Wind-Induced Torsional Loads on Low- and Medium-Rise Buildings

Mohamed Ragab Elsharawy

A Thesis
In the Department
of
Building, Civil and Environmental Engineering

Presented in Partial Fulfillment of the Requirements
For the Degree of
Doctor of Philosophy (Civil Engineering) at
Concordia University
Montréal, Québec, Canada

April 2014

CONCORDIA UNIVERSITY

School of Graduate Studies

This is to certify that the thesis prepared

By: Mohamed Ragab Elsharawy

Entitled: **Wind-Induced Torsional Loads on Low- and Medium-Rise Buildings**

and submitted in partial fulfillment of the requirements for the degree of

Doctor of Philosophy (Civil Engineering)

complies with the regulations of the university and meets the accepted standards with respect to originality and quality.

Signed by the final examining committee:

_____ Chair
Dr. Wahid Ghaly

_____ External Examiner
Dr. Yukio Tamura

_____ External to Program
Dr. Georgios Vatistas

_____ Examiner
Dr. Oscar Pekau

_____ Examiner
Dr. Lucia Tirca

_____ Thesis Co-supervisor
Dr. Ted Stathopoulos

_____ Thesis Co-supervisor
Dr. Khaled Galal

Approved by

_____

Dr. M. Elektorowicz, GPD
Department of Building, Civil and Environmental Engineering

_____

Dr. C. Trueman, Dean
Faculty of Engineering and Computer Science

Date _____

ABSTRACT

Wind-Induced Torsional Loads on Low- and Medium-Rise Buildings

Mohamed R. Elsharawy, Ph.D.
Concordia University, 2014

Proper building design against wind loads depends primarily on the adequacy of the provisions of codes of practice and wind load standards. During the past decades, much has been learned about along- and across-wind forces on buildings. However, studies on wind-induced torsional loads on buildings are very limited. The recent trends towards construction of more complex building shapes and structural systems can result in an increase of the unbalanced wind loads yielding an increase of torsional moments. Thus, re-visiting the wind load provisions is of an utmost concern to ensure their adequacy in evaluating torsion on low- and medium-rise buildings and to achieve safe, yet economic building design. It is noteworthy that most of the wind loading provisions on torsion have been developed from the research work largely directed towards very tall and flexible buildings for which resonant responses are significant. However, the dynamic response of most low- and medium-rise buildings is dominated by quasi-steady gust loading with little resonant effect. Moreover, the lack of knowledge regarding wind-induced torsion is reflected in having different approaches in evaluating torsion in the international wind loading codes and standards.

The current research program undertakes the investigation of shear and torsional wind loads on low- and medium-rise buildings. The study demonstrates that North American and European Codes and Standards have quite different provisions for wind-

induced torsion acting on low- and medium-rise buildings with typical geometries – namely, for horizontal aspect ratios (L/B) equal to 1, 2, and 3. In the experimental phase, several buildings with different configurations, i.e. different roof angles (0°, 18.4°, 45°) and heights (ranging from 6 m to 60 m) were tested in the boundary layer wind tunnel of Concordia University for different wind directions (every 15°). The measured shear and torsional loads were compared with the Canadian and American code provisions. The study found that NBCC 2010 underestimates torsion on low-rise buildings significantly, while discrepancies were found for medium-rise buildings. In addition, wind load combinations for low- and medium-rise buildings were studied. For flat-roofed buildings, it was found that maximum torsion for winds in transverse direction is associated with 80% of the overall shear force perpendicular to the longer horizontal building dimension; and 45% of the maximum shear occurs perpendicular to the smaller horizontal building dimension. Suggested approaches and load combination factors were introduced to enhance the current building codes and standards aiming at an adequate evaluation of wind load effects on low- and medium-rise buildings.

ACKNOWLEDGEMENTS

During this PhD marathon, I must admit that I was fortunate to be advised by excellent researches and mentored by wonderful teachers. My greatest appreciation goes to my supervisors Dr. Ted Stathopoulos and Dr. Khaled Galal. I believe that this research would not have been completed without their continuous support.

I would also like to dedicate this work to my parents and my wife for their invaluable support during my study. I also dedicate it from the bottom of my heart to the source of happiness in my life and the gift from God; my older son Omar and my lovely twins Ahmed and Salma. Their presence in my life encouraged and gave me the motivation to reach my goals and achieve my dreams.

Last but not least, many thanks are due to my dear friends and colleagues as well as the lab technicians at Concordia University.

To My Beloved Parents

Table of Contents

CHAPTER 1 - INTRODUCTION

CHAPTER 2 - BACKGROUND AND LITERATURE REVIEW

CHAPTER 3 – WIND-INDUCED TORSION IN CURRENT WIND CODES AND STANDARDS

CHAPTER 4 - WIND TUNNEL METHODOLOGY

CHAPTER 5- EXPERIMENTAL RESULTS AND DISCUSSION

CHAPTER 6 - LOAD COMBINATIONS

CHAPTER 7 – PROPOSED WIND LOAD COMBINATIONS FOR DESIGN CODES

CHAPTER 8 - CONCLUSIONS

LIST OF FIGURES

LIST OF TABLES

NOMENCLATURE

f_n building natural frequency

Z height from the ground

Z_g gradient height

α power law index

q_h mean dynamic wind pressure at mean roof height

p_t instantaneous pressure at pressure taps

$A_{i,\,effective}$ area effective for pressure tap allocated in X-direction

$A_{j,effective}$ area effective for pressure tap allocated in Y-direction

$f_{i,t}, f_{j,t}$ wind forces at pressure taps

H eave building height

B smallest horizontal building dimension

L largest horizontal building dimension

r_i, r_j perpendicular distances between the pressure taps and the building center in X- and Y-directions, respectively

F_X, F_Y Horizontal force components

V total base shear force

M_T torsional moment

C_{Sx} shear coefficient in X-direction

C_{Sy} shear coefficient in Y-direction

$C_{T\,Mean}$ mean torsion coefficient

C_{Tx} torsional coefficient due to winds in transverse direction

C_{Ty} torsional coefficient due to winds in longitudinal direction

e, e_x, e_y eccentricities

$|C_{Sx}|_{corr.}$ corresponding shear force coefficient in transverse direction

$|C_{Sx}|_{Max.}$ peak shear force coefficient in transverse direction

$|C_{Sy}|_{corr.}$ corresponding shear force coefficient in longitudinal direction

$|C_{Sy}|_{Max.}$ peak shear force coefficient in longitudinal direction

$|C_{Tx}|_{Max.}$ peak torsional coefficient due to winds in transverse direction

$|C_{Ty}|_{Max.}$ peak torsional coefficient due to winds in longitudinal direction

$C_{Sx\ overall}$ the most critical shear coefficient in X-direction found from testing the buildings for all wind directions

$C_{Sy\ overall}$ the most critical shear coefficient in Y-direction found from testing the buildings for all wind directions

$C_{T\ overall}$ the most critical torsion coefficient found from testing the buildings for all wind directions

CHAPTER 1
INTRODUCTION

The characteristics of wind-induced loads on buildings continuously vary in temporal and spatial dimensions. Adequate design of buildings depends on the success in predicting the actual effects of turbulent wind forces in order to account for the most critical design scenarios which may occur during a certain design period. Along-wind force fluctuations are generated to a large extent by approaching flow turbulence; but fluctuations in across-wind force and torsion are generally dominated by vortex shedding causing asymmetric pressure distributions around building envelopes (Tamura *et al.* 2003). The variation of local wind pressures on building envelope and the total effective wind forces (base shear/overturning moment) on the main structural building systems of low- and medium-rise buildings have been investigated extensively in the past few decades (Krishna, 1995, Stathopoulos and Dumitrescu, 1989, and Sanni et al, 1992). However, studies on wind-induced torsional loads on low- and medium-rise buildings are very limited. Moreover, most of building codes and standards provide very little or, sometimes ambiguous guidance to evaluate wind-induced torsion on buildings.

1.1 WIND-INDUCED TORSIONAL LOADS ON BUILDINGS

Wind causes a three-dimensional dynamic load which varies on building surfaces in both, space and time. Modeling of the comprehensive building-wind interaction effects in the building design standards for predicting the actual turbulent wind loads is not an easy or straightforward process. Meteorological data, geographical information, in addition to building geometries and surroundings affect significantly the variation of the turbulent wind loads on buildings. The essential need for adequate building design was the reason behind extensive investigation of wind effects on buildings in the last few decades. The precise simulation of wind in the boundary layer wind tunnel (BLWT) and the development of pressure measurements techniques made a significant contribution to improvement of the current wind design standards. Despite this, it is surprising to realize that there is still a lack of adequate reliable approaches for predicting the torsional effects of wind on buildings.

The wind flow around any building is very sensitive to the building's shape and geometry as well as the layout of the surroundings. The turbulence of the wind velocity itself in addition to the turbulence due to the interaction between the wind and the building, in case of stiff or flexible structures, introduce variable wind loads that vary in time and in space. Previous wind tunnel tests and field measurements emphasized that there is always a lack of correlation in space and time of the wind pressure over the building faces even for simple geometrical and structural systems of buildings. In other words, wind loads on the building surfaces are, in general, non-uniform. Wind load provisions always require the design wind loads to be safe and economic as well as simple to be implemented in design code provisions. The simplified methods introduced

2

in the current design standards to predict the actual wind load effects on buildings were not sufficiently examined to ensure that these provisions are adequate for predicting the wind-induced torsion on buildings. Figure 1.1 shows an example for an actual low building damage possibly caused by torsion (AAWE, 2013). As illustrated, the non-uniform wind load distribution, which is the main source for generating torsion on the building, is likely to be the reason for damage. Overlooking the accurate representation of wind-induced torsional loads on buildings due to the limited knowledge in this area, would lead to unrealistic spatial equivalent wind design loads. These unrealistic loads can be conservative in certain design situations and detrimental in others. Accordingly, accurate evaluation of wind-induced torsional loads has a significant effect on the serviceability and survivability of designed buildings.

Figure 1.1: Low-rise building damage likely caused by wind-induced torsion (AAWE, 2013)

Wind-induced torsional moments are generated as a result of the natural eccentricities between the center of building rigidity and the center of the instantaneous aerodynamic wind loads. It is also well known that the determination of torsion or unbalanced wind loads requires information about instantaneous wind pressure distribution on building surfaces. Identifying wind load for design purposes through capturing experimentally or analytically wind pressure envelope, as presented in Figure 1.2, is one of the main reasons for overlooking the torsional moments induced by wind. Wind pressure envelope is a reliable treatment for evaluating the maximum effective wind force generated on the building. On the other hand, the distribution of these peak wind pressures is not representative of the real instantaneous wind distribution since the peaks acting on the building surface will not occur simultaneously. The trend of focusing on evaluating peak pressures envelope only resulted in overlooking the instantaneous realistic wind distribution acting on the building surface. Consequently, this resulted in uncertainties in predicting the level of torsional wind loads stated in the current wind standards.

When compared to the loads in the along- and cross-wind directions, wind-induced torsional loads on buildings have clearly received less attention in previous research. This mainly arose from three main reasons. First, the complexity and sensitivity of the wind flow around the building and any obstacle that wind might face within its path. Second, the limited capacity of equipment and the difficulties faced in fabricating building models for testing in wind tunnel. The third reason is the simplicity often adapted by buildings codes and standards. Shortcomings and discrepancies that are found when comparing the provisions of wind-induced torsional loads in different international

wind standards and codes of practice highlight the necessity for investigating the fundamental behaviour associated with this phenomenon.

In general, torsion wind load case may govern the design for buildings or at least, it will reduce the design safety index due to increasing the stresses in some structural elements more than what is expected. On the other hand, the continuous development of new structural materials and advanced building techniques introduces a smart generation of tall and flexible buildings. Significant mean and dynamic torsional loads that can be generated on tall buildings due to wind pressure unsteadiness will cause uncomfortable accelerations for building habitants. This was the reason behind the escalating awareness of the need for more research efforts towards investigating wind-induced torsional wind loads on tall buildings. However, still the current building design standards provide little guidance and sometimes unclear input to the designer in this regard.
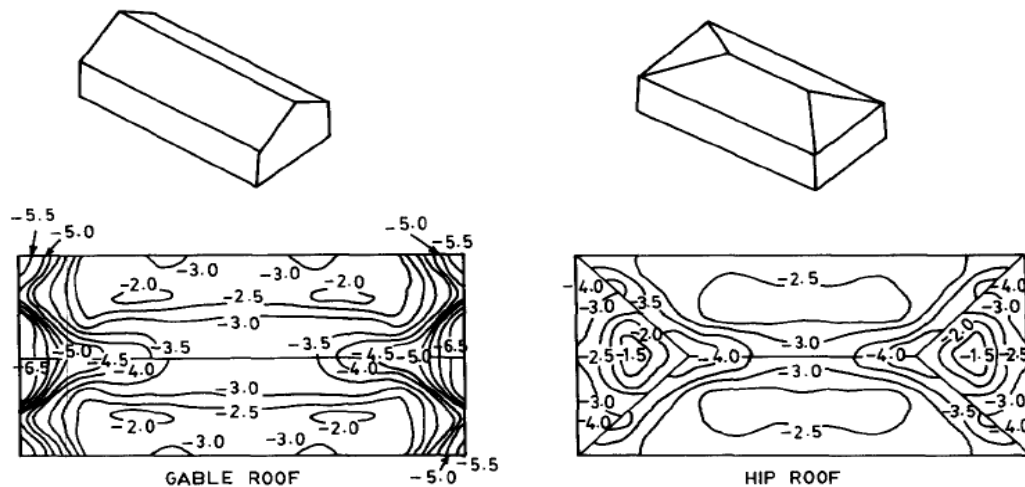
Figure 1.2: Worst peak negative pressure coefficients- all azimuths (Krishna, 1995)

1.2 PROBLEM STATEMENT

There has been a confusion regarding wind-induced torsion on low- or medium-rise buildings due to the different provisions available in current design codes and standards. For instance, the ASCE 7 (2010) American standard introduces two load cases in the envelope method to estimate torsion, namely; maximum torsion with corresponding shear and maximum shear with corresponding torsion. The National Building Code of Canada, NBCC, (2010) specifies only one load case in the static method assigned for low-rise buildings to evaluate maximum shear as well as maximum torsion. Similar to ASCE 7 (2010), the European code (EN 1991-1-4 (2005)) introduces two load cases to evaluate the design shear and torsional loads but for buildings with all heights. Figure 1.3 shows a schematic of the different wind load distributions introduced in these three wind load provisions for estimating the wind-induced torsion loads for building design.

Wind-induced torsion provisions in the three codes/standards are also different for medium-rise buildings. ASCE 7 (2010) requires introducing 75% of the full wind load with eccentricity of 15% of the facing building horizontal dimension for evaluating maximum torsion. On the other hand, NBCC (2010) requirements for design of medium-rise buildings specifies applying 50% of the full wind load on half of the along wind wall in order to predict the maximum torsion. Non-uniform wind loads were simulated by applying triangular loading in the EN 1991-1-4 (2005). The non-uniform wind loads applied for torsion, in EN 1991-1-4 (2005), allow for torsional moment equivalent to applying the full design wind load with 6% eccentricity.

Notwithstanding these differences among the mentioned wind load provisions, it is remarkable to note that other codes/standards neglect torsion in the design of low- and medium-rise buildings. For instance, the Australian standard (AS/NZS 1170.2-2011) does not require wind-induced torsion to be considered for the design of buildings with heights lower than 70 m.

The limited information and the little guidance available in the current wind loads codes/standards show clearly the need for examining wind induced torsion on buildings. Therefore, an experimental wind tunnel study was undertaken in this study to examine wind-induced torsion on low- and medium-rise buildings.

NBCC (2010)

ASCE 7 (2010)

EN 1991-1-4 (2005)
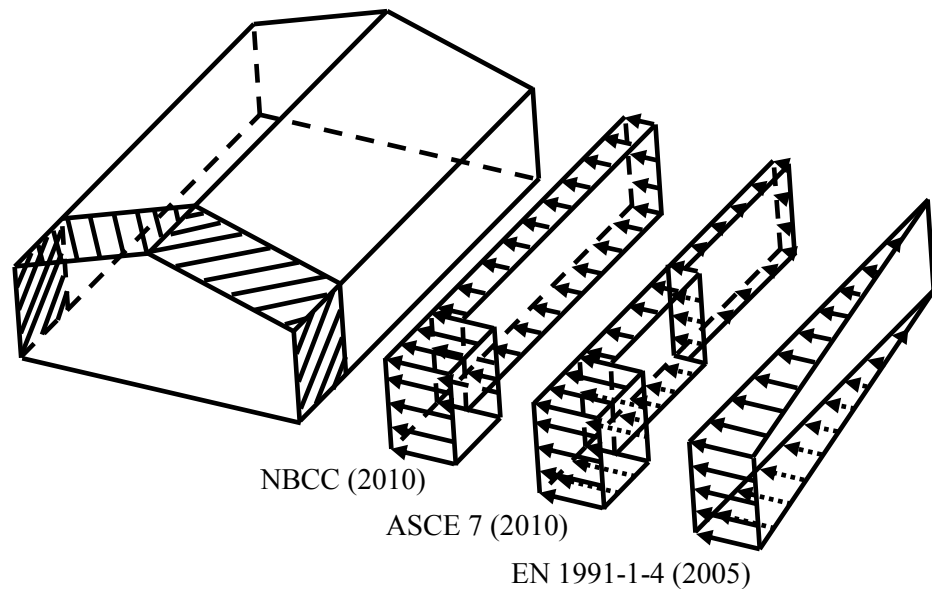
Figure 1.3: Schematic representation of load configurations used to evaluate wind-induced torsion in three international design codes and standards

1.3 RESEARCH OBJECTIVES:

The main objective of this research is to investigate experimentally and analytically the wind-induced torsional loads on low- and medium-rise buildings.

1.4 SCOPE OF RESEARCH

In order to achieve the above-mentioned objective, the scope of this research is to:

1- Compare the current design codes and standards provisions approaches for predicting torsional wind loads on buildings. The research will focus on the NBCC (2010), ASCE 7 (2010), and the EN 1991-1-4 (2005).

2- Assess the current building codes and provisions analytical approaches for predicting wind induced torsional loads on low-rise and medium-rise buildings.

3- Conduct wind tunnel tests on low- and medium-rise buildings to study the effect of the following key variables on the wind-induced torsional loads: Building height; Roof slope; Terrain exposure; and Wind direction.

4- Analyse the wind tunnel measurements. In this task, wind-induced measured pressures are numerically integrated over all building surfaces and results are obtained for along-wind force, across-wind force, and torsional moment. Torsion load case (i.e. maximum torsion and corresponding shear) and shear

load case (i.e. maximum shear and corresponding torsion) are evaluated to reflect the maximum actual wind load effects in the two horizontal directions (i.e. transverse and longitudinal).

5- Develop two analytical methods to predict wind-induced torsion for low rise- and medium-rise buildings. In this task, the evaluated torsion and shear load cases are also compared with the current torsion- and shear-related provisions in the NBCC 2010, ASCE 7 (2010). Finally, shear and torsion load cases are suggested for evaluating wind loads considering torsion effects to be used in the design of low- and medium-rise rectangular buildings.

1.5 STRUCTURE OF THE THESIS

The research work conducted in this thesis is presented in eight chapters.

Chapter 1 describes the background and the motivation for the research program.

Chapter 2 contains a detailed literature review. All literature relevant to wind-induced torsional loads on low- and medium-rise buildings were presented.

Chapter 3 presents comparisons among the current North American (NBCC 2010, ASCE 7 (2010)) and European (EN 1991-1-4) wind provisions in evaluating shear and torsion load cases for low- and medium-rise buildings. Part of these comparison results (i.e. comparing provisions for low-rise buildings) were published in (Elsharawy et al. 2012).

Chapter 4 describes the wind tunnel methodology, pressure measurements, velocity measurements and the analytical approach to get the shear and torsional coefficients.

Chapter 5 presents the discussion of the wind tunnel results along with the comparisons with the NBCC 2010 and ASCE 7 (2010) wind provisions.

Chapter 6 presents the load combinations evaluated from the measured data. The effect of the wind direction on wind load combinations for rectangular low- and medium-rise buildings was investigated. The maximum torsion along with corresponding shear forces in transverse and longitudinal directions were examined. Similarly, the maximum shear forces with corresponding torsion were studied. The results discussed in this chapter were published in (Stathopoulos et al. 2013).

Chapter 7 provides general recommendations, based on the wind tunnel results, for better evaluating wind effect including torsion. The chapter also provides specific proposed values for wind-induced loads, including torsion, on buildings for possible implementation in the NBCC 2010 and ASCE 7 (2010) codes.

Lastly, Chapter 8 summarizes the contributions of the current work, drawing the final conclusions and stating recommendations for future work.

CHAPTER 2

BACKGROUND AND LITERATURE REVIEW

Understanding wind-building interaction has a significant impact on effective building design for both serviceability and survivability states. The demand for a proper design for buildings is inevitable for human safety and nation's economy. Historically, prediction of the wind loads on buildings is a major subject of interest for designers. Wind-structure interactions were investigated extensively during the past decades in wind tunnel facilities and few field measurements in addition to, more recently, the computational fluid dynamics (CFD). Unfortunately, realistic modeling of the obtained data and providing designers with simple and reliable design procedures for wind loads is still difficult for some reasons. The main difficulties are attributed to the infinite scenarios of buildings' geometry in addition to the complexity of the wind flow interaction around the buildings and their surrounding environment (Stathopoulos 1984).

2.1 REVIEW OF WIND-INDUCED TORSIONAL LOADS ON BUILDINGS

2.1.1 Low-rise buildings

The majority of residential and commercial buildings worldwide are categorized as low buildings. Wind loads on low-rise buildings have not received sufficient attention, particularly when the large investment in such structures is considered. Wind loads

generally govern the design of lateral structural systems of low-rise buildings in low seismicity areas and where there is high probability of occurrence of severe wind events. Comprehensive reviews of the previous field measurements, wind tunnel tests, and analytical studies for wind loads on low-rise buildings have been introduced by Holmes (1983), Stathopoulos (1984) and Krishna (1995). The development of provisions for the evaluation of wind loads on low-rise buildings was based on the research carried out at the University of Western Ontario in the late 70's, when an extensive experimental program in a boundary layer wind tunnel considered a variety of rectangular low-rise buildings with different dimensions, roof slopes and upstream terrain exposures (Davenport et al., 1977, 1978). The tested buildings were exposed to wind from directions vary from 0° to 360°. Depending on the idea of time average and spatially average the peak measured pressures, the study tried to develop the pseudo values of wind pressures (GC_{pf}) for appropriate design of low-rise buildings. The calculation process is illustrated in Figure 2.1. Only the following structural actions were evaluated:

1. Total uplift;

2. Total horizontal shear;

3. Bending moment at knees (two-hinged frame);

4. Bending moment at knees (three-hinged frame); and

5. Bending moment at ridge (two-hinged frame).

Nevertheless torsional load was not investigated; the simultaneous occurrence of the peak of different wind load components was not also examined. For instance, ASCE 7 (2010) introduces two load cases in the envelope method to estimate torsion, namely;

maximum torsion with corresponding shear and maximum shear with corresponding torsion. NBCC (2010) specifies one load case in the static method assigned for low-rise buildings to evaluate maximum shear as well as maximum torsion. Significant effects may occur due to neglecting or not considering adequately the non-uniformity of the real wind distribution on building surfaces.
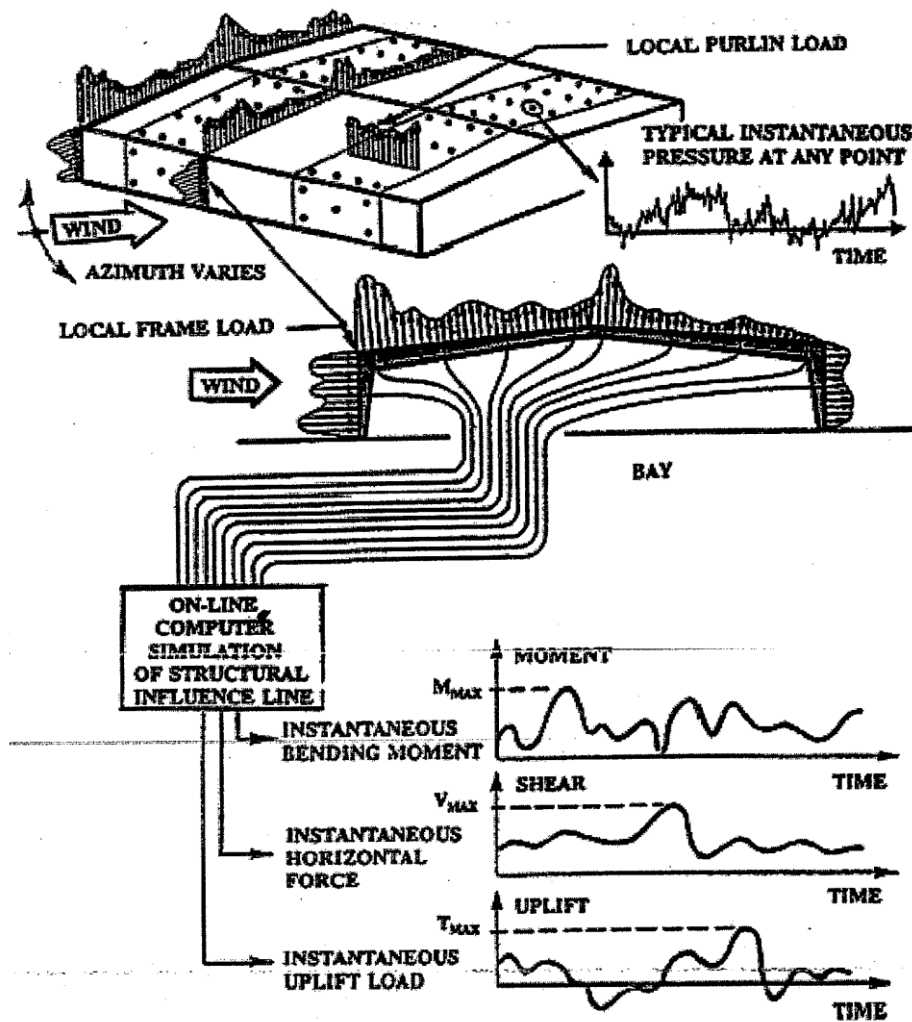
Figure 2.1: Unsteady wind loads on low-rise buildings, not including torsion (ASCE 7, 2010)

13

A study by Tamura and et al. (2000), showed that even for wind direction perpendicular for a symmetric building shape, the instantaneous wind pressure distribution is always non uniform –see Figure 2.2. However for a $0^{°}$ wind direction, while wind perpendicular to the building the mean torsion may be zero in the symmetric building case, the peak torsion may be significant. It would be of great importance to have more information about the effect of wind direction on buildings with symmetric and non-symmetric plans.

There are limited reported studies addressing wind-induced torsional loads on low-rise buildings in full detail. In addition to the scarcity of information in this area, it was found that there are significant differences when comparing the wind torsional loads in the current international building codes as it will be shown in detail in the following chapter. Notwithstanding these differences among wind load provisions, other codes/standards neglect torsion in the design of low- and medium-rise buildings. For instance, the Australian standard (AS/NZS 1170.2-2011) does not require wind-induced torsion to be considered for the design of buildings with heights lower than 70 m. For taller buildings, torsion shall be applied based on eccentricity of 20% of building width with respect to the center of geometry of the building on the along-wind loading.

Isyumov and Case (2000) measured wind-induced torsion for three low-rise buildings with different aspect ratios (length/width = 1, 2, and 3) in open terrain exposure as modeled in the wind tunnel. It was suggested that applying partial wind loads, similar to those implemented for the design of medium-rise buildings, would improve the design of low-rise buildings until more pertinent data becomes available. Based on this study's recommendation of embedding the partial load approach to eliminate this shortage of

increasing wind pressure only on the end zone, the American Society of Civil Engineers

standard ASCE 7-05 was modified. In addition, the ASCE 7 (2010) also used the partial

loads by reducing the wind pressure over half of building face to 25% of the total wind

pressure, which creates more severe design situation. However, the afore-mentioned

approach still needs more experimental work to identify more details regarding the

configuration of the partial wind load cases in order to ensure that they adequately

represent actual wind load conditions.

(a) When the maximum along-wind base shear was recorded

(b) When the maximum across-wind base shear was recorded

(c) When the maximum torsional moment was recorded
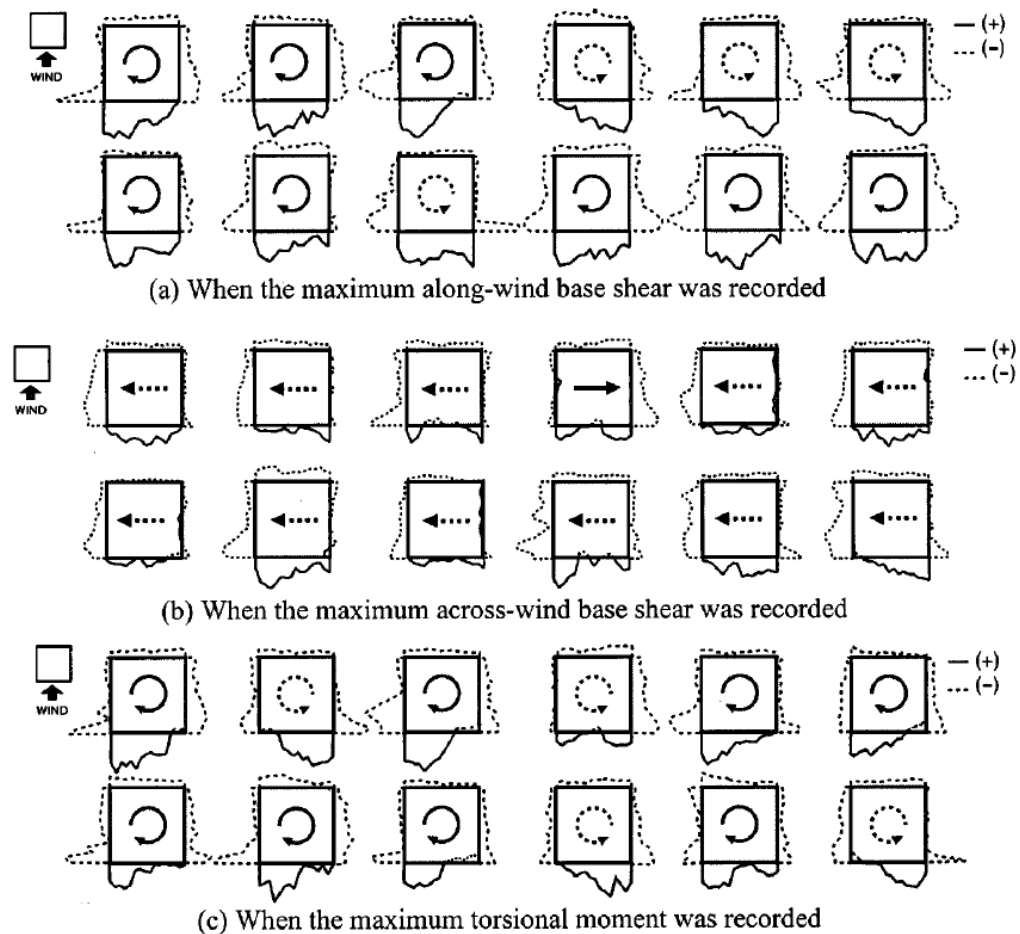
Figure 2.2: Examples of instantaneous pressure distributions causing maximum wind
force and torsion coefficients (Tamura et. al., 2000)

2.1.2 Medium-rise buildings

Most of the wind loading provisions on torsion have been developed from the research work largely directed towards tall and flexible buildings (Melbourne 1975, Greig 1980, Vickery and Basu 1984, Tallin 1985, Lythe et al. 1990, Xie et al. 2000, Zhou et al. 2000 and Boggs et al. 2000) for which resonant responses are significant. However, the dynamic response of most medium-rise buildings is dominated by quasi-steady gust loading with little resonant effect. Moreover, the lack of knowledge regarding wind-induced torsion is apparent in the different approaches in evaluating torsion in the international wind loading codes and standards.

Tamura et al. (2003, 2008 and 2012) conducted extensive research on wind load combinations for low-, medium and high-rise buildings. Different building models were tested in open and urban terrain exposures. Focus was given to wind load combinations but mainly for wind perpendicular to building face. Wind load combination in these studies were evaluated based on wind load effects on buildings (i.e. normal stresses in columns and displacements) with one structural system (i.e. buildings with only four corner columns), which is required more experimental data to generalize the findings. Keast et al. (2012) studied wind load combinations including torsion for medium-rise buildings. Three building models were tested, two with rectangular planes and one with L-shape. Based on testing of these building models, the study concludes that for rectangular buildings the peak overall torsion occurs simultaneously with 30-40% of the peak overall drag force. Additional experimental results for testing different building configurations are still required to confirm and generalize these results.

2.1.3 Tall buildings

Wind-induced torsional loads on tall buildings have received more attention compared to low buildings, since more complex interactions between the fluctuating wind forces and main wind force resisting systems may result in significant dynamic wind torsion for tall buildings. Moreover, any rotational motion of a building could be a reason for disturbance and for causing discomfort to building habitants. Wind tunnel studies are recognized as a reliable source of information for engineers to design such buildings. Ten multi-degree-of-freedom aeroelastic models have been tested in the wind tunnel by Greig (1980) to measure the mean and the dynamic torsional wind-induced moments. This is the first study that introduced an empirical formula for predicting the torsional wind moment on tall buildings, although this was an empirical formula based on a finite data set; indeed, to be used as a general estimator, this formula must be validated and improved through performing additional wind tunnel tests.

Isyumov and Poole (1983) tested buildings with square and rectangular cross-sections in the wind tunnel by using the weighted pneumatic averaging technique to measure the mean and dynamic torque components. This study was trying to overcome the limitation of the pressure instrumentation to measure simultaneously the wind pressure over the building surfaces. It was shown that the pressure fluctuation on the back face induced by vortex shedding has a significant contribution to the dynamic torsional moment in the studied buildings. Also, the study showed that the quasi-static assumptions can provide reasonable estimates of the dynamic torque. A comparison between measuring the base torque using a force balance method in wind tunnel and the integration of the pressures measured on the sides of the model has been published by

Tallin (1985) where it was shown that although the force balance technique requires smaller computational effort, it over-estimates the torsional moment. Lythe et al. (1990) conducted a wind tunnel study, in which torsional wind loads for different building shapes (simple, complex symmetrical, and complex non-symmetrical) were measured in detail. Instrumentation and computational limitations at the time restrained the study to only examine the mean torsional wind loads.

As a kind of simplicity and by using two dimensionless factors, the equivalent eccentricity, e, and the load reduction factor, r, the magnitudes of torsional wind loads were investigated in wind tunnel for several tall buildings with respect to horizontal loads, as reported by Xie et al. (2000). In general, it was illustrated that for most buildings the overall equivalent eccentricities are found to be more than 10% (20% for torsional sensitive buildings). Some real-life tall buildings have been tested through wind tunnel tests and results presented by Boggs et al. (2000). In general, the equivalent eccentricity for these buildings might reach up to 30% of the building width and the wind-induced torsion effects cannot be eliminated but can possibly be minimized by changing the building geometry or the structural properties of the tall buildings. The tests also showed the effects of the structural properties on the elimination of the coupling between the torsional and sway vibrations.

Zhou et al. (2000) introduced a gust load factor (GLF) formulation to estimate the torsional wind response for tall buildings. This was based on data collected from High Frequency Force Balance (HFFB) wind tunnel tests. The study discussed the effect of a nonuniform mode shape on the HFFB results since the rigid model used allowed only for linear mode building shape. This GLF procedure can be used in the preliminary design

18

stages prior to the detailed wind tunnel tests. This procedure requires also more validations, possibly through aeroelastic model testing in the wind tunnel, to become a generalized approach. More recently, the development of the solid state switching technology has allowed the use of the High Frequency Pressure Integration (HFPI) method to determine the overall wind loads on tall buildings. The effectiveness of using this method has been studied by Ho et al. (1999) who compared the traditional HFFB with HFPI method. The results collected from testing two tall building models in the wind tunnel demonstrated that wind tunnel testing with HFPI method is capable of providing improved information on the overall wind-induced building forces and torsional moments.

Summary:

Very limited information is available in the literature regarding wind-induced torsion on low- and medium-rise buildings. This lack of information has been reflected in the current provisions and support the high demand for more experimental work to investigated wind-induced torsion on low- and medium-rise buildings.

CHAPTER 3

WIND-INDUCED TORSION IN CURRENT WIND CODES AND STANDARDS

Modern building codes and standards introduce various analytical load patterns to evaluate the actual wind load effects on buildings. For wind-induced torsional loads on buildings, inadequate information and sometimes unclear or ambiguous statements are found in these descriptive code models, as it will be indicated in the following sections. Some standards do not even have provisions for wind-induced torsional loads on buildings. As mentioned in chapter 2, the current Australian standard (AS/NZS 1170, 2:2011) does not require wind-induced torsion to be considered in the design of rectangular buildings with heights lower than 70 m. For buildings with heights greater than 70 m, torsion shall be applied based on eccentricity of 20% of building width with respect to the center of geometry of the building on the along-wind loading. Ongoing updates and sufficient assessment are always considered critical towards reliable analytical approaches aiming at better evaluation of actual wind effects on buildings. In this section the wind-induced torsional load provisions in ASCE 7 (2010), NBCC (2010), and EN 1991-1-4 (2005) will be presented, discussed and compared with available experimental data from past and current studies.

3.1 OVERVIEW OF THE CURRENT WIND-INDUCED TORSION PROVISIONS

Wind-induced loads on buildings vary instantaneously in temporal and spatial dimensions. Buildings may experience a significant torsional moment due to the shift between the resultant of aero elastic wind forces and the building center of rigidity. This torsional moment should be accounted for during the building design process. Unfortunately, due to the limited available sources, most of the building codes provide inadequate information about wind-induced torsion on buildings. As a step towards better estimation of wind-induced torsional loads on low-rise buildings – defined generally as having heights less than 20 m – an assessment of the wind-induced torsional load provisions is necessary.

Two main approaches are being used in the wind loading standards for the evaluation of the actual effects of wind-induced torsional loads on buildings. The first approach is implemented by applying reduced uniform wind loads on building surfaces with additional equivalent eccentricity from the building dimensions (used in ASCE 7 (2010)), while the other way is by applying non-uniform wind loads (used in NBCC (2010) and EN 1991-1-4 (2005)). The non-uniform wind loads can be simulated by either increasing the wind pressure on building corners, by using partial wind load acting on one part of a building face, or by applying a triangular wind load on building surfaces. The following sections discuss the different approaches used to calculate the wind-induced torsional loads in the American, the Canadian and the European wind codes/standards:

3.1.1 American Society of Civil Engineers (ASCE 7 (2010))

Wind load provisions in ASCE 7 (2010) include two analytical methods to estimate wind forces on the main wind force resisting system (MWFRS): the static (envelope) method, which is applicable to low buildings – (defined as having mean roof height, $h < 18$ m and $h <$ smallest horizontal building dimension, B) – and the simplified (directional) method, which can be used for designing buildings of all heights. The simplified method has three main load cases; namely transverse (perpendicular to ridge) load case, longitudinal (parallel to ridge) load case, and torsional load case. The description of the three load cases is given in ASCE 7 (2010) in chapter 28, figure 28.4-1 (Appendix I). In the third case, the torsional effects are taken into account by applying only 25% of the full design wind pressure on half of the building faces. As an exceptionally, one-story buildings with $h < 9.1$ m and two-story buildings framed with light frame construction or designed with flexible diaphragms need not be designed for torsional loads. On the other hand, the simplified/directional method has four load cases described in ASCE 7 (2010), chapter 27, figure 27.4-8 (Appendix I). In the first and third cases, uniform wind loads are applied without any torsional loads. Torsional wind loads are specified in cases 2 and 4 by introducing two non-dimensional parameters, 15% equivalent eccentricity of the building dimension and 0.75 and 0.563 reduction factors respectively for the equivalent static wind pressure. Specific exemptions are provided in Appendix D of the Commentary of ASCE 7 (2010), which also says:

"Although this is more in line with wind tunnel experience on square and rectangular buildings with aspect ratios up to about 2.5, it <u>may not cover</u> all cases, even for symmetric and common building shapes where larger torsions have been observed" (C27.4.6)

3.1.2 National Building Code of Canada (NBCC (2010))

The National Building Code of Canada was the first that adopted in its provisions the effect of wind-induced torsional loads on buildings. Since the early 70's and till 2005, the NBCC subcommittee on wind loads introduced unbalanced wind loads to generate wind-induced torsion on medium-rise buildings. It was suggested to remove 25% of the full wind load from any portion on building surfaces in order to maximize torsion according to the most critical design scenario states. This allowance for torsion is equivalent to applying the full design wind load at an eccentricity, which was 3 or 4 percent of the building width. In the NBCC 2005 edition, the 25% removal of the full wind load was modified into a complete removal of the full wind loads from those areas that would lead to maximize torsion. Accordingly, limiting the load on half of windward and leeward building faces will generate torsion, equivalent to applying the full design wind load at an eccentricity equal to 12.5 percent of the horizontal dimension perpendicular to the wind direction.

In NBCC (2010), the static method specifies wind loads on low-rise buildings (defined as having mean roof height, h < 10 m, or h < 20 m and h < smallest horizontal building dimension, B) –see figure I-7 (Appendix II). One load case is described in the static approach to evaluate maximum shear, as well as maximum torsion. For instance, the NBCC 2010 identifies the horizontal wind load distribution over the building surface by increasing the wind pressure on the end zones. The width of this end zone depends mainly on the building width and is not related to the building's length. Moreover, there is limitation in such analogy for buildings with heights less than 7.5 m and widths less than 30 m where the end zone has a fixed width of 6.0 m, no matter how long the

building is. The simplified method is suggested for medium-rise buildings, defined as having h < 60 m, h/B < 4, and lowest natural frequency, f_n > 1 Hz. It is important to mention here that most of the torsion provisions in the simplified method were formulated from testing tall and flexible buildings (Isyumov, 1982; ASCE 1999). The method identifies four load cases: in Cases A and C, symmetric uniform loads are considered, in order to estimate the maximum base shears and overturning moments; and, partial wind loads are recommended to create equivalent torsional building loads in Cases B and D. Nevertheless, the choice of partial loads could be difficult for design engineers following the code statements quoted below:

"In case B, the full wind pressure should be applied only to parts of the wall faces so that the wind-induced torsion is maximized" (note (2) to figure I-16)*; and "To account for potentially more severe effects induced by diagonal wind, and also for the tendency of structures to sway in the cross-wind direction, taller structures should be designed to resist 75% of the maximum wind pressures for each of the principal directions applied simultaneously as shown in figure I-16, Case C. In addition, the influence of removing 50% of the case C loads from parts of the face areas that maximizes torsion, as shown in figure I-16, case D, should be investigated"* (Commentary I, paragraph 37).

As can be noted, it might not be easy to determine the parts of the wall faces on which the reduced wind loads should be applied in order to account for the appropriate torsion and shear combinations needed for a proper design of the building.

3.1.3 European Building Code (EN 1991-1-4)

The Eurocode defines one unified analytical method that can be used for predicting the wind forces on all building types regardless of height. Wind pressure and force coefficients are described in Eurocode part 4 section 7. Torsional effects are taken into account by applying non-uniform pressures and forces, as shown in EN 1991-1-4 (2005), figure 7.1 (Appendix III). A triangular wind load is applied on the windward surface with a rectangular load on the leeward face of the building. Limited information regarding wind-induced torsional loads only for rectangular buildings can be found in this code. In addition, EN 1991-1-4 includes a rather difficult to apply statement regarding the torsional wind load case:

"For other cases an allowance for asymmetry of loading should be made by completely removing the design wind action from those parts of the structure where its action will produce a beneficial effect". (Section 7.1.2 – note (b))

In summary, a review of the current approaches stated in ASCE 7 (2010), NBCC (2010), and EN 1991-1-4 (2005) for predicting torsional wind loads on low-rise buildings are presented in Figure 1.2. In ASCE 7 (2010), the wind pressure is increased on areas close to building corners (end zone). Moreover, a 75% reduction of the wind loads on half of the building faces is required. In NBCC (2010), only increasing the wind pressure on the end zone is required while a triangular wind load is implemented in EN 1991-1-4 (2005). In general, these procedures lack the full details for describing the torsional wind load cases. As clearly seen in some code statements for partial wind load cases the decision has to be made by designer to specify from where the wind loads should be

removed in order to maximize torsion. Yet, these are simple and typical building configurations (i.e. buildings with symmetrical rectangular or square plan).

3.2 COMPARISONS OF TORSION PROVISIONS USING CURRENT CODES AND STANDARDS

3.2.1 Low-rise buildings

In this section, comparisons among ASCE 7 (2010), NBCC (2010), and EN 1991-1-4 (2005) provisions for wind-induced torsional loads on low-rise buildings are presented. Different building configurations are analyzed using the three codes/standards selected. In particular, three low-rise buildings - gabled roof angle 18.4° width (B =16 m), and eave height (H = 6 m) with different aspect ratios (L/B =1, 2, and 3) in an open terrain have been examined. The static methods assigned for low-rise buildings are applied. Also, it is of interest to apply the simplified methods provided for medium-rise buildings, as the structural behaviour of these buildings is quasi-similar with that of low-rise buildings. The directional approach in ASCE 7 (2010) (called herein simplified method) assigned for all building heights and simplified method in NBCC (2010) assigned for medium-rise buildings, have been applied, in addition to the analytical method available in EN 1991-1-4 (2005). The assessment of the torsional load cases in the code provisions has been carried out by estimating both the maximum torsional moment and the corresponding shear force. On the other hand, the wind velocity was adjusted by using the so-called Durst curve also provided in the ASCE 7 (2010) Commentary, figure C26.5.1. This curve describes the relation between the wind speed averaged over t seconds, and the mean hourly wind speed at reference height (10 m). This

is used in order to alleviate the effect of using the 3-sec reference wind speed in ASCE 7 (2010), as opposed to the mean hourly and 10-minute wind speed in NBCC (2010) and EN 1991-1-4 (2005), respectively. Thus, the ASCE 7 (2010) and EN 1991-1-4 (2005) reference wind speeds were multiplied by 1.51 and 1.06, respectively in order to be comparable with the experimental and NBCC 2010 values based on a mean-hourly wind speed. The results were presented in terms of shear coefficient and equivalent eccentricity estimated in transverse direction as per the following equations:

$$C_V = \frac{\text{Base shear force}}{0.5\rho\, V_H^2\, B\, H} \tag{1}$$

where ρ = air density (kg/m^3); and V_H = mean wind velocity at eave height (m/s).

$$e\,(\%) = \frac{\text{Base torsional moment}}{L * \text{Base shear force}} \tag{2}$$

It is also important to compare the magnitude of the torsional moment estimated for the three low-rise buildings based on the application of the wind load patterns introduced (simplified and detailed methods) in the standards considered with the past wind tunnel results. The estimated torsional moment is normalized to get the torsional coefficient according to:

$$C_T = \frac{\text{Base torsional moment}}{0.5\rho\, V_H^2\, B\, L\, H} \tag{3}$$

Comparisons among ASCE 7 (2010), NBCC (2010), and EN 1991-1-4 (2005) for three low building geometries are presented. Figure 3.1 shows the results for torsional loads case, maximum torsional moment and the corresponding shear. These values are estimated by applying the static/envelope method assigned for low-rise buildings in ASCE 7 (2010) and NBCC (2010) respectively, in addition to the analytical method in EN 1991-1-4 (2005). As clearly shown, significant differences are found among the three national codes/standards in evaluating the torsional moment, whereas smaller differences are found in evaluating corresponding shear forces. The distribution of wind loads introduced in this load case (maximum torsion and the corresponding shear force) is also very different in these codes. ASCE 7 (2010) introduces equivalent eccentricity about 17% of the building length while the NBCC (2010) and EN 1991-1-4 (2005) have eccentricities about 4%, and 8% of the building length, as Figure 3.1 clearly shows. The results show that ASCE 7 (2010) torsional moment estimated for buildings with aspect ratios 2 and 3 are three times higher than those of NBCC (2010), and more than twice the torsional moments calculated by EN 1991-1-4 (2005) for buildings with aspect ratios 1 and 2. Clearly, NBCC (2010) provides significantly lower values for the torsional moment on the three low buildings compared to ASCE 7 (2010) and EN 1991-1-4 (2005).
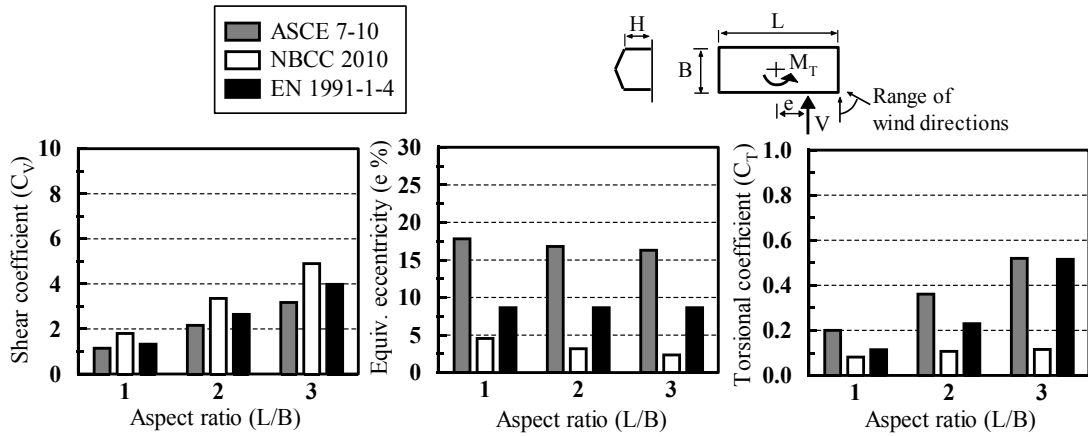
Figure 3.1: Static method – load case: maximum torsion and corresponding shear force

In Figure 3.2, comparisons among the three codes/standards are presented using the simplified methods (directional method in ASCE 7 (2010), static method for medium-rise buildings and the analytical method in EN 1991-1-4 (2005)) for the same buildings. Although significant differences of equivalent eccentricities have been found among the codes/standards, different values of the corresponding shear forces compensate and produce more comparable torsional moments with the exception of the Eurocode values being on the low side. For example, NBCC (2010) introduces the highest equivalent eccentricity value, which is equal to 25% of the building length but it also has the smallest value for the corresponding shear force. Thus, it appears the simplified method fixes an appropriate equivalent eccentricity depending on the value of shear coefficient in

order to produce comparable torsional moments for all cases. Although the torsional load cases required by the simplified methods in ASCE 7 (2010) and NBCC (2010) provide comparable torsional moments, the latter were generated by applying different wind loads with different eccentricities/distributions. Indeed, ASCE 7 (2010) requires applying 75% of the full wind loads (maximum shear force), while NBCC (2010) requires applying 50% of the total wind loads (see Figure 3.3). On the other hand, the torsional coefficients evaluated by EN 1991-1-4 (2005) for the same buildings are 0.10, 0.24, and 0.50, i.e. almost half of the torsional coefficients proposed by the ASCE 7 (2010) and NBCC (2010). This may be attributed to the very small equivalent eccentricity proposed by the EN 1991-1-4 (2005) which is about 8% of the building length compared to ASCE 7 (2010) (15%) and NBCC (2010) (25%).
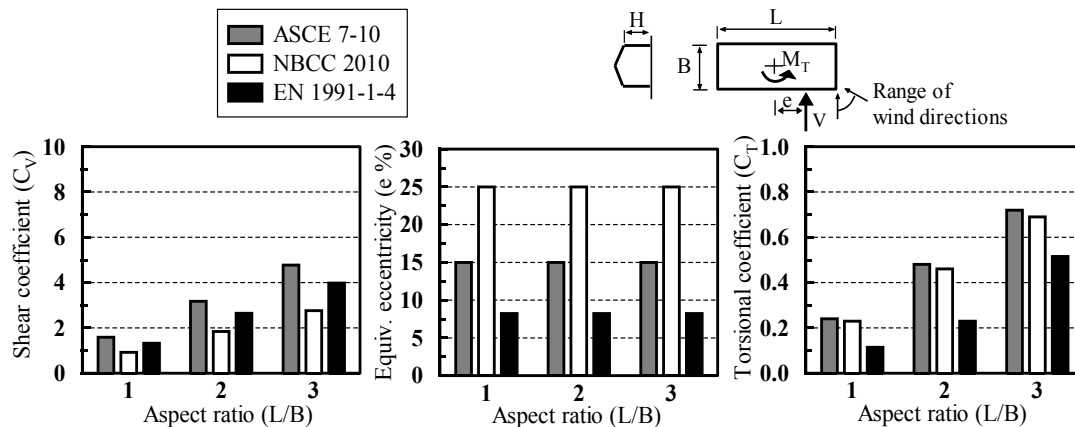
Figure 3.2: Simplified method – load case: maximum torsion and corresponding shear force
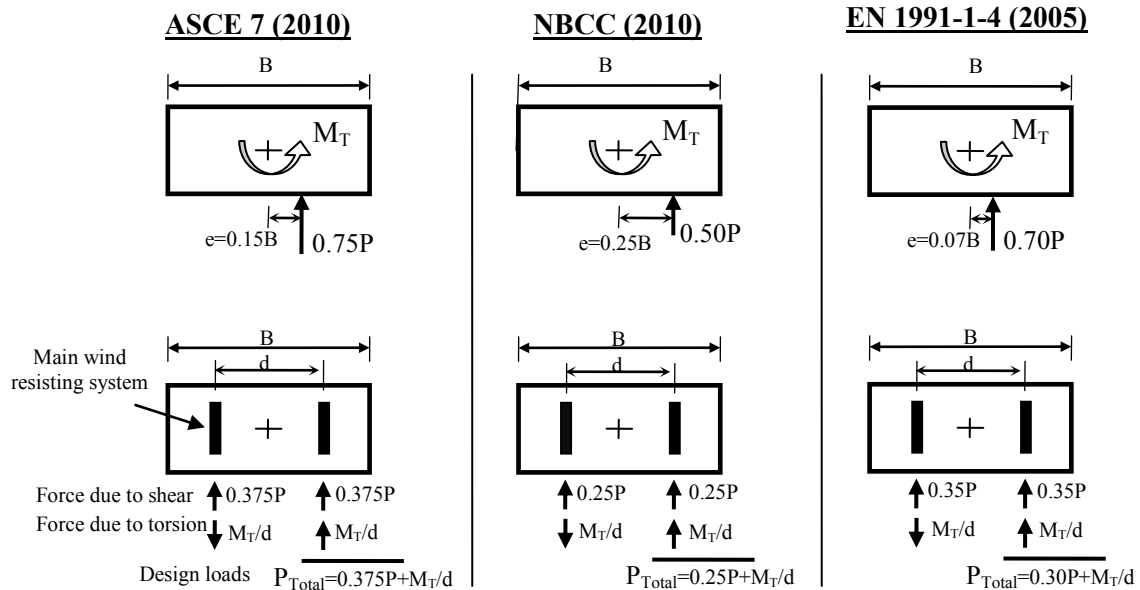
Figure 3.3: Comparison of the torsional load cases specified for low-rise buildings in ASCE 7 (2010), NBCC (2010), and EN 1991-1-4 (2005)

3.2.2 Medium-rise buildings

The National Building Code of Canada was the first adopted in its provisions the effect of wind-induced torsional loads on buildings. Since the early 70's and till 2005, the NBCC subcommittee on wind loads introduced the unbalanced wind loads or wind-induced torsion by removing 25% of the full wind load from any portion on building surfaces in order to maximize torsion according to the most critical design scenario states. This allowance for torsion is equivalent to applying the full design wind load at 3 or 4

percent of the building width. In the absence of detailed research in this area and based on some wind tunnel observations the 25% removal of the full wind load has been modified in the NBCC 2010 edition to a complete removal of the full wind loads from those areas that would lead to maximizing torsion. This allowance for torsion is equivalent to applying the full design wind load at 12.5 percent of the building width in case of loading half of the width of the building. On the other hand, the ASCE-7 subcommittee on wind loads has taken the initiative to add wind loading provisions for wind-induced torsional loads on buildings since the 1995 edition of the standard. These provisions were similar to the NBCC provisions at that time (i.e. removing 25% of the full wind loads on 50% of the projected area bounded by the extreme projected edge of the building). Since the 2002 edition, torsion load case was characterized by applying 75% of the full wind load with equivalent eccentricity 15% of the building dimension. This allowance for torsion is equivalent to applying the full design wind load at 11.25 percent of the building width.

In EN 1991-1-4 (2005), the non-uniform applied wind loads in torsion load case allow for torsional moment equivalent to applying the full design wind load with 6 percent eccentricity. Such differences in torsion provisions for medium-rise buildings in the current codes and standards are questionable. Furthermore, the torsional load case is always described in wind provisions on the basis of the full wind load case (shear load case). Although, the fluctuating wind forces allow torsion to develop even for buildings of symmetric shape and wind perpendicular to their facade. Therefore, the oversimplifications for the shear load case implicit in the wind provisions need to be examined.

As with the low-rise building cases, Figure 3.4 compares the code/standard provisions for three medium-rise buildings (B = 30 m, h = 60 m) with horizontal aspect ratios (L/B =1, 2, and 3) located in suburban terrain. For these buildings, the directional-part I method (ASCE 7 (2010)) assigned for enclosed, partially enclosed, and open buildings of all heights was applied. The side wall external pressure coefficient (C_p) was estimated according to figure 27.4-1. Suburban terrain exposure B was considered, with the directional factor (K_d) and the gust factor (G) taken as 1 and 0.85, respectively. Maximum torsion and corresponding shear were estimated by applying 75% of the full wind load and equivalent eccentricity of 15% of building width, as indicated in Case 2 in figure 27.4-8. The external pressure estimation by the simplified method (NBCC 2010) is taken from figure I-16, Commentary I, and the gust factor (Cg) was taken as 2. The partial load case was implemented by completely removing the full wind loads from half of building faces to estimate maximum torsion and corresponding shear as specified in Case B in figure I-16, Commentary I. In the Eurocode 2005, the same approach used for low-rise buildings has been applied for medium-rise buildings. The terrain factor roughness (C_r) was calculated for terrain category III which is expressed in Eurocode 2005 as a peer for the suburban terrain exposure.

As can be clearly seen from the figure, NBCC (2010) estimates torsional coefficient 40% and 60% higher than the proposed values in the ASCE 7 (2010) and the EN 1991-1-4 (2005), whereas the corresponding shear in the three sets of provisions are different. Moreover, significant differences of equivalent eccentricities imply significant differences in wind load distributions. Applying different loads with different eccentricities yield to different torsional moments. These discrepancies in the definition

of the torsional loads case in these codes/standards -in addition to neglecting torsion totally in some other international codes/standards- dictate the urgent need for examining experimentally, the wind-induced torsion forces on low- and medium-rise buildings.
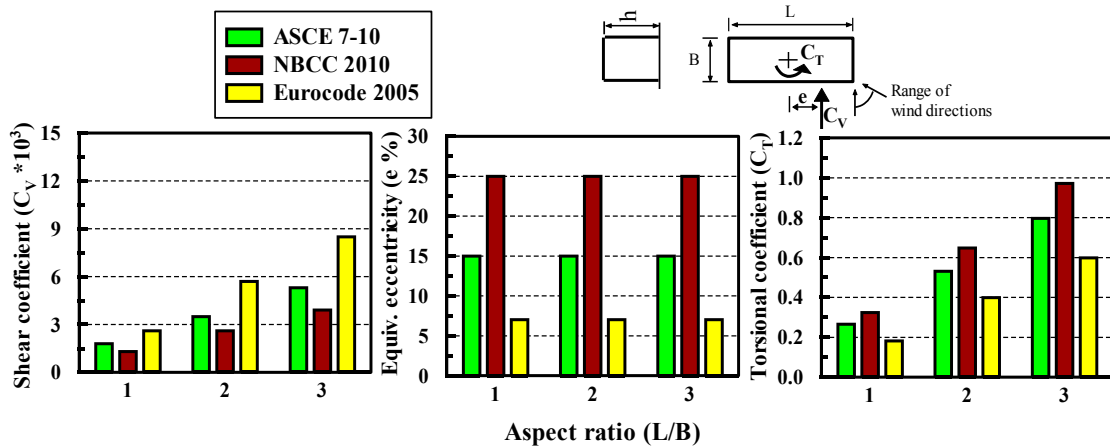
Figure 3.4: Comparison of torsion load case in wind code and standard provisions for three medium-rise buildings with aspect ratios (L/B) = 1, 2, and 3

Summary:

There has been a clear discrepancy between different provisions available in current codes and standards in quantifying the value of wind-induced torsion for the design of low- or medium-rise buildings. For instance, ASCE 7 (2010) introduces two load cases in the envelope method to estimate torsion, namely: maximum torsion with corresponding shear and maximum shear with corresponding torsion. NBCC (2010) specifies only one load case in the static method assigned for low-rise buildings to

evaluate maximum shear as well as maximum torsion. Similar to ASCE 7 (2010), the European code (EN 1991-1-4, 2005) introduces two load cases to evaluate the design shear and torsional loads to be used for buildings with all heights. Wind-induced torsion provisions in the three codes/standards are also different for medium-rise buildings. ASCE 7 (2010) requires introducing 75% of the full wind load with eccentricity of 15% of the facing building horizontal dimension for evaluating maximum torsion. On the other hand, NBCC (2010) requires for design of medium-rise buildings to apply 50% of the full wind load on half of the along wind wall in order to predict the maximum torsion. Non-uniform wind loads were simulated by applying triangular loading in the EN 1991-1-4 (2005). The non-uniform wind loads applied for torsion, in EN 1991-1-4 (2005), allow for torsional moment equivalent to applying the full design wind load with 6% eccentricity. When these provisions were compared for three low- and medium-rise buildings with different aspect ratios (L/B= 1, 2, 3), significant differences were found in evaluating design wind loads. Notwithstanding these differences among these wind load provisions, it was alarming to note that other codes/standards, such as the Australian standard, do not address torsion altogether in the design requirements for low- and medium-rise buildings.

CHAPTER 4
WIND TUNNEL METHODOLOGY

Wind tunnel studies have been accepted as a reliable tool for predicting wind loads on buildings (Davenport et al. 1976). Wind tunnel tests are also deemed effective due to the fact that field tests are time consuming and costly. This was emphasized by the good agreement obtained between the measured wind loads in the wind tunnels and the field tests. Unlike wind tunnel tests, the wind flow characteristics cannot be controlled in real environment. A pioneer study conducted by Jensen (1958) led to a significant contribution in wind engineering, which is the correction of the simulation of the atmospheric wind in the boundary layer wind tunnel (BLWT). The friction between the wind flow and the built-up land surface is treated by Jensen number (H/z_o), i.e. the ratio between the building height, H, and the effective aerodynamic surface roughness of the flow, z_o. Since then, a subsequent revolution in wind engineering studies started, however, one of the main ongoing challenges in wind tunnel testing is to achieve adequate similarities for buildings and the turbulent wind flow. The geometric scale of the atmospheric boundary layer, the geometric similarity of the structural shape, an accurate modeling of building features, and the match between the frequency response of the available pressure measurement system and the desired full-scale frequency response should be considered. Another similarity fact is related to the Reynolds number. Although the full-scale Reynolds number cannot be achieved in the wind tunnel, the very

sharp edges for the building models could be used for ensuring the place of the separation flow points around the building model. However, to minimize local viscous effects, it is important to attain a minimum value of Reynolds number. Generally, distortion of the flow and the resulting variation in pressure distributions are considered negligible for Reynolds numbers in excess of 10^4 (Isyumov, 1982; ASCE 1999).

4.1 WIND TUNNEL SETTING

In order to achieve the objectives of this research, the experimental phase were carried out in the boundary layer wind tunnel of Concordia University. The working section of the tunnel is approximately 12.2 m long x 1.80 m wide. Its height is adjustable and ranges between 1.4 and 1.8 m to maintain negligible pressure gradient for different simulated exposures along the test section. A turntable of 1.2 m diameter is located on the test section of the tunnel and allows testing of models for any wind direction (see Figure 4.1). An automated Traversing Gear system provides the capability of probe placement to measure wind characteristics at any spatial location around a building model inside the test section. A geometric scale of 1:400 was chosen. This meets the minimum requirements for capturing the most important variables of the atmospheric boundary layer under strong wind conditions (Stathopoulos 1984).

Figure 4.1: Boundary layer wind tunnel at Concordia University (Front view)

4.2 VELOCITY MEASUREMENTS AND TERRAIN SIMULATIONS

Open country and urban terrain exposures were simulated in the wind tunnel. The flow approach profiles of mean wind velocities and turbulence intensities were measured using a 4-hole Cobra probe (TFI) for the simulated terrain exposures (see Figure 4.2). The wind velocity at free stream was 13.6 m/s for open and urban exposures. The power law exponent α of the mean wind velocity profile for open country exposure was set at α = 0.15 and 0.30 for urban terrain exposure. Typical spectra of the longitudinal turbulence component measured by Stathopoulos (1984) at sixth of the boundary layer depth and compared with the well-known Von Karman's equation and Davenport's empirical expression – Figure 4.3. The length scale of the turbulence in the longitudinal direction was estimated as 112 m.

38
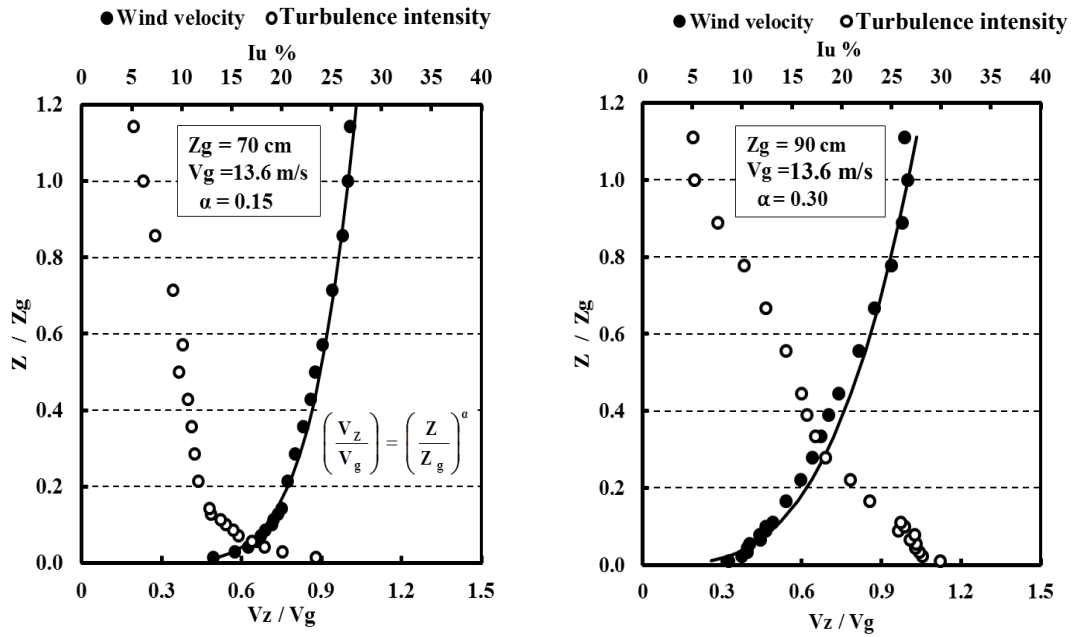
Figure 4.2: Wind tunnel velocity and turbulence intensity profiles for open and urban terrain exposures
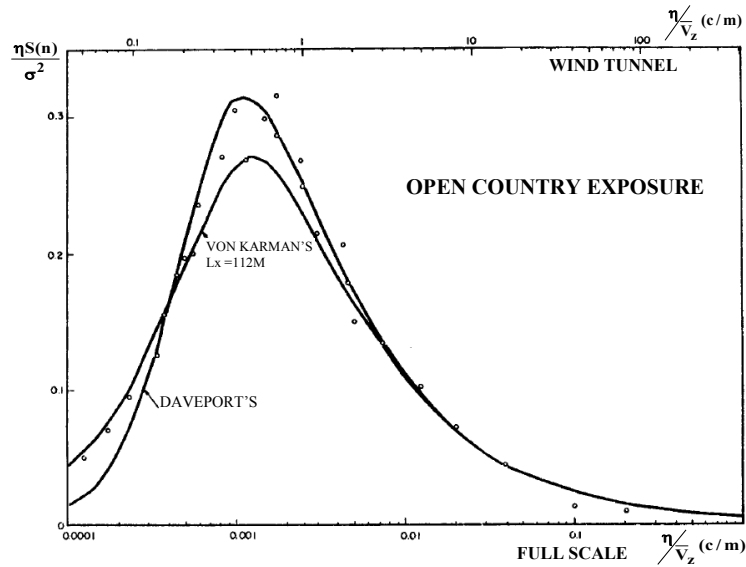
Figure 4.3: Spectra of the longitudinal turbulence component at $Z/Z_g = 1/6$ (Stathopoulos 1984)

4.3 BUILDING MODELS

The current study used a low-rise building model with three gabled roof angles (0°, 18.4° and 45°) and full-scale equivalent horizontal dimensions 61x39 m –see Figure 4.4. These particular building dimensions were used mainly because data on wind-induced pressures and forces (but not torsion) were available from previous studies, thus comparisons with previous measurements would enrich the current study. An extension part was manufactured and connected to the low rise-building model to test medium-rise buildings, as it can be seen in Figure 4.5. The 1:400 building model with a flat-roof was equipped by a total 146 pressure taps on its side walls and 192 for the gabled-roof buildings tested (18.4° and 45°). The flat-roof does not have any pressure taps, since uplift forces do not contribute to torsion or horizontal shear forces. Focuses were directed towards the effect of roof slope, building height, and wind directions on the wind-induced torsional loading, as it is believed that would be very useful for structural engineering practitioners and code development authorities. It was also decided to use rectangular building models of different heights but with a single (L/B) aspect ratio, namely 1.6. This was selected because such a ratio is typically representative of most of the low- and medium-rise buildings, further to being complementary of what has been used to the limited number of previous studies of wind-induced torsion available in the literature. The building model was tested at different heights, by sliding it downwards in a tightly fit slot in the turntable, such that it represents different actual buildings with heights 6, 12, 20, 30, 40, 50 and 60 m. Model dimensions and the tested building heights are given in Table 4.1. In this study, all tested buildings were assumed to be structurally rigid and follow the limitations stated in the three wind load codes/standards (NBCC (2010),

ASCE 7 (2010), EN 1991-1-4 (2005)). Buildings were tested in open and urban exposures for different wind directions.
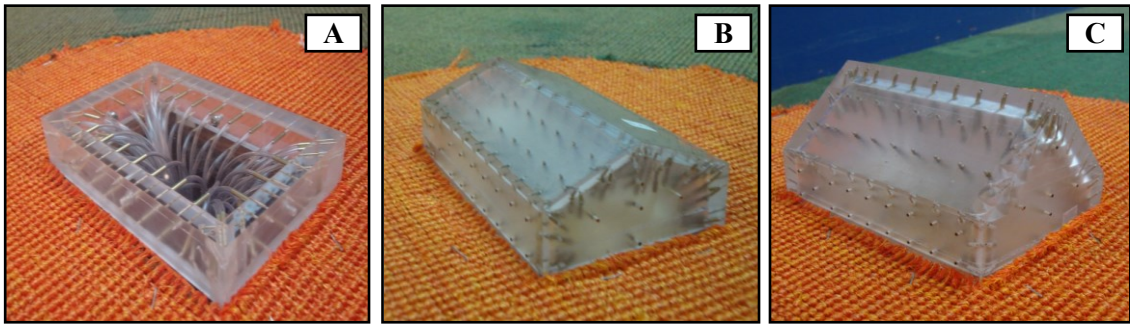
Figure 4.4: Low-rise building models: A) Building with a flat-roof, B) Building with 18.4$^{°}$ roof angle, C) Building with 45$^{°}$ roof angle
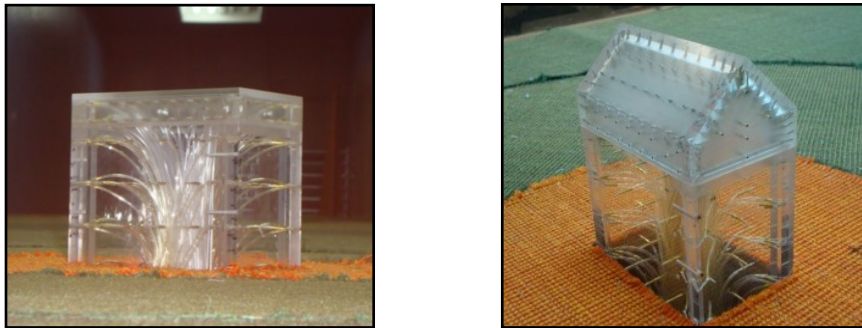
Figure 4.5: Medium-rise building models: A) Building with a flat-roof, and B) Building with 45$^{°}$ roof angle

Table 4.1: Model dimensions and building heights tested for all roof slopes

Building	Dimensions	
	Scaled (1:400, mm)	Actual (m)
Width (B)	97.5	39
Length (L)	152.5	61
Tested eave heights (H)	15	6
	30	12
	50	20
	75	30
	100	40
	125	50
	150	60

4.4 PRESSURE MEASUREMENTS

The pressure measurements on the models were conducted using a system of miniature pressure scanners from Scanivalve (ZOC33/64Px) and the digital service module DSM 3400. Figure 4.6 shows the experimental instrumentations and the connection among the different devices (i.e. the building model, thermal ZOC units, pitot tube, air supply and pressure scan computers). Figures 4.7a and 4.7b show thermal units (T.U. ZOC 64) used to measure wind pressure and the pressure scan computer (DSM 3400). A standard tubing system was used in these measurements, in order to minimize the Gain and Phase shifts of pressure signals due to Helmholtz's resonance effects. Corrections were made by using traditional restrictors properly calibrated. The pressure measurement tubes have an outer and inner diameter of 2.18 and 1.37 mm respectively, their length is 55 cm and restrictors are installed at 30 cm from the location of the pressure tap. As the tubing system was used in these measurements, the Gain and Phase shifts of pressure signals due to Helmholtz's resonance effects were corrected by using traditional restrictors.

The characteristics of the boundary layer flow developed by the wind tunnel essentially dictate the appreciate length and velocity scales for a rigid pressure model. These are approximately 1:400 and 1:3 respectively. Thus the time scale is typically of the order of 1:133. All measurements were synchronized with a sampling rate of 300 Hz on each channel for a period of 27 sec (i.e. about one hour in full scale). The frequency response of the pressure measurement system is capable of modeling full scale fluctuations up to about 2.27 Hz. It is well known that the mean wind speed has the tendency to remain relatively steady over smaller periods of time (i.e. 10 minutes to an hour) assuming stationarity of wind speed, as reported by Van der Hoven (1957). This period is also suitable to capture all gust loads, which may be critical for structural design. Since building models are symmetric in both directions and located in open terrain exposure, the tested wind directions were limited to the interval of 0° to 90°. Figures 4.8a and 4.8b show pictures for the models during the connecting process of the pressure tubes and their restrictors. Figures 4.9a and 4.9b show the ZOC thermal units and their connected to the building model underneath the wind tunnel and during the test.
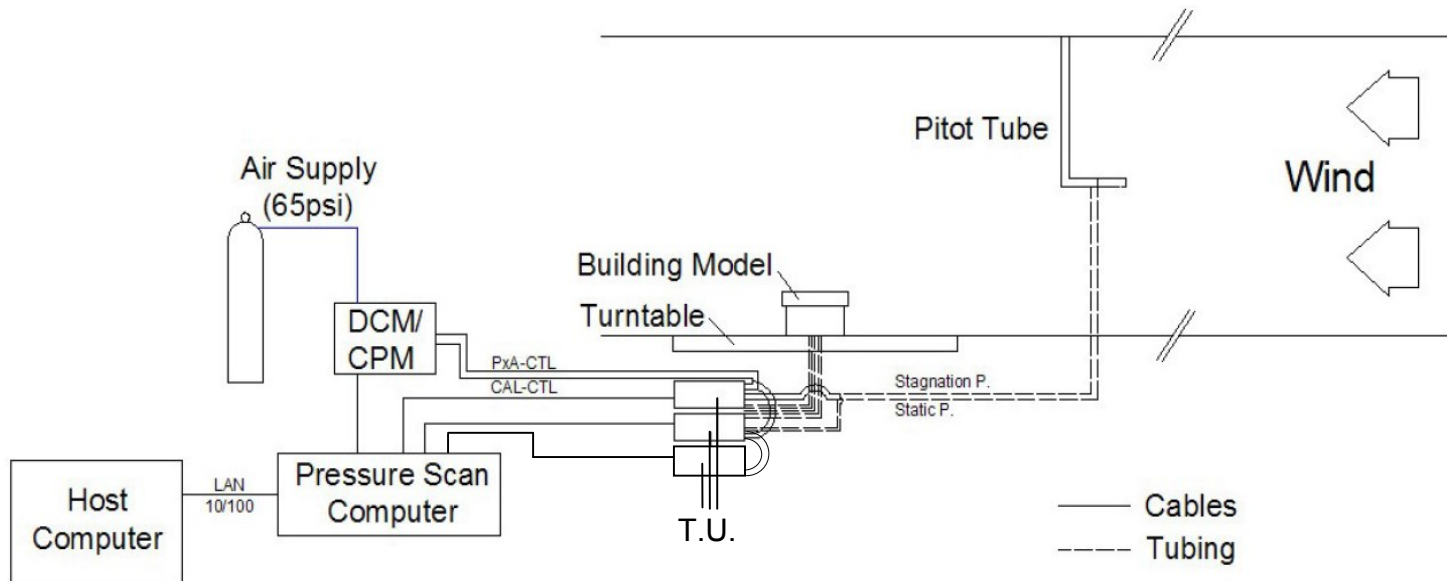
Figure 4.6: Instrumentation schematic of the wind tunnel experiments (modified –Zisis (2006))

Figure 4.7: Pressure measurement equipment a) Thermal units (T.U. ZOC 64) b) Pressure scan computer (DSM 3400)
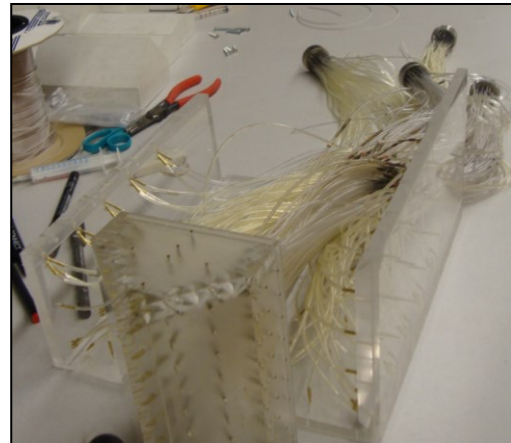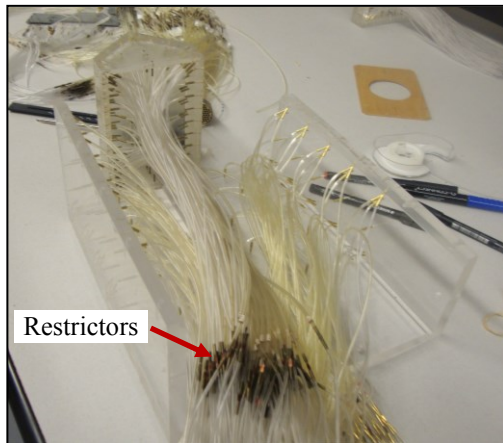
Restrictors

Figure 4.8: Tubing installation and the restrictors
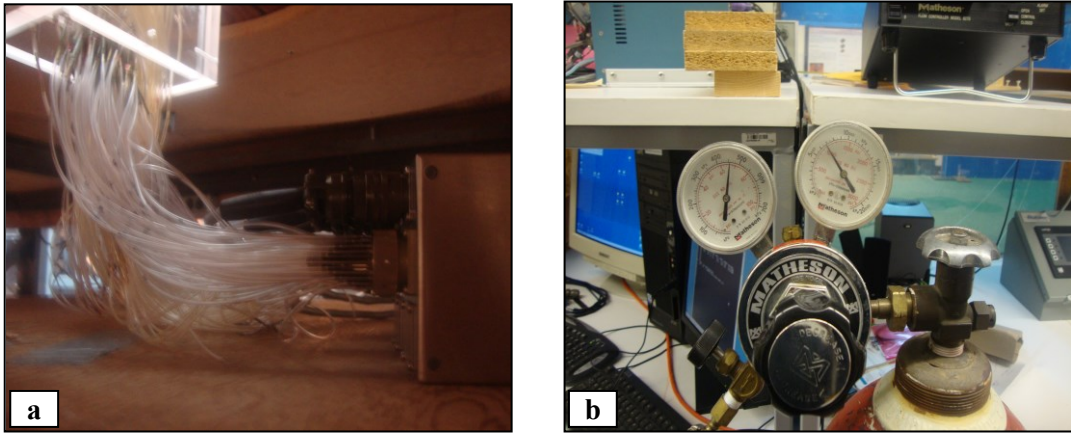
Figure 4.9: Part of pressure instrumentation a) tube connections with the ZOC units b) air pressure regulator connected to the air supply

4.5 ANALYTICAL APPROACH

Figure 4.10 shows a schematic representation of external pressure distributions on building envelope at a certain instant, the exerted shear forces, F_X and F_Y, along the two orthogonal axes of the buildings, as well as the torsional moment, M_T, at the geometric centre of the building. Pressure measurements are scanned simultaneously. The instantaneous wind force at each pressure tap is calculated according to:

$$f_{i,t} = p_{i,t} \times A_{\text{effective}} \qquad\qquad f_{j,t} = p_{j,t} \times A_{\text{effective}} \qquad\qquad (1)$$

where $p_{i,t}$, and $p_{j,t}$ are instantaneous pressures measured at each pressure tap. The wind forces exerted at pressure tap locations in X- and Y-directions are noted by $f_{i,t}$ and $f_{j,t}$, respectively.
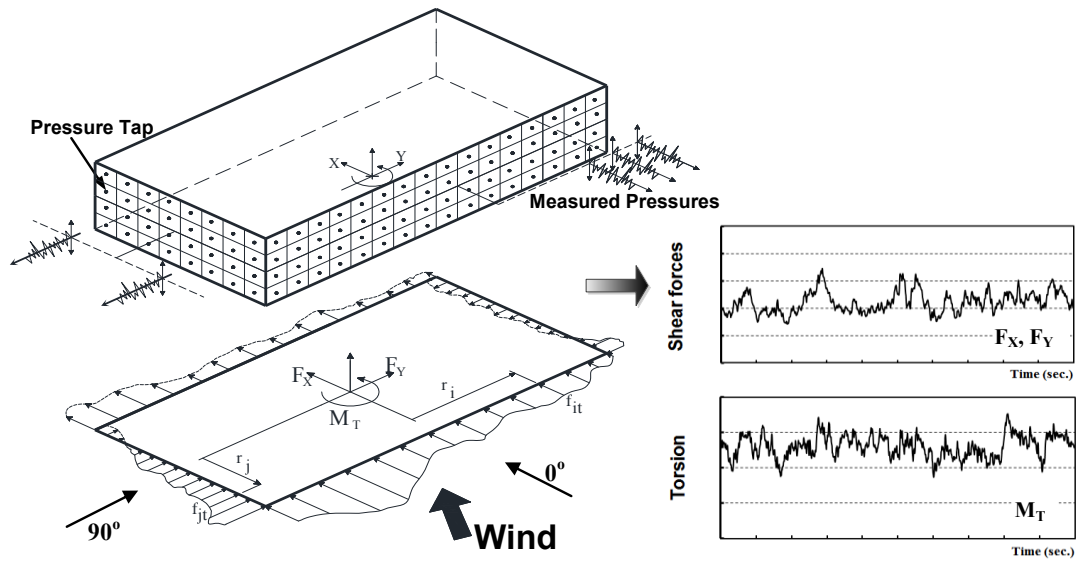
Figure 4.10: Measurement procedure for horizontal wind forces, F_X and F_Y, and torsional moment, M_T

For each wind direction, the horizontal force components in X- and Y-directions and the total base shear are evaluated according to:

$$F_X = \sum_{i=1}^{N} f_{i,t} \qquad F_Y = \sum_{j=1}^{M} f_{j,t} \qquad V = \sqrt{F_X^2 + F_Y^2} \qquad (2)$$

where N and M are the numbers of pressure taps on the longitudinal and transverse directions, respectively. It should be noted that in order to compare easily the results of this study with design load cases stated in the NBCC wind load provisions, shear coefficients where referred to be in X- and Y-directions or in transverse- and longitudinal-directions, as can be seen in Figure 4.11. This is different from previous studies expressing their results in terms of drag and lift coefficients. In this study, the torsional moment is estimated as follows:

$$M_T = \sum_{i=1}^{N} f_{i,t} * r_i + \sum_{j=1}^{M} f_{j,t} * r_j \qquad (3)$$

where r_i and r_j are the perpendicular distances between the pressure taps and the building center in X- and Y-directions, respectively.

All these forces are normalized with respect to the mean dynamic wind pressure at the mean roof height as follows:

$$C_{Sx} = \frac{F_X}{q_h B^2} \qquad\qquad C_{Sy} = \frac{F_Y}{q_h B^2} \qquad (4)$$

where q_h = mean dynamic wind pressure (kN/m^2) at mean roof height h (m), B = smallest horizontal building dimension (m). The torsional coefficient, C_T, and equivalent eccentricity, e, are evaluated based on:

$$C_T = \frac{M_T}{q_h B^2 L} \qquad\qquad e = \frac{M_T}{V} \qquad\qquad (5)$$

where L= largest horizontal building dimension
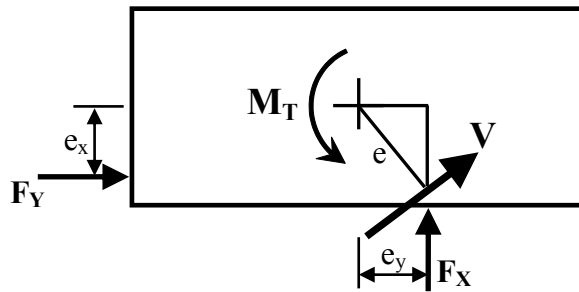
Figure 4.11: Resultant and wind force components along with the eccentricities in transverse (X) and longitudinal (Y) directions

It is acknowledged that different normalization factors for shear and torsion coefficients have been used in the literature. However, the definitions used herein were

selected for better presentation of the effect of building height on the variation of shear and torsional coefficients for all tested buildings.

In addition, for the scope of comparisons with the NBCC and ASCE 7 wind load provisions, eccentricity and torsional coefficient were also calculated in transverse direction, as follows:

$$e_y(\%) = e \times \frac{F_X}{V} \times \frac{1}{L} \times 100 \tag{6}$$

$$C_{Tx} = C_{Sx} \times e_y \tag{7}$$

Similarly, the eccentricity and torsion coefficient in longitudinal direction were evaluated based on:

$$e_x(\%) = e \times \frac{F_Y}{V} \times \frac{1}{B} \times 100 \tag{8}$$

$$C_{Ty} = C_{Sy} \times e_x \times \frac{B}{L} \tag{9}$$

All peak shear and torsional coefficients ($\left|C_{Sx}\right|_{Max.}, \left|C_{Sy}\right|_{Max.}, \left|C_T\right|_{Max.}, \left|C_{Tx}\right|_{Max.}, \left|C_{Ty}\right|_{Max.}$) were considered as the average of the maximum ten values occurring within a 1-hr full-

scale equivalent time history of the respective signal. This approach has been considered as a good approximation to the mode value of detailed extreme value distribution and it has been used in previous wind tunnel studies. Recently, in a similar approach used by Keast et al. (2012), the peaks were evaluated as the average of the 10 highest values from 10 one-hour equivalent samples. Although the two approaches are not identical, comparison between the two methods has yielded similar shear and torsion coefficients of buildings tested in similar experimental conditions, as it will be presented later. The corresponding shear force $(|C_{Sx}|_{corr.}, |C_{Sy}|_{corr.})$ and torsion $(|C_T|_{corr.}, |C_{Tx}|_{corr.}, |C_{Ty}|_{corr.})$ coefficients were evaluated as the average of ten values occurring simultaneously with the ten peaks used to define the respective source maximum value.

4.6 REPEATABILITY:

It was also important to check the stability of the measurements and that it does not change from time to time. For this reason, the test measurements were taken for a rectangular configuration in Dec. 2011 and repeated for the same case in May 2012. Figure 4.12 shows the peaks and mean torsional coefficient values measured in these two different tests, 6 months apart, for a 20-m building located in open terrain exposure. This comparison shows that the repeatability is very good. Similarly, the measurements for the shear force coefficients in x- and y-axes show also good agreement as indicated in Figures 4.13 and 4.14. Clearly, the differences are may be considered negligible. Such a good agreement is typical for the other tested cases.
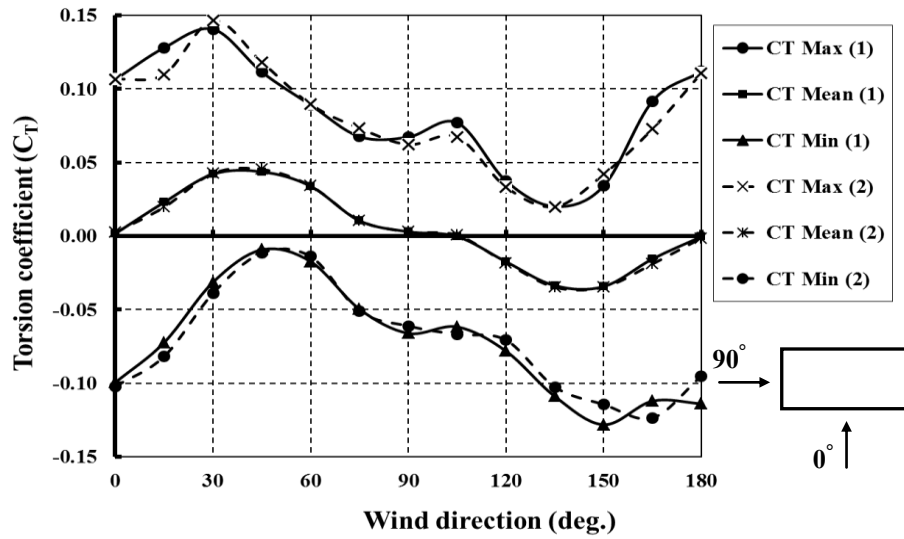
Figure 4.12: Torsional coefficient (C_T) measured in two different tests for the 20m-building ($\alpha=0.15$)
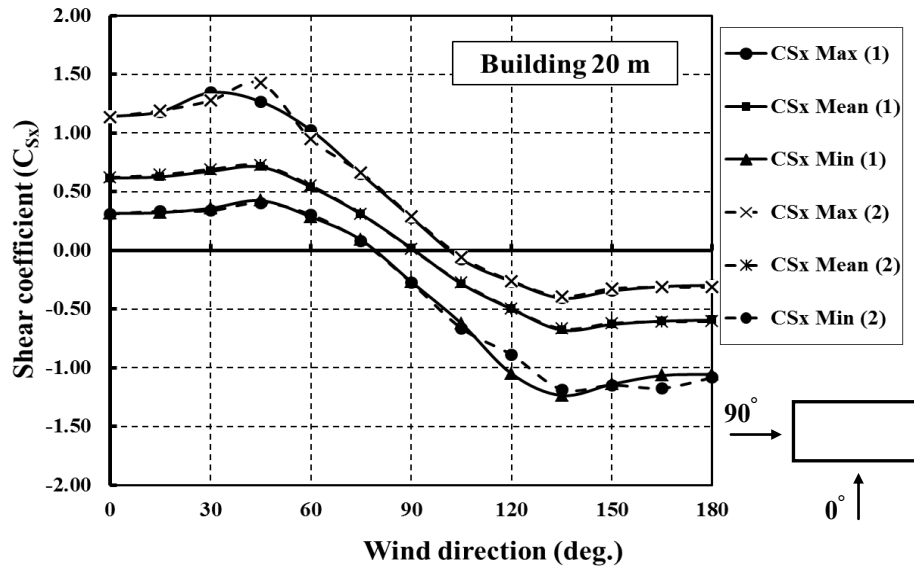
Figure 4.13: Shear coefficient in X-direction (C_{Sx}) measured in two different tests for the 20m-building ($\alpha=0.15$)
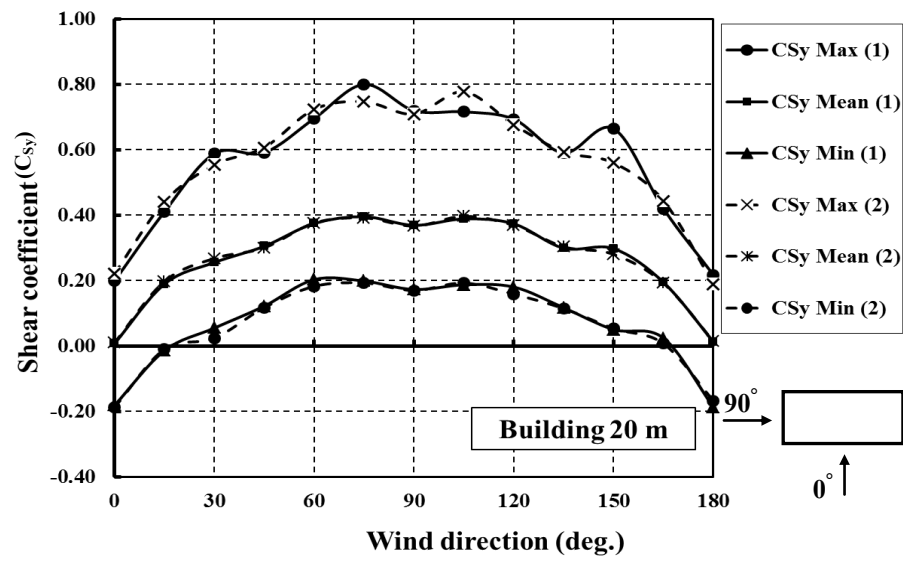
Figure 4.14: Shear coefficient in Y-direction (C_{sy}) measured in two different tests for the 20m-building (α=0.15)

CHAPTER 5

EXPERIMENTAL RESULTS AND DISCUSSION

In this chapter, wind tunnel experimental results will be presented including the effects of terrain exposure, roof slop, and building height on the generated shear and torsion coefficients. In addition, comparisons with previous reported studies and with the NBCC (2010) and ASCE 7 (2010) provisions were also conducted. Shear and torsional loads cases in transverse and longitudinal directions evaluated using wind tunnel, NBCC (2010) and ASCE 7 (2010) were compared for the design purpose of low- and medium-rise buildings.

5.1 WIND TUNNEL MEASUREMENT RESULTS

The three building models with gabled roof angles 0°, 18.4° and 45° were tested in open and urban terrain exposure for several wind directions at full scale eave heights ranging from 6 to 60 m. The evaluated torsion and shear forces were normalized by the mean dynamic wind pressure at the mean roof height (see Eqs. 3 and 4 in Chapter 4). Shear coefficients in X- and Y-axes along with the resultant shear force coefficient were evaluated for all the cases.

5.1.1 Effect of terrain exposure

Figure 5.1 shows the variation of the peak torsional coefficient with wind direction for all three buildings in open-country and urban terrain exposures. As can be seen from the figure, the maximum torsional moments occur for wind directions from 15° to 45° for all buildings. As a result of the building models having symmetric shapes, the evaluated mean torsions are zero for wind directions perpendicular to building faces, i.e. 0° and 90°. However, there are significant maximum and minimum torsional coefficients for these wind directions due to the natural lack of wind pressure correlation over the building envelope in the horizontal direction, as expected.

Table 5.1 presents the most critical values of shear coefficients evaluated in open and urban terrain exposures for all three buildings tested at full and half eave heights, while Table 5.2 presents the most critical values of torsional coefficients. The mean wind velocity at the mean roof height has been decreased by about 35% in urban than open terrain exposure. This is associated with increasing the turbulence intensity in urban terrain by about 33.5% in comparison with open terrain exposure. Thus, the shear and torsion measured in open terrain are higher than those in urban terrain. For instance, the ratios between the shear forces measured in open terrain to those measured in urban terrain exposure for buildings A, B, and C are 1.15, 1.23 and 1.10 respectively, for full building height while these ratios for torsional moments are 1.10, 1.23 and 1.12. On the other hand, the shear and torsional coefficients for the low-rise building models tested in urban terrain exposure are higher (about double) than those in open terrain exposure (see Tables 5.1 and 5.2). It may be concluded that buildings located in open terrain exposure are exposed to higher shear and torsional loads by about 10 to 25%. Therefore, the

current study focused more on the buildings in open terrain exposure as it would be more

critical for design load purposes.
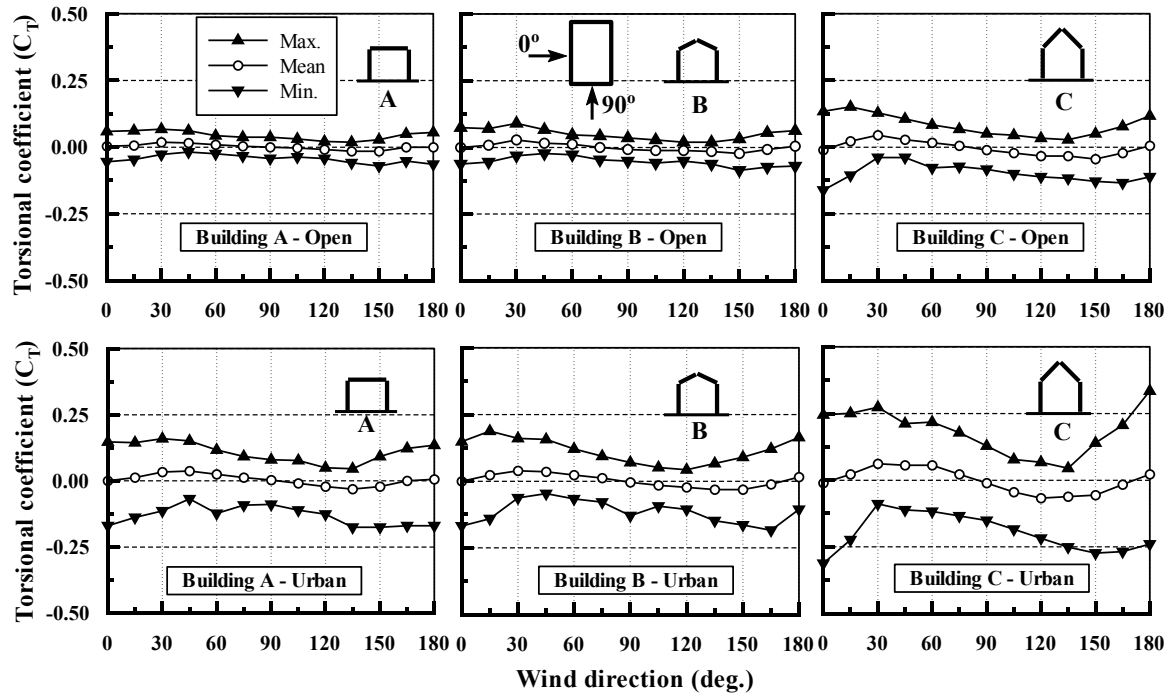
Figure 5.1: Torsional coefficients for the three buildings (A, B, and C) tested at full eave heights in open and urban terrain exposure

Table 5.1: Most critical values for shear coefficients (open and urban terrain exposures)

						Building B (18.4°)			Building C (45°)		
			X-dir.	Y-dir.	Total	X-dir.	Y-dir.	Total	X-dir.	Y-dir.	Total
Shear Coefficient	**Open terrain**	Full height	0.69	0.47	0.73	0.95	0.63	0.96	2.23	0.92	2.24
		Half height	0.33	0.22	0.33	0.60	0.32	0.62	1.80	0.67	1.80
	Urban terrain	Full height	1.82	1.09	1.70	1.96	1.26	1.99	4.60	1.67	4.61
		Half height	1.01	0.64	1.02	1.61	0.85	1.66	3.78	1.34	3.84

Table 5.2: Most critical values for torsional coefficients (open and urban terrain exposures)

			Building A (0°)	Building B (18.4°)	Building C (45°)
Torsional Coefficient	**Open terrain**	Full height	0.07	0.09	0.16
		Half height	0.03	0.05	0.13
	Urban terrain	Full height	0.18	0.19	0.33
		Half height	0.10	0.14	0.32

5.1.2 Effect of roof slope

Figure 5.2 shows the variation of peak shear coefficients (i.e. in X-, Y-direction, and resultant shear force), with wind direction for the three building models tested in simulated open-country exposure. For buildings A and B, the shear coefficients have almost similar values for most of the tested wind directions, while building C has significantly higher shear coefficient values. The maximum shear forces in X-direction occur for wind directions from $0°$ to $45°$; while in Y-direction when wind is almost perpendicular to building face, i.e. $90°$. It is also important to mention that increasing the number of pressure taps used in Y-direction to measure the pressure distributions will help obtaining more details about the variation of shear force in this direction. Although, the determination of the shear coefficient is important to propose equivalent wind loading, identification of horizontal distribution of these wind loads on building structural system still requires information about the torsional moment.

The shear and torsional coefficients for the building models have not been affected much by changing the roof slope from $0°$ to $18.4°$ for most wind directions, as shown in Figure 5.1 and 5.2. However, significant difference for shear coefficient has been noticed when roof angle was changed to $45°$. Increasing the roof slope leads to an increase of shear forces and torsional moments. At the same time, mean wind velocity and mean roof height are increased. In open terrain exposure, changing the roof angle from $0°$ to $45°$ for buildings tested at full eave height results in an increase of the shear coefficient by about 40% and the torsional coefficient by about 20%.
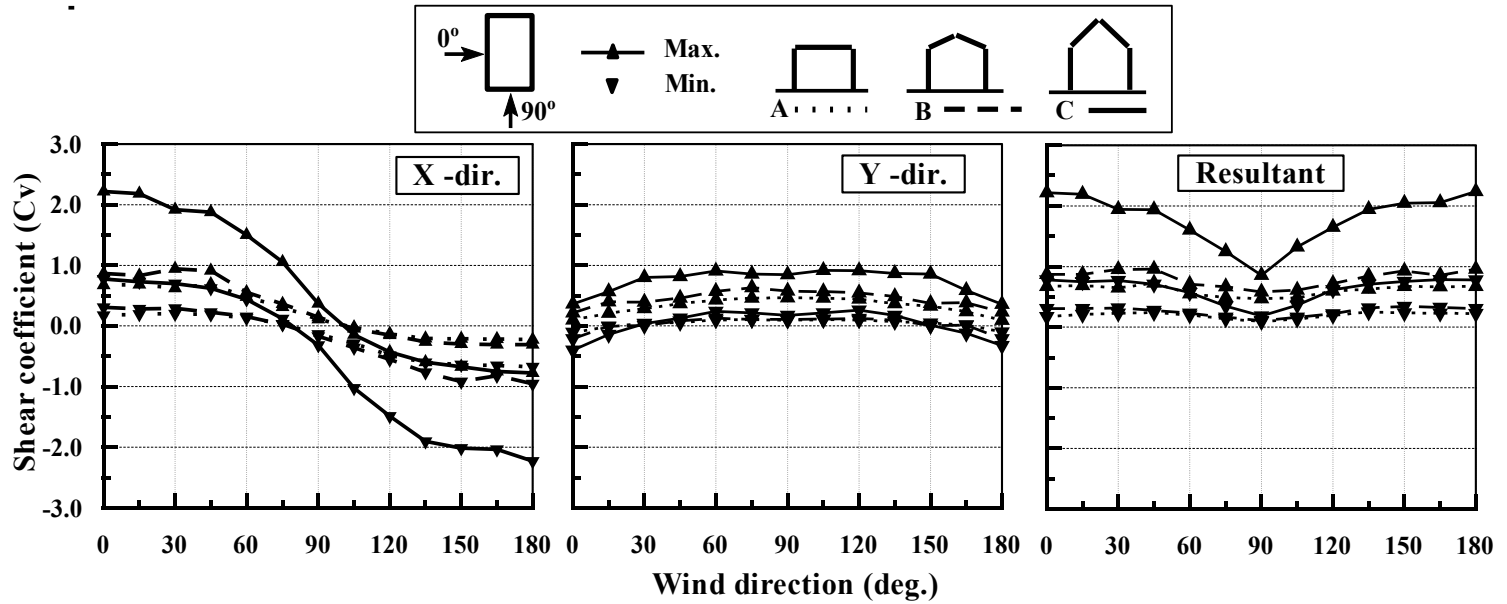
Figure 5.2: Shear coefficients in X direction, Y direction and their resultant for each building model in open terrain exposure

5.1.3 Effect of building height

The two buildings with $0^°$ and $45^°$ gabled-roof angles were tested in open terrain exposure at different full scale eave heights (H = 6, 12, 20, 30, 40, 50, and 60 m) for different wind directions ($0^°$ to $90^°$ every $15^°$ intervals). Figure 5.3 presents the variation of maximum torsion coefficient ($|C_T|_{Max}$) with wind direction for the two buildings tested at different heights. As can be seen from the figure, $|C_T|_{Max}$ has increased significantly when building height was increased from 6 to 60 m for both buildings with $0^°$ and $45^°$ roof angles. The lowest torsional coefficients are found for wind direction around $60^°$ for all heights. The $|C_T|_{Max}$ occurs for wind directions ranging from $15^°$ to $45^°$ for the first three buildings (6, 12, 20 m) while for the other heights, another peak torsional coefficient zone has been recorded for wind directions between $75^°$ and $90^°$. This may be attributed to different characteristics of wind flow interactions with buildings of heights lower than 20 m, particularly flow reattachment and 3-dimensionality compared to taller buildings. Further study for this matter is recommended.
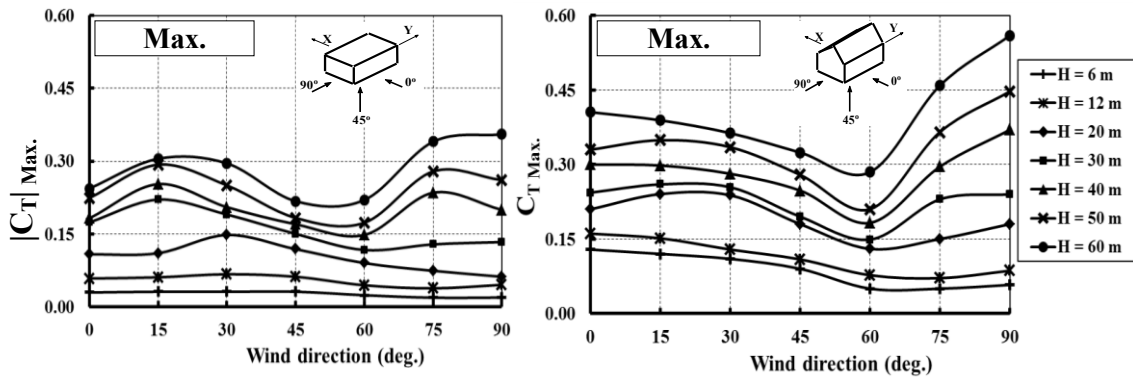
Figure 5.3: Variation of peak torsion coefficient ($C_{T\,Max.}$) with wind direction for the tested buildings

Figures 5.4 and 5.5 show the measured peak shear coefficients in X-direction, and Y-direction when the two buildings were tested at different eave heights for different wind directions. As expected, the shear coefficient in X-direction decreases when the wind direction varies from $0°$ to $90°$, as shown in Figure 5.4 On the other hand, for the same wind directions range the shear coefficient in Y-direction somewhat increases. The maximum shear force in the X-direction occurs for wind direction ranging from $0°$ to $45°$; whereas in the Y-direction for wind almost perpendicular to building face, ($75°$ to $90°$). The significant effect of increasing the building height and the roof slope on the generated shear forces is clear. Maximum shear force coefficient ($|C_{Sx}|_{Max}$) has increased by almost 3 and 2 times when the eave height increases from 20 to 60 m for the buildings with flat-roof and gabled-roof ($45°$), respectively. Changing roof angle from $0°$ to $45°$ results in increasing $|C_{Sx}|_{Max}$ by about 2.5 times for building with a 20 m eave height. This increase in $|C_{Sx}|_{Max}$ is smaller for higher buildings and reaches 1.5 for the 60 m high building. Thus, it is clear that the effect of increasing roof slope on the $|C_{Sx}|_{Max}$ decreases with increasing building height. This may be attributed to the reduction of the ratio of the inclined roof area facing wind relative to the total surface building area as the building height increases from 20 to 60 m. The $|C_{Sx}|_{Max}$ has not been affected much by changing wind incidence from $0°$ to $45°$ while rapid decrease was noticed from $45°$ to $90°$. Similar to the shear force in X-direction, the maximum shear force coefficient in Y-direction ($|C_{Sy}|_{Max}$) has increased significantly (about 2.8 times) by increasing the height of the flat-roofed building from 20 to 60 m and by about 1.8 times for the gabled-roof ($45°$) building. Changing roof angle from $0°$ to $45°$ results in doubling $|C_{Sy}|_{Max}$ for building with eave height of 20 m, yet it resulted in 30% increase only for the 60 m high building. The

maximum shear coefficient in Y-direction has not been affected much by changing wind direction from 45° to 90° while rapid decrease occurred from 45° to 0°, as expected.
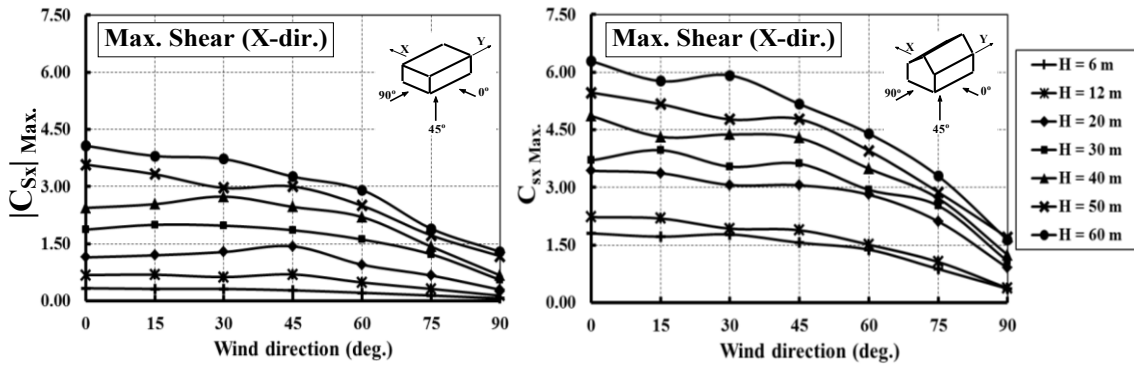
Figure 5.4: Variation of peak shear coefficient ($C_{Sx\ Max.}$) with wind direction for the tested buildings
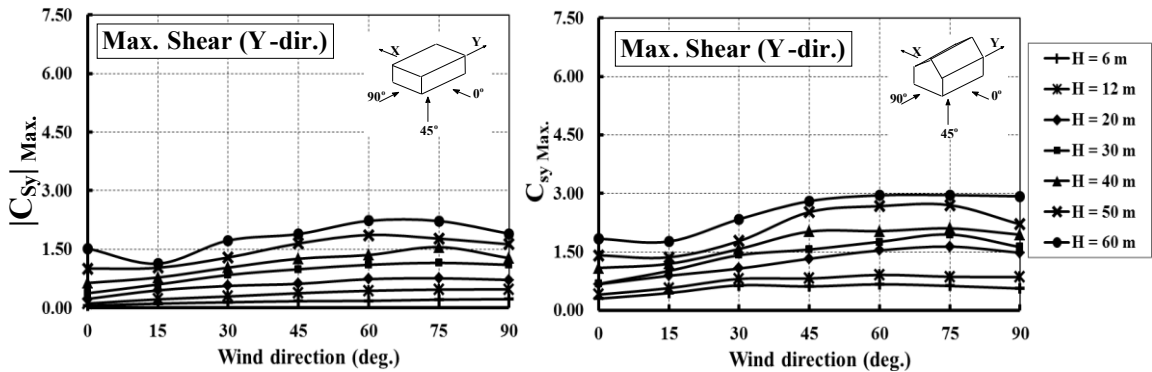
Figure 5.5: Variation of peak shear coefficient ($C_{Sy\ Max.}$) with wind direction for the tested buildings

5.2 COMPARISON WITH PREVIOUS STUDIES

A comparison of the results with those from a previous study by Isyumov and Case (2000) for a building with dimensions L = 19.5 x B = 9.75 x H = 4.88 m was made using the wind tunnel measurements in the current study for a modeled full-scale building with L = 61 x B = 39 m x H = 6 m. The two low-rise buildings have gabled roof 4:12 and located in open terrain exposures. Table 5.3 shows the experimental conditions and building configurations. The current study used the same definition of the torsion coefficient used in Isyumov and Case (2000) study. Torsional coefficient was defined as C_T = Base torsion/ (q_H BLH) where q_H = mean dynamic wind pressure at eave height, B = width, L = length, H = eave height. The two torsional coefficient evaluated in the two studies are in a very good agreement considering the differences in the geometries and scales.

Table 5.3: Comparison with Isyumov and Case (2000)

	Isyumov and Case (2000)	Current study
Building	(L = 19.5 x B = 9.75 x H = 4.88) m	(L = 61 x B = 39 x H = 6) m
Gabled roof slope	4:12	4:12
Model scale	1:100	1:400
Building model	(195x97.5x48.8) mm	(152.5x97.5x15) mm
Terrain exposure	Open country (α= 0.16)	Open country (α= 0.15)
Wind direction	$\perp$ building dimension (L= 19.5 m)	$\perp$ building dimension (L= 61 m)
Torsional coefficient ($C_{T Max.}$*)	0.48	0.42

*Where Torsional coefficient C_T = Base torsion/ (q_H BLH); q_H = mean dynamic wind pressure at eave height,
 B = width, L = length, H = eave height

Another comparison was made with Tamura et al. (2003) study for two low-rise buildings but with flat-roof. Building configurations and wind tunnel experimental conditions are given in Table 5.4. The two buildings were tested in open and urban terrain exposures. In this comparison, the definitions of torsional and shear coefficients in the Tamura et al. (2003) study were followed. The torsional coefficient was considered as C_T = Base torsion/(q_H LHR) where; $R=\sqrt{(L^2+B^2)}/2$, B = smaller horizontal building dimension, and shear coefficient Cv= Base shear/(q_H LH). For this comparison also, only wind direction perpendicular to the largest horizontal building dimension was considered due to the lack of data for other cases in Tamura et al. (2003). Table 5.5 show the comparison results for the shear and torsion coefficients evaluated by the two studies. The comparison show good agreement between the two studies for the evaluated shear and torsion coefficients.

Table 5.4: Comparison with Tamura et al. (2000)

	Tamura et al. study	Current work
Buildings	(L = 42.5x B = 30 x h = 12.5) m	Building (L = 61x B = 39x h = 12) m
Model Scales	1:250	1:400
Building models	(170x120x50) mm	(152.5x97.5x30) mm
Terrain exposures	Urban terrain (α= 0.25) & Open country (α= 0.16)	Urban terrain (α= 0.3) & Open country (α= 0.16)
Wind direction	$\perp$ building dimension (L= 42.5 m)	$\perp$ building dimension (L= 61 m)

Table 5.5: Results of the comparison between Tamura et al. (2000) and the current study

	Urban winds		Open country winds	
	Tamura et al. (2003)	Current study	Tamura et al. (2003)	Current study
Torsional coefficient ($C_{T\,max}$*)	0.55	0.60	0.30	0.25
Shear coefficient ($C_{Sx\,max}$*)	3.42	3.50	1.80	1.60
Shear coefficient ($C_{Sy\,max}$*)	0.90	1.10	0.60	0.85

*Where Torsional coefficient CT = Base torsion/ (q_h LhR); q_H = mean dynamic wind pressure at mean roof height, L = length, h = mean roof height, R=√(L²+B²)/2, B = length; Shear coefficient C_S = Base shear/(q_h Lh)

A comparison of the results with those from a previous study by Isyumov and Poole (1983) for a building with dimensions L = 91.45 x B = 45.7 x H = 231.65 m and a more recent study from Keast et al. (2012) for a building with dimensions L = 40 x B = 20 x H = 60 m was made using the wind tunnel measurements in the current study for a modeled full-scale building with L = 61 x B = 39 m x H = 60 m. As the building tested by Isyumov and Poole (1983) was very tall and the power law index (α) for actual exposure was also not specified, the mean torsion evaluated for different wind directions was only considered for this comparison. For the case of Keast et al. (2012), the building dimensions and the terrain exposure were similar, therefore a complete comparison was carried out. Past studies have used shear and torsional coefficients defined as; C_v = Base shear/(q_H LH) and C_T = Base torsion/(q_H L^2H), respectively, where q_H = mean dynamic wind pressure at mean roof height, L = larger horizontal building dimension. For comparison purposes, the results of the current study have been transformed to the same definitions of shear and torsional coefficients. Additionally, shear coefficients for only $0^°$ and $90^°$ wind directions were considered in this comparison, as Keast et al. (2012) introduced shear force in terms of drag and lift force coefficients. Table 5.6 presents the experimental parameters as well as the evaluated shear and torsional coefficients for the

buildings considered. Figure 5.6 shows good agreement of the mean torsional coefficients for different wind directions evaluated by the three studies; and the peak torsional coefficients of the present study with those by Keast et al. (2012). Results show relatively good agreement for the measured peak shear forces and torsion in the two studies. Small differences could be attributed to the difference in building dimensions, the scale used, and the number of pressure taps.

Table 5.6: Comparison with Isyumov and Poole (1983) and Keast et al. (2012)

	Isyumov and Poole (1983)	Keast et al. (2012)	Current study
Wind tunnel technique	Weighted pneumatic averaging	A 6 degree-of-freedom high frequency balance	High frequency pressure integration
Building dimensions (m)	L=91.45 x B=45.7 x H=231.65	L=40 x B=20 x H=60	L=61 x B=39 x H=60
Aspect ratio (L/B)	2	2	1.56
Scale	1:500	1:400	1:400
Model dimensions (mm)	182.9x 91.4x463.3	100 x 50 x150	152.5 x97.5 x150
Terrain exposures	Suburban	Open	Open
Wind direction	$0°$ to $90°$	$0°$ to $90°$	$0°$ to $90°$
Torsional coeff. ($|C_T|_{max}$)	N/A	0.14	0.15
Shear coefficient ($|C_{vx}|_{max}, 0°$)	N/A	($C_{drag}, 0°$) = 2.00	1.70
Shear coefficient ($|C_{vy}|_{max}, 90°$)	N/A	($C_{drag}, 90°$) = 0.75	0.80
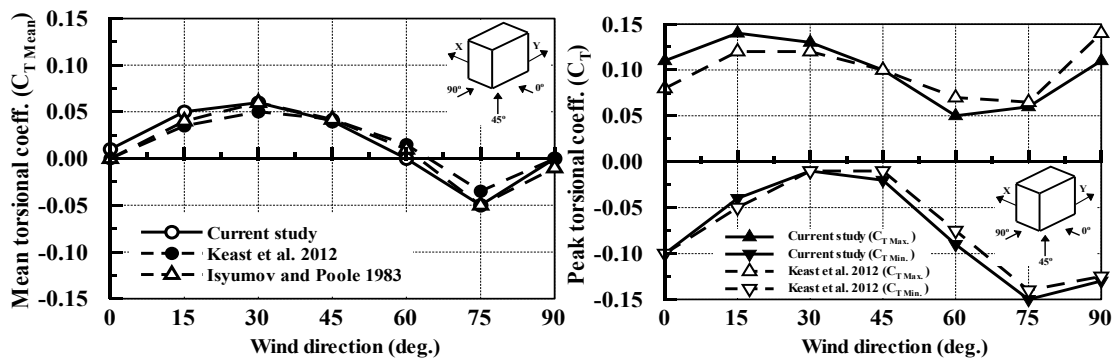
Figure 5.6: Torsional coefficient comparison for flat-roofed rectangular buildings with height 60 m located in open country exposure

Another comparison with a previous study by Tamura et al. (2003) for a building with dimensions L = 50 m x B = 25 m x H = 50 m was made using a building model having L = 61 m x B = 39 m x H = 50 m. The two flat-roofed buildings have the same height and aspect ratios of their plan dimensions L/B = 2 and 1.56. In this comparison, the definitions of torsional and shear coefficients in the Tamura et al. (2003) study were followed. The torsional coefficient was considered as C_T = Base torsion/(qH LHR) where; R=√(L2+B2)/2, B = smaller horizontal building dimension, and shear coefficient Cv= Base shear/(qH LH). For this comparison also, only wind direction perpendicular to the largest horizontal building dimension was considered due to the lack of data for other cases in Tamura et al. (2003). Tamura et al. study shows higher coefficients by about 60% (see Table 5.7), but this may be attributed to the different terrain exposures used in these studies. Indeed, the mean wind velocity at the roof height in urban terrain is much lower than that in open terrain exposure.

Table 5.7: Comparison with previous study by Tamura et al. (2003)

Experimental variables	Tamura et al. (2003)	Current study
Wind tunnel technique	High frequency pressure integration	High frequency pressure integration
Building dimensions (m)	L = 50 x B = 25 x h = 50	L = 61 x B = 39 x h = 50
Aspect ratio (L/B)	2.0	1. 6
Scale	1:250	1:400
Model dimensions (mm)	200 x 100 x 200	152.5 x97.5 x125
Terrain exposures	Urban (α= 0.25)	Open (α= 0.15)
Wind direction	$\perp$ to building length (L= 50 m)	$\perp$ to building length (L= 61 m)
Torsional coefficient ($|C_T|_{max}$)	0.30	0.20
Shear coefficient ($|C_{vx}|_{max}$)	3.00	1.90
Shear coefficient ($|C_{vy}|_{max}$)	0.90	0.50

5.3 COMPARISON OF WIND TUNNEL RESULTS WITH NBCC 2010 PROVISIONS

The experimental results were used to introduce four load cases, namely: shear and torsion load cases in both transverse and longitudinal wind directions (see Table 5.8). These load case values were compared to the evaluated shear and torsion values using the NBCC (2010) provisions. In the shear load case, maximum shear was considered along with the corresponding torsion, whereas in the torsion load case, maximum torsion and the corresponding shear were evaluated. The most critical shear and torsion values reported for wind direction range of $0^{°}$ to $45^{°}$ were considered for the transverse load cases; and from $45^{°}$ to $90^{°}$ for the longitudinal load cases. Furthermore, in transverse torsion load case, maximum torsion ($|C_{Tx}|_{Max.}$) resulting from winds in transverse direction ($|C_{Sx}|_{corr.}$) was only considered. Similarly, $|C_{Ty}|_{Max.}$ and $|C_{Sy}|_{corr.}$ were evaluated for comparison in the longitudinal torsion load case. Transverse shear load case was also defined as the maximum shear force ($|C_{Sx}|_{Max.}$) and the corresponding torsion ($|C_{Tx}|_{corr.}$) while in longitudinal shear load case ($|C_{Sy}|_{Max.}$) and ($|C_{Ty}|_{corr.}$) were considered. The eccentricities were noted by e_y and e_x in transverse- and longitudinal-direction as defined in Eqs. 5 and 7 and shown in Figure 4.10.

Table 5.8: Wind load cases in transverse and longitudinal directions

Load case	Transverse direction	Longitudinal direction
Shear	Max. shear in X-dir. ($|C_{Sx}|_{Max.}$) and corresponding torsion ($|C_{Tx}|_{Corr.}$)	Max. shear in Y-dir. ($|C_{Sy}|_{Max.}$) and corresponding torsion ($|C_{Ty}|_{Corr.}$)
Torsion	Max. torsion ($|C_{Tx}|_{Max.}$) and corresponding shear in X-dir. ($|Cs_{x}|_{Corr.}$)	Max. torsion ($|C_{Ty}|_{Max.}$) and corresponding shear in Y-dir. ($|Cs_{y}|_{Corr.}$)

In NBCC (2010), the static method, as mentioned earlier in Chapter 3, is introduced for low-rise buildings while the simplified method is proposed for medium-rise buildings. The static method calculations for the torsional and shear coefficients were derived based on figure I-7 in Commentary I of NBCC 2010, where the external peak (gust) pressure coefficients (C_pC_g) are provided for low-rise buildings. Likewise, for the simplified method, the external pressure is taken from figure I-15, Commentary I (Appendix II). Partial and full load cases were considered to estimate maximum torsion and corresponding shear, as well as maximum shear and corresponding torsion. Calculations were carried out considering the open terrain exposure. Static method values were increased by 25% to eliminate the implicit reduction (0.8) due to directionality (Stathopoulos, 2003).

Figure 5.7 shows the wind tunnel results along with the evaluated torsional load case parameters using the static and simplified methods in the transverse direction. Although the static method requires applying higher loads in comparison with wind tunnel measurements, it significantly underestimates torsion on low-rise buildings. This is mainly due to the fact that it specifies a significantly lower equivalent eccentricity (e_y (%)) which is about 3% of the facing horizontal building dimension compared to the equivalent eccentricity evaluated in the wind tunnel tests which is around 8% and 15% for buildings with gabled and flat-roof, respectively. Also, for the building with flat-roof, the simplified method requires applying almost the same wind loads as those measured in the wind tunnel. The eccentricity specified by the simplified method is 25% of the facing building width, which is significantly higher than the measured eccentricity (i.e. about 15%), hence the evaluated torsion using the simplified method exceeds the measured

torsion significantly. For the building with $45^°$ roof, the corresponding shear seems to exceed that on the flat-roofed building by 50%. However, lower eccentricities were noticed for buildings with roof angle $45^°$.
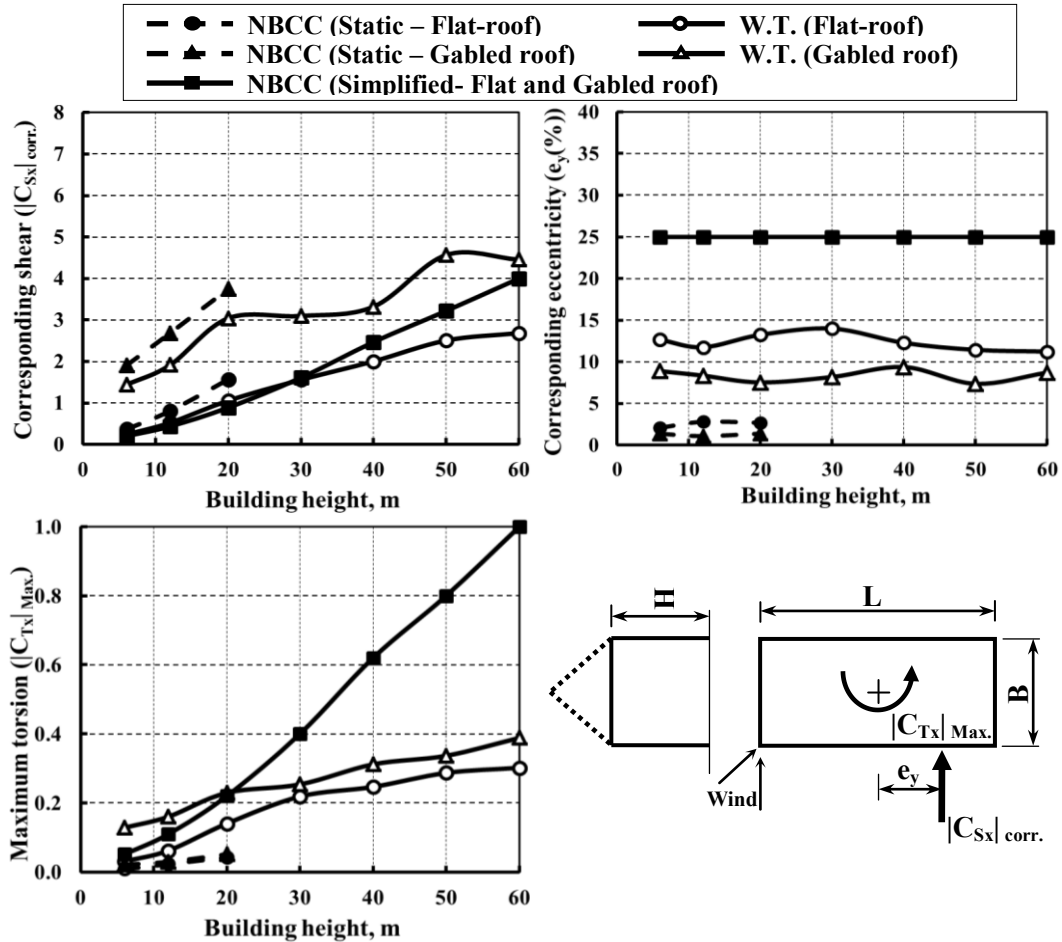
Figure 5.7: Comparison of torsional load case evaluated using NBCC (2010) and wind tunnel measurements for buildings with $0^°$ and $45^°$ roof angles (Transverse direction)

Figure 5.8 presents shear load case in the transverse direction evaluated by NBCC (2010) and measured in the wind tunnel. The static method compares well with the wind tunnel measurements in evaluating maximum shear while it underestimates the corresponding torsion on low-rise building with $45°$. The simplified method overestimates shear on buildings with flat-roof, however it underestimates shear on building with $45°$ roof angle with heights up to 40 m. Moreover, the simplified method neglects the corresponding torsion by applying wind loads uniformly distributed to evaluate maximum shear; this may be inadequate for the design of buildings sensitive to torsion.
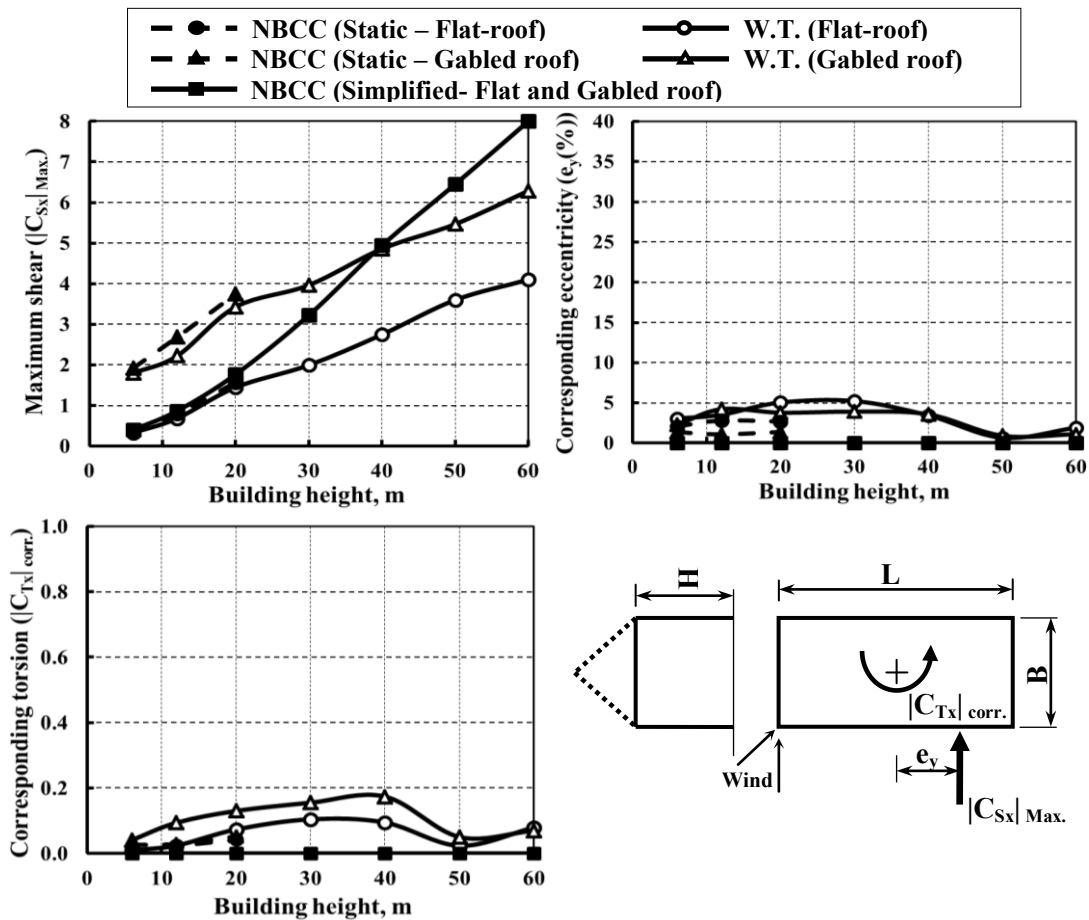
Figure 5.8: Comparison of shear load case evaluated using NBCC (2010) and wind tunnel measurements for buildings with $0°$ and $45°$ roof angles (Transverse direction)

Similarly, Figures 5.9 and 5.10 present torsional and shear load cases in the longitudinal direction. The static method also in this direction underestimates maximum torsion on low-rise buildings with flat-roof significantly. As Figure 5.9 shows, the measured eccentricity for low-rise buildings is about 25% of building width (B) while the static method applies higher wind loads with eccentricity of 5%. For buildings with flat-roofs, the simplified method compares well with wind tunnel in predicting the maximum torsion and overestimates maximum shear; while, the simplified method underestimates maximum torsion and succeeds in predicting maximum shear on buildings with $45°$ roof angle. However, the corresponding shear estimated by the simplified method shows good agreement with the wind tunnel data but the equivalent eccentricity for the building with gabled-roof is low. Figure 5.10, also shows that the corresponding torsion to the maximum shear has been neglected completely in longitudinal direction, as in Figure 5.8 for transverse direction. Neglecting the corresponding torsion, as mentioned previously, may not be always prudent.
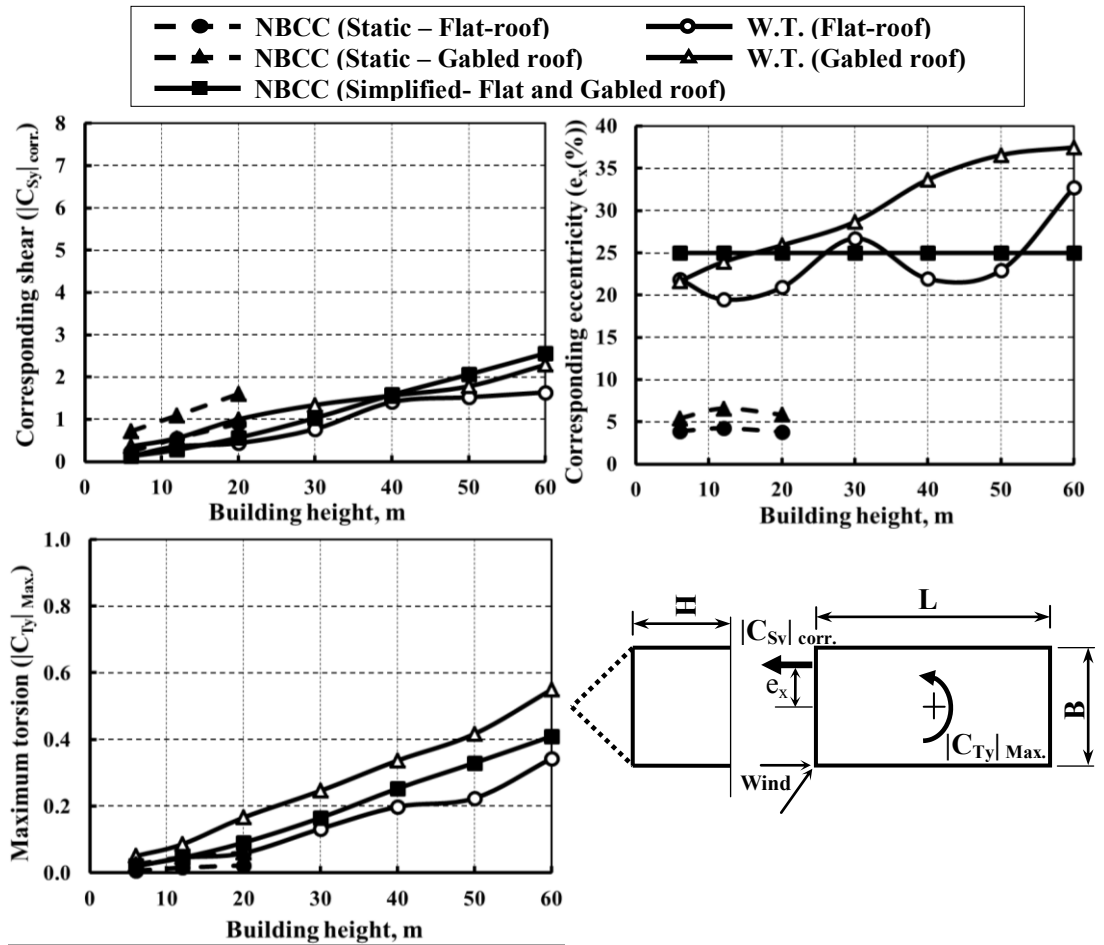
Figure 5.9: Comparison of torsional load case evaluated using NBCC (2010) and wind tunnel measurements for buildings with 0° and 45° roof angles (Longitudinal direction)
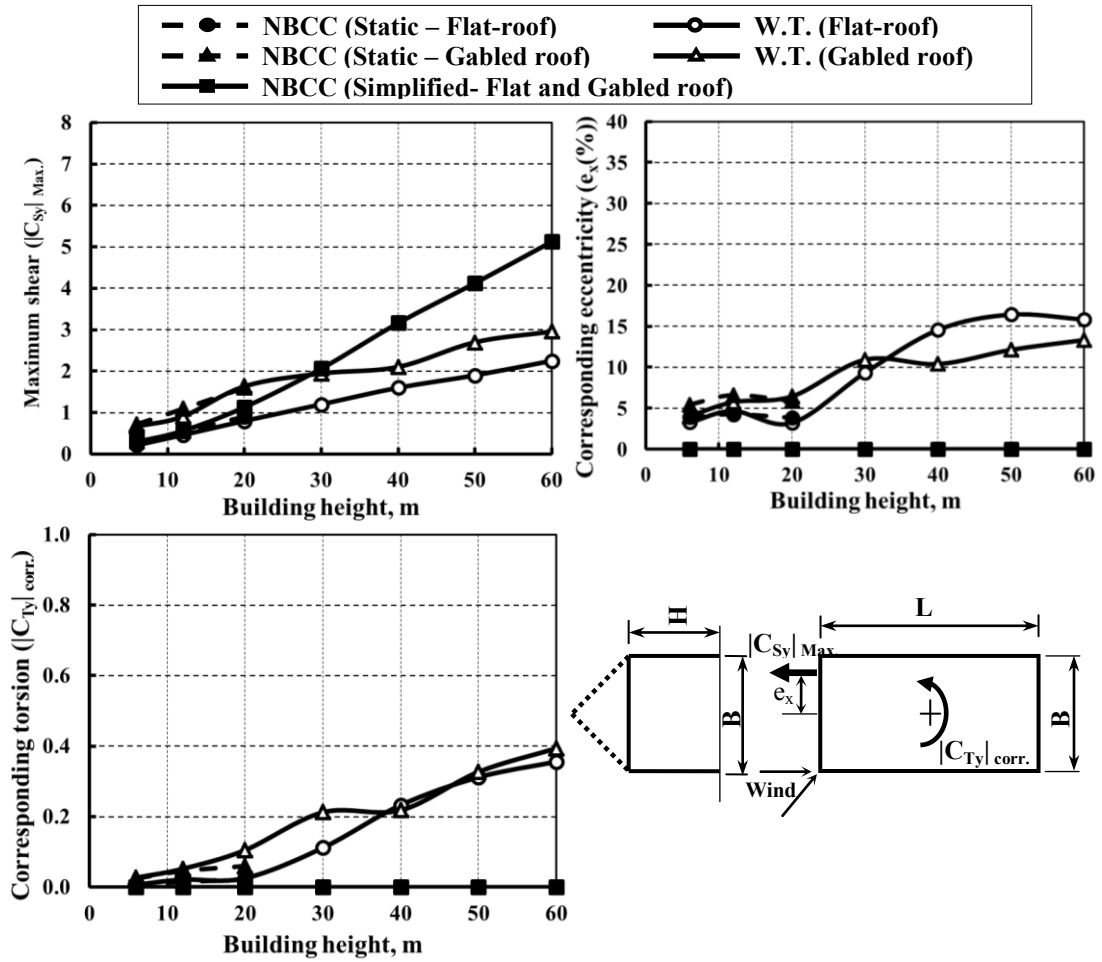
Figure 5.10: Comparison of shear load case evaluated using NBCC (2010) and wind tunnel measurements for buildings with $0°$ and $45°$ roof angles (Longitudinal direction)

Results summary for the comparisons with the NBCC 2010:

Tables 5.9 and 5.10 summarize the findings of the comparisons of the wind tunnel data with the static and simplified methods proposed in NBCC 2010 for the design of low- and medium rise buildings. The following could be concluded:

- The static method assigned for low-rise buildings underestimates torsion significantly.

- Significant differences were found between the simplified method and the wind tunnel results. In some cases, the simplified method requires torsion about double the measured, while in others it underestimates torsion and shear force.

- The simplified method does not introduce any guidance for the design of medium-rise buildings with gabled-roofs.

Table 5.9: Results summary for the comparison with the static method (NBCC (2010))

	Direction	Maximum torsion (NBCC (2010))	Maximum shear (NBCC (2010))
Flat-roof building	Transverse	Underestimates significantly	Compares well
	Longitudinal		
Gabled-roof building	Transverse	Underestimates significantly	Compares well
	Longitudinal		

Table 5.10: Results summary for the comparison with the simplified method (NBCC (2010))

	Direction	Maximum torsion (NBCC (2010))	Maximum shear (NBCC (2010))
Flat-roof building	Transverse	Overestimates	Overestimates
	Longitudinal	Compares well	Overestimates
Gabled-roof building	Transverse	Overestimates	Underestimates
	Longitudinal	Underestimates	Compares well

5.4 COMPARISON OF WIND TUNNEL RESULTS WITH ASCE 7 (2010) PROVISIONS

The three analytical procedures stated in ASCE 7 (2010) to evaluate wind loads were applied for this comparison. The envelope method appropriate for low-rise buildings (with conditions that h < 18 m and h < B) where h and B are the mean roof height and the smallest horizontal dimension, respectively, was used. Also, the ASCE's figure 28.4-1(Appendix I) is used to get the external pressure coefficients (GC_{pf}). The basic (transverse) and torsional load cases presented in figure 28.4-1 (Appendix I) of ASCE 7 (2010) are used to estimate the maximum torsional moment and the maximum base shear. In ASCE 7 (2010), directional methods, Part I proposed for all building heights and Part II recommended for buildings up to 48.8 m high, are also considered in this comparison. External pressure coefficients were collected from figure 27.4-1 (Appendix I). Pressure coefficients are provided in table 27.6-1 (Appendix I) for buildings with height up to 48.8 m. For consistency, ASCE 7 (2010) calculations were carried out considering the open terrain exposure C. Similar to the comparison with the NBCC 2010, four load cases are introduced, as given above in Table 5.8. Torsion and shear load cases in both traverse and longitudinal directions were compared with the corresponding wind tunnel measurement results.

As the ASCE 7- 10 has proposed guidance for design of medium-rise buildings with flat- and gabled-roofs, the comparison herein was made separately for each building configurations. Figures 5.11 to 5.14 show the comparison of torsion and shear load cases in transverse and longitudinal directions for flat-roof buildings, while Figures 5.15 to 5.18 are for the gabled-roof buildings.

Figure 5.11 summarizes the results for torsion load cases in transverse direction for flat low- and medium-rise buildings. Peak torsional coefficients ($|C_{Tx}|_{Max.}$), corresponding shear ($|C_{Sx}|_{corr.}$), and equivalent eccentricity (e_y (%)) are evaluated using the wind tunnel study and ASCE 7 (2010). For low-rise buildings, the envelope method in ASCE 7 (2010) shows relatively good agreement with the measured $|C_{Tx}|_{Max.}$, whereas the measurements show that the equivalent eccentricity e (%) could be reduced from about 18% to 15%. The directional methods (Parts I and II) necessitate equivalent eccentricity 15% which seems to be in relatively good agreement with the wind tunnel results (≈13%). At the same time, it can be seen from the figure that the directional methods apply significantly higher $|C_{Sx}|_{corr.}$. Consequently, the $|C_{Tx}|_{Max.}$ evaluated using these two methods is significantly greater than the measured wind tunnel torsion. For instance, the Directional I method applies torsion that is almost three times higher than the values measured in the wind tunnel for the 60 m high building. Directional II provided even higher torsion for buildings range from 20 to 50m high. As such, reducing the $|C_{Sx}|_{corr.}$ would improve the directional methods' predictions for torsion on rectangular low- and medium-rise buildings. Hence, it could be suggested for the torsion load case of the directional methods in ASCE 7 (2010) to apply 50% instead of 75% of the full wind load with the same eccentricity, i.e. 15% of the facing building horizontal dimension.

Figure 5.11: Comparison of torsional load case evaluated using ASCE 7 (2010) and wind tunnel measurements for flat-roof buildings (Transverse direction)

A comparison between the shear load case predicted using the provisions of the ASCE 7 (2010) wind standard, and that measured in the wind tunnel, is presented in Figure 5.12. The shear load case in transverse direction; the maximum shear ($|C_{Sx}|_{Max.}$), corresponding torsion ($|C_{Tx}|_{Max.}$) and equivalent eccentricity (e_y (%)) clearly indicates that the envelope method for low-rise buildings in ASCE 7 (2010) is indeed capable of predicting $|C_{Sx}|_{Max.}$ and $C_{T\ corr.}$ on low-rise buildings.
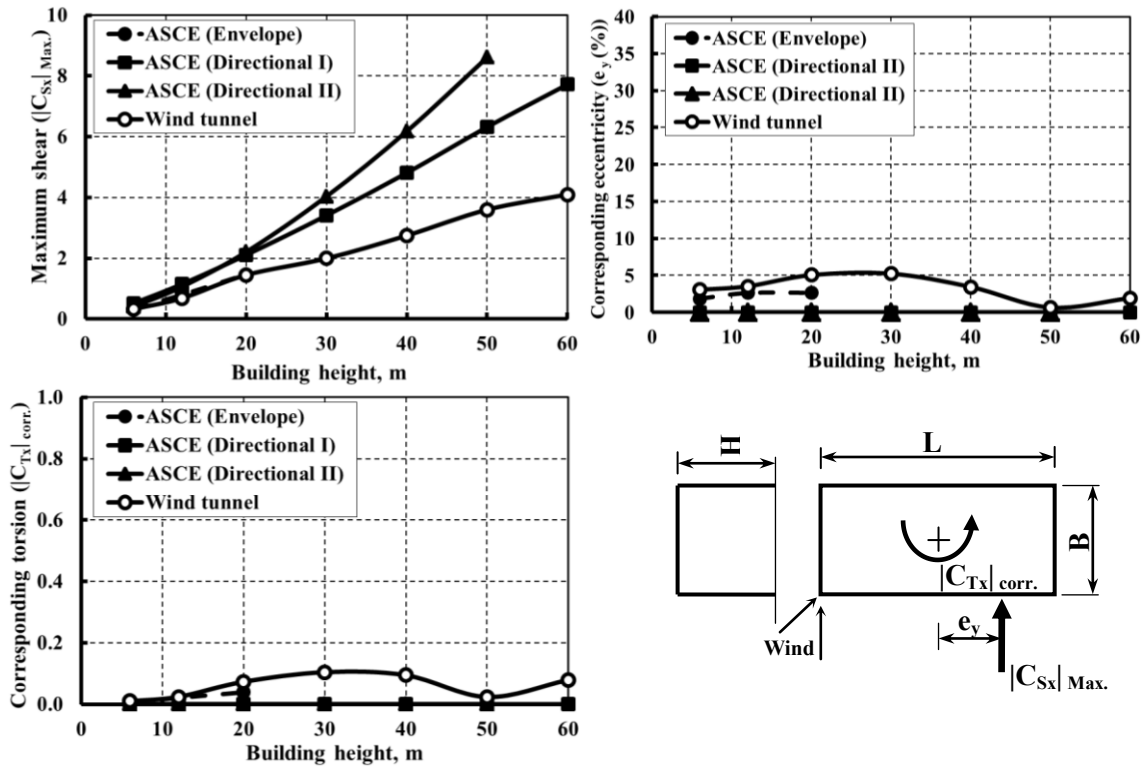
Figure 5.12: Comparison of shear load case evaluated using ASCE 7 (2010) and wind tunnel measurements for flat-roof buildings (Transverse direction)

Although, the directional methods (Parts I and II) of ASCE 7 (2010) provisions significantly overestimate the shear forces on the studied buildings, it has to be noted that the wind loads introduced in these shear load cases are uniformly distributed on building face. Thus, the directional methods do not consider the corresponding torsion. For instance, the directional method part II applies shear force that is about two times the measured in the wind tunnel for the 50 m high building. Although this high shear force (without torsion) may be conservative in the case of designing buildings that have their

main structural elements placed at the exterior building perimeter, it may not be safe for those buildings that have their main structural elements located near to the core, i.e. buildings that are sensitive to torsion or unbalanced wind loads. Therefore, designing the building for equivalent shear force similar to that measured in the wind tunnel along with the measured corresponding torsion is seen to be more representative of the actual wind loads acting on rectangular low- and medium-rise buildings.

For the design of low-rise buildings, Figure 5.13 shows the comparison of torsion loads case for flat-roof buildings in the longitudinal direction. Similar to transverse direction, the envelope method succeeded in predicting the maximum torsion and the corresponding shear with slightly higher equivalent eccentricity than the evaluated using the wind tunnel. Although, the directional methods (I and II) seems to be in a good agreement with the measured torsion, the distribution of wind forces defined in this load case is not appropriately considered. As it could be seen in Figure 5.13, the applied corresponding shear force is higher than the measured and the eccentricity is lower than the wind tunnel eccentricity.

Figure 5.13: Comparison of torsional load case evaluated using ASCE 7 (2010) and wind tunnel measurements for flat-roof buildings (Longitudinal direction)

Shear load case in longitudinal direction for flat-roof buildings, were also compared and presented in Figure 5.14. It appears also that the envelope method is in relatively good agreement with the experimental results. The directional methods overestimate the maximum shear and fully neglect the corresponding torsion. As mentioned previously, this may not be considered critical for the design of buildings sensitive to torsion (i.e. when the structural elements of main wind resisting system are distributed around building core)

Figure 5.14: Comparison of shear load case evaluated using ASCE 7 (2010) and wind tunnel measurements for flat-roof buildings (Longitudinal direction)

The four load cases (i.e. shear and torsion in transverse and longitudinal directions) evaluated using the ASCE 7 (2010) and wind tunnel for the design of gabled-roof buildings will now be presented. Again, the three analytical methods stated in the ASCE 7 (2010) were applied. The Envelope method was used to evaluate wind loads on low-rise buildings (up to 20 m), as per previous provided. The directional method was applied for all building heights. Because the directional II method limited to evaluate wind loads on building with mean roof heights lower than 48.8 m (160 ft), it was used for buildings having eave heights up to 40 m.

For gabled-roof buildings, Figure 5.15 shows the comparison between the ASCE 7 (2010) and wind tunnel measurements for the shear load case in transverse direction. Starting with low-rise buildings, it was found that the envelope method applies torsion higher than what was measured in the wind tunnel. It could also be seen that the corresponding shear proposed by envelope method is slightly lower than the wind tunnel values and associated with eccentricity higher than the expected eccentricity using the wind tunnel. Clearly, increasing the corresponding shear with reducing the associated eccentricity (from 16 to 10%) would improve the envelope method for better evaluating torsion on rectangular low-rise buildings with gabled roofs (45°). Looking at the performance of the directional methods I and II, it appears clearly that these two methods overestimate torsion significantly on low and medium-rise buildings with gable roofs. For instance, the directional method II requires applying torsion three times higher than the measured value for design of the 40-m high building. Therefore, applying the appropriate corresponding shear (close to the measured corresponding shear) with the suitable

eccentricity (10%) will improve the directional methods I and II to predict the actual wind effects including torsion for adequate building design.
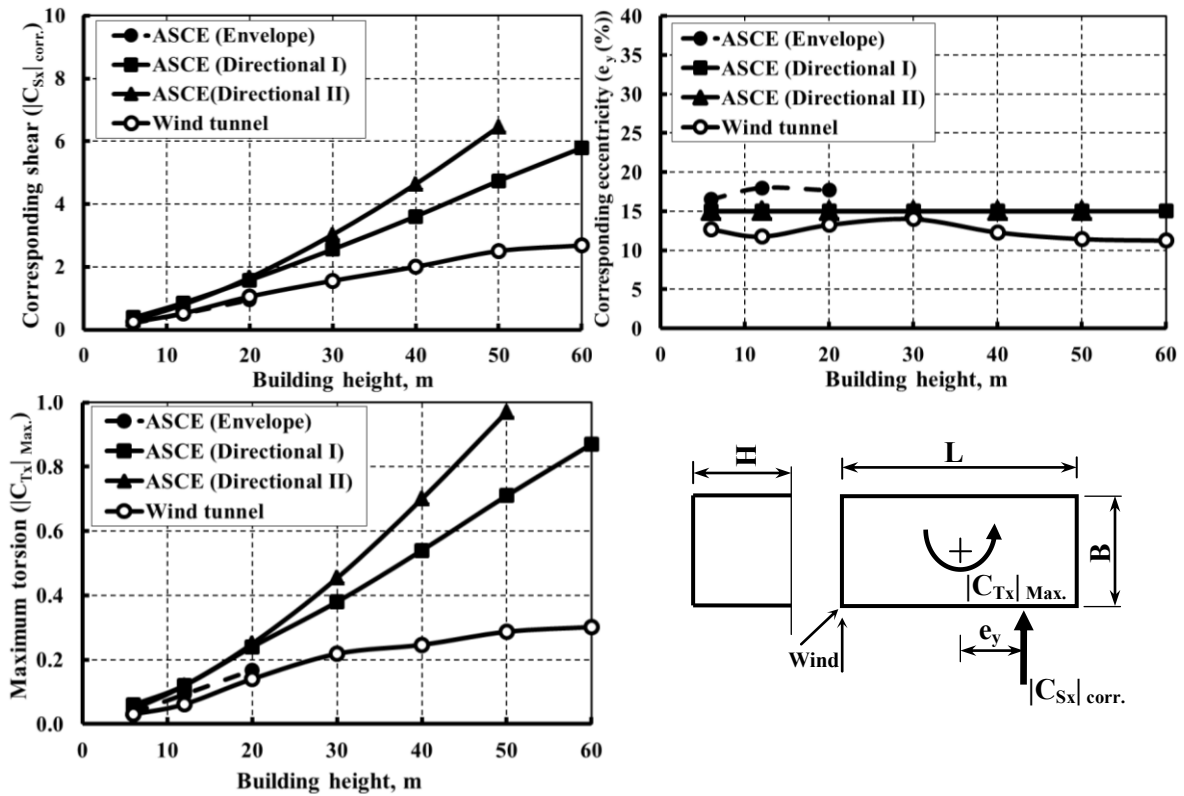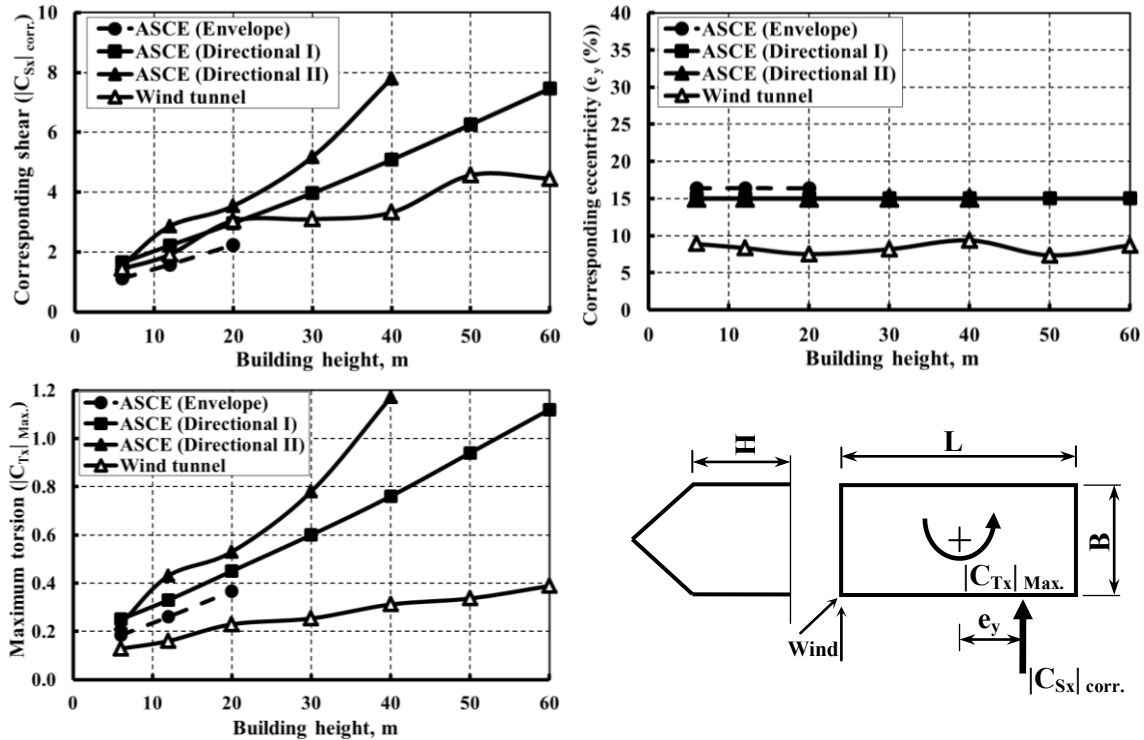

Figure 5.15: Comparison of torsional load case evaluated using ASCE 7 (2010) and wind tunnel measurements for buildings with $45°$ roof angle (Transverse direction)

Figure 5.16 shows the shear load case in transverse direction for gabled-roof buildings evaluate using ASCE 7 (2010) provisions and wind tunnel. For low-rise buildings, the envelope method succeeds in predicting the maximum shear but it underestimates the corresponding torsion. This could be improved by increasing the

corresponding eccentricity to 5% from the facing horizontal building dimension. Directional methods I and II overestimate maximum shear and fully neglect the corresponding torsion. It would be recommended to apply the appropriate maximum shear and the corresponding torsion, as this will produce the actual wind loads to achieve adequate building design. This will be discussed further in Chapter 7.
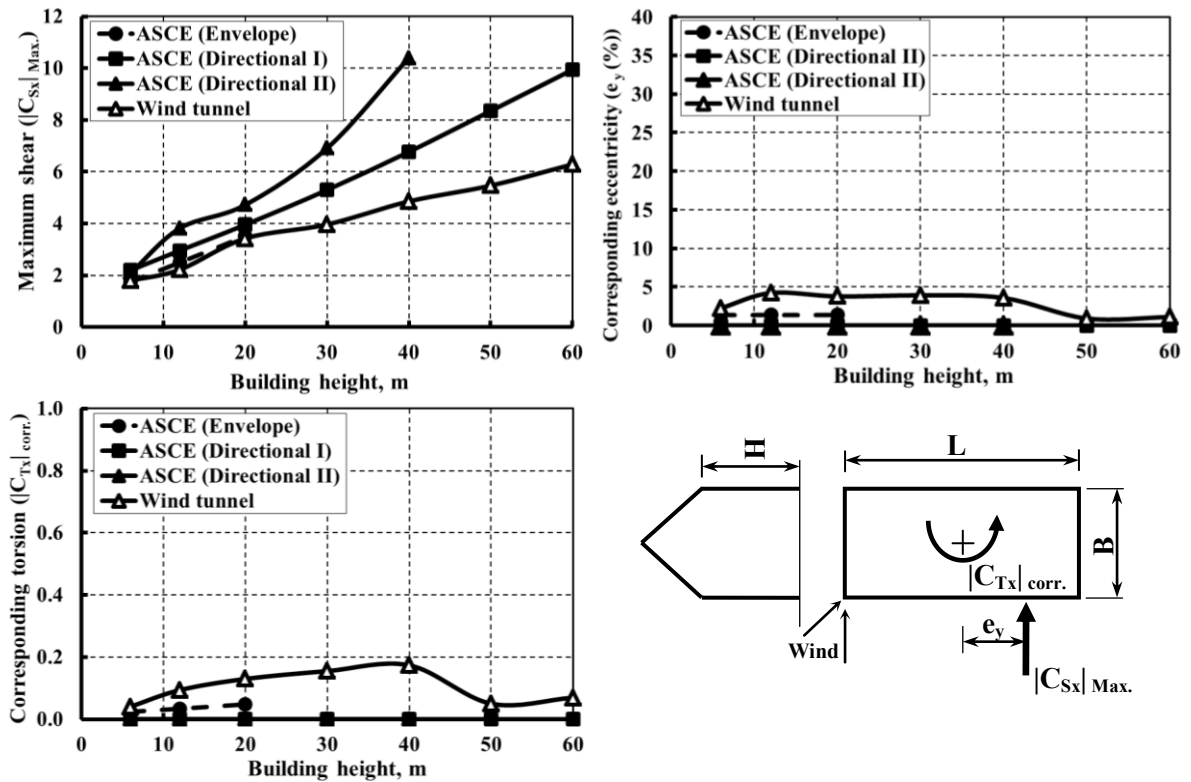
Figure 5.16: Comparison of shear load case evaluated using ASCE 7 (2010) and wind tunnel measurements for buildings with $45°$ roof angle (Transverse direction)

Figure 5.17 presents the comparison results for the torsion load case for gabled-roof buildings in longitudinal direction evaluated using the ASCE 7 (2010) and the wind

tunnel. For low rise buildings, the envelope method succeeds to evaluate the maximum

torsion and the corresponding shear. While directional method I shows good agreement

in predicting maximum torsion, it requires a corresponding shear higher than that

measured in the wind tunnel with associated eccentricity (15 to 20%), i.e. much lower

than the equivalent eccentricity (22 to 37%) evaluated in the wind tunnel - see Figure

5.17. The case even worse with the directional method II, as it overestimates maximum

torsion significantly. For instance, for the 40 m-high building directional II applies

torsion double than the measured in the wind tunnel. Clearly, the corresponding shear is

overestimated significantly and is applied with associated equivalent eccentricity (15%),
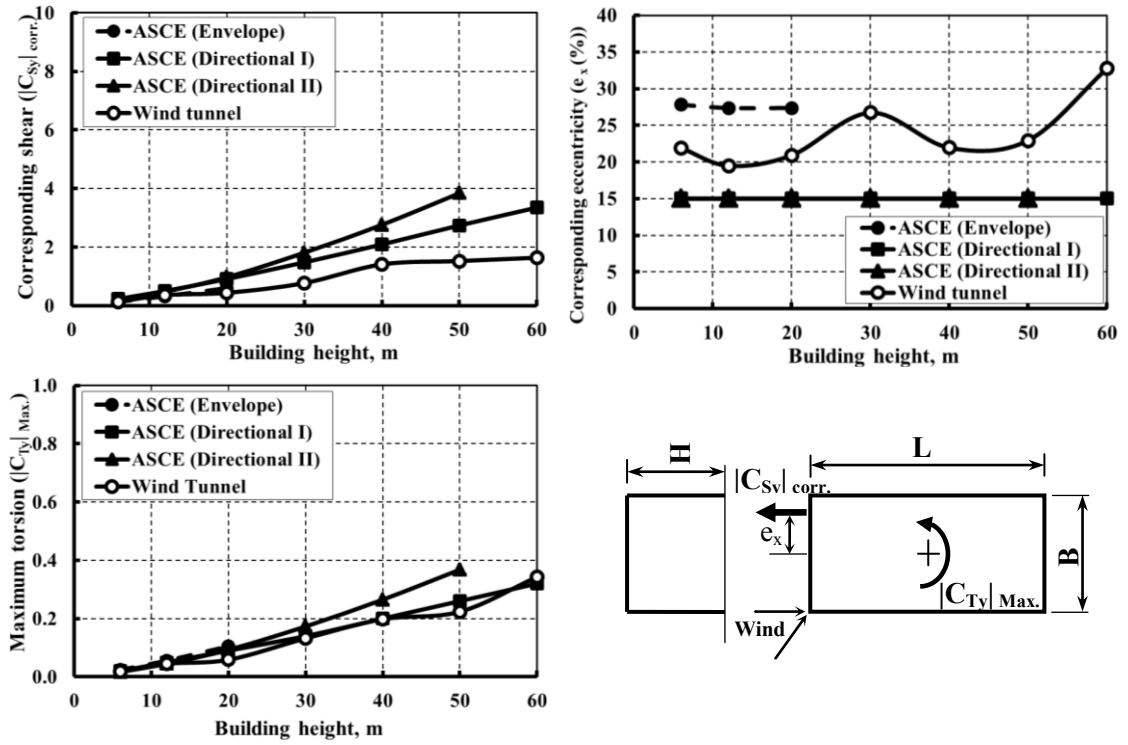
which is lower than the evaluated using the wind tunnel (22 to 37%).
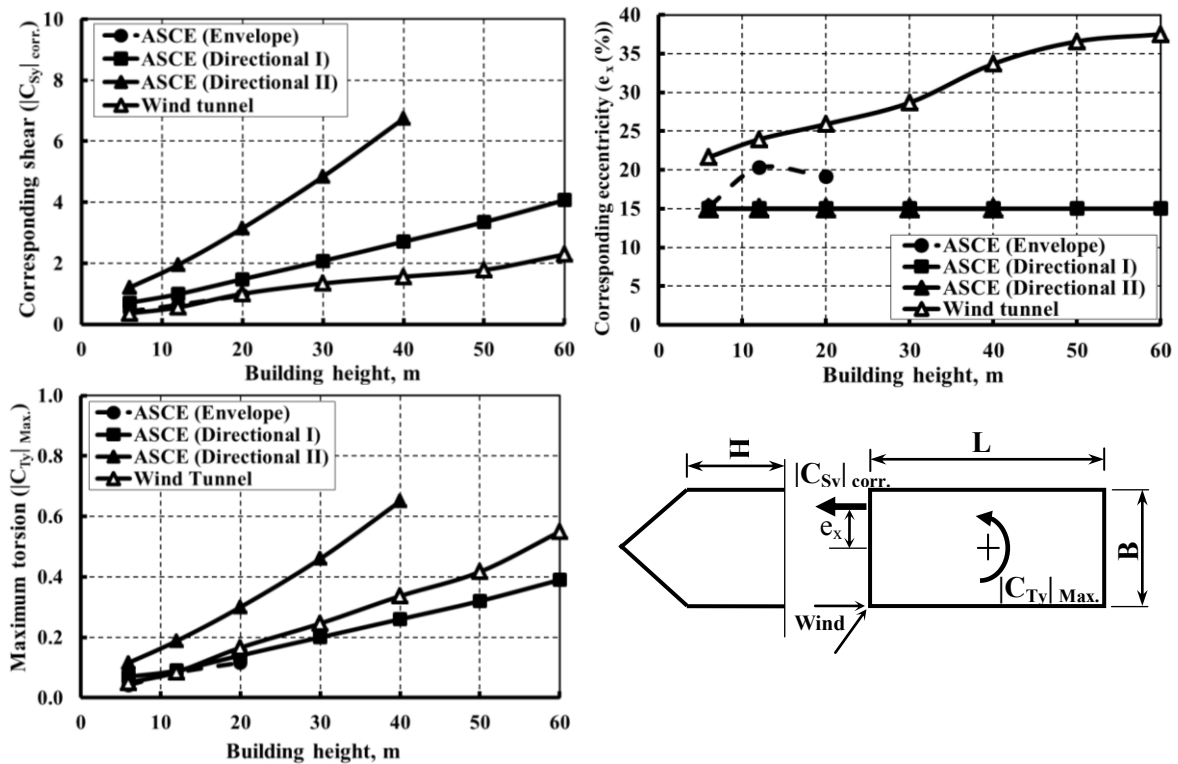
Figure 5.17: Comparison of torsional load case evaluated using ASCE 7 (2010) and wind tunnel measurements for buildings with 45° roof angle (Longitudinal direction)

The shear load case in longitudinal direction for gabled-roof buildings is also presented in Figure 5.18, and compared with ASCE 7 (2010) as previously. It appears that the envelope method is in relatively good agreement with the experimental results for predicting the maximum shear but underestimates the corresponding torsion. The directional methods I and II overestimate the maximum shear and fully neglect the corresponding torsion. However, as mentioned previously, this may not be considered critical for the design of buildings sensitive to torsion.

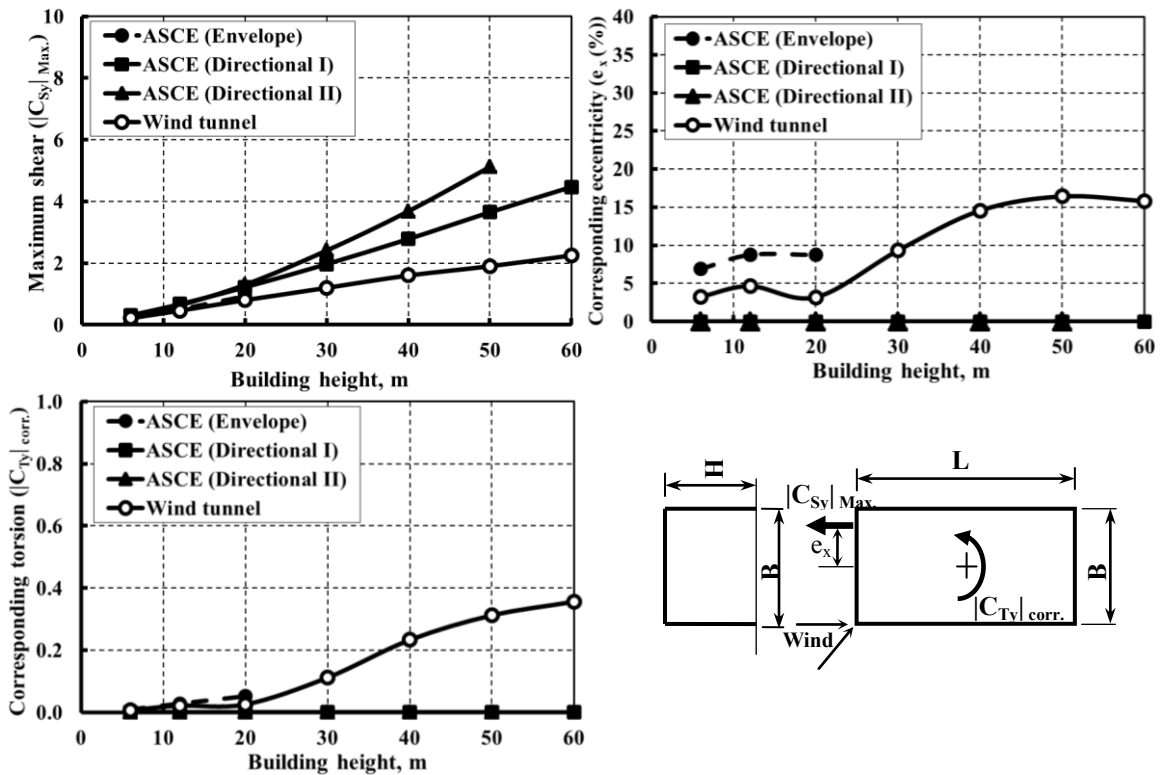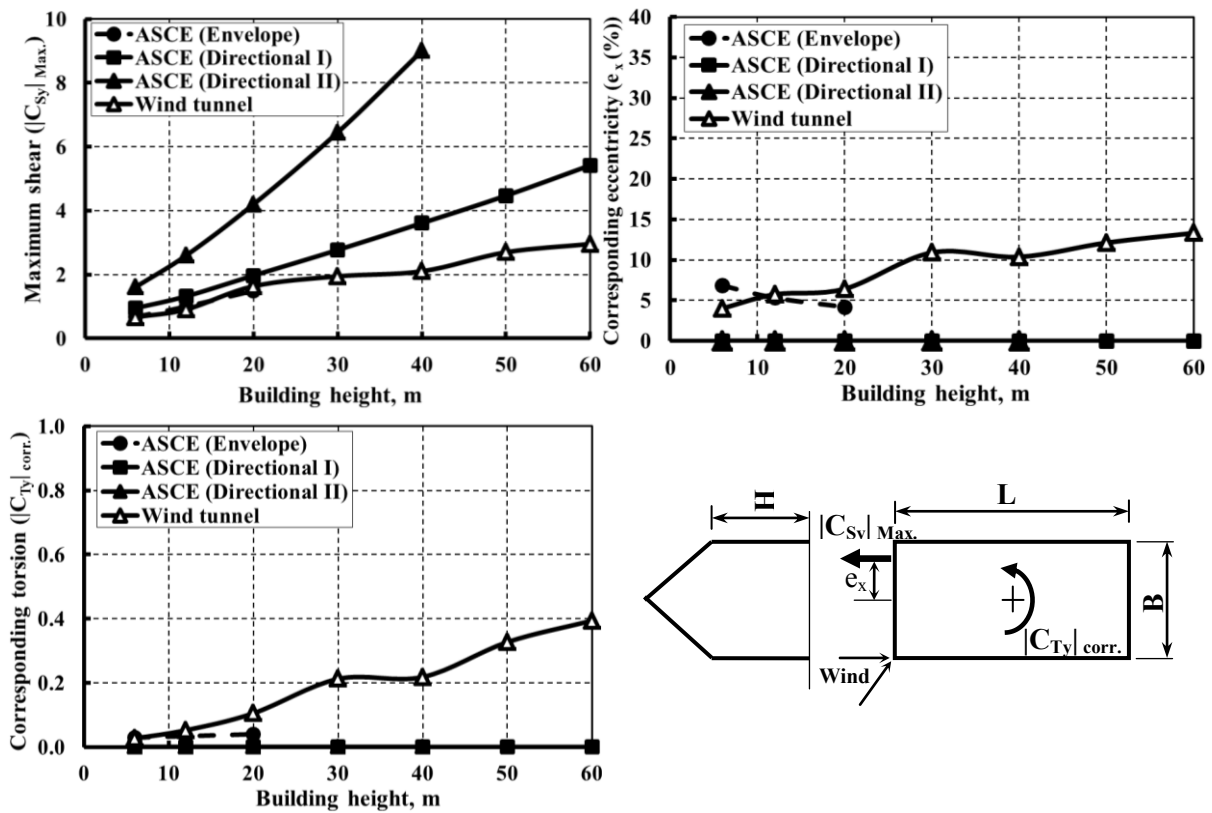
Figure 5.18: Comparison of shear load case evaluated using ASCE 7 (2010) and wind tunnel measurements for buildings with $45°$ roof angle (Longitudinal direction)

Results summary for the comparisons with the ASCE 7 (2010):

Tables 5.11, 5.12 and 5.13 summarize the findings of the comparisons among the wind tunnel data and static and simplified methods proposed in ASCE 7 (2010) for the design of low- and medium rise buildings. Results can be briefly summarized as:

- The envelope method assigned for low-rise buildings show generally good agreement with the wind tunnel measurements.

- Significant differences were found between the simplified method and the wind tunnel results. In some cases, the directional methods require torsion about three times the measured values, whereas they underestimate torsion and shear force in other cases. Considering the inherent code/standard conservatism, some overestimation may be desirable.

Table 5.11: Results summary for the comparison with <u>the envelope method</u> (ASCE 7 (2010))

	Direction	Maximum torsion (ASCE 7 (2010))	Maximum shear (ASCE 7 (2010))
Flat-roof building	Transverse	Compares well	Compares well
	Longitudinal	Compares well	Compares well
Gabled-roof building	Transverse	Overestimates	Compares well
	Longitudinal	Compares well	Compares well

Table 5.12: Results summary for the comparison with <u>the directional I method</u> (ASCE 7(2010))

	Direction	Maximum torsion (ASCE 7 (2010))	Maximum shear (ASCE (2010))
Flat-roof building	Transverse	Overestimates	Overestimates
	Longitudinal	Compares well	Overestimates
Gabled-roof building	Transverse	Overestimates	Overestimates
	Longitudinal	Compares well	Overestimates

Table 5.13: Results summary for the comparison with <u>the directional II method</u> (ASCE 7 (2010))

	Direction	Maximum torsion (ASCE (2010))	Maximum shear (ASCE (2010))
Flat-roof building	Transverse	Overestimates	Overestimates
	Longitudinal	Overestimates	Overestimates
Gabled-roof building	Transverse	Overestimates	Overestimates
	Longitudinal	Overestimates	Overestimates

CHAPTER 6

LOAD COMBINATIONS

In this chapter, the results of a set of wind tunnel tests carried out to examine wind-induced overall structural loads on rectangular low- and medium-rise buildings will be presented. Emphasis was directed towards the effect of wind direction on torsion and its correlation with peak shear forces in both transverse and longitudinal directions. The two building models with the same horizontal dimensions but different gabled-roof angles (0° and 45°) were tested at different full-scale equivalent eave heights (6, 12, 20, 30, 40, 50, and 60 m) in open terrain exposure for all wind directions (every 15°). Wind-induced pressures were integrated over building surfaces and results were obtained for the along-wind force, the across-wind force, and the torsional moment. Maximum wind force component was given associated with the other simultaneously-observed wind force components normalized by the overall peak. Suggested load combination factors for potential use in design codes will be introduced in Chapter 7 aiming at an adequate evaluation of wind load effects on rectangular low- and medium-rise buildings. This chapter examines the effect of building height, roof slope, and wind direction on wind load combinations; shear forces (in X- and Y- directions) occurring simultaneously with maximum torsion, as well as maximum shears and corresponding torsions.

6.1 BACKGROUND

Peak torsion and its correlation with peak along- and across-wind forces are of utmost importance for adequate building design. Wind load combinations (i.e. along-wind force associated with across-wind forces and vice versa) for medium-rise buildings, defined by ASCE 7 (2010) as having height less than 60 m but greater than 18 m with lowest natural frequency > 1Hz, have been simplified by applying 0.75 of the full wind loads in both along- and across-wind directions simultaneously (ASCE 7 (2010), NBCC (2010)). In another load combination case including torsion, the ASCE 7 (2010) requires applying 0.563 of the full wind loads with an equivalent eccentricity equal to 15% of the facing building horizontal dimension in both along- and across-wind directions simultaneously. However, a similar torsional load case in NBCC (2010) applies 0.75 of the full wind load on half of building face and 0.38 of the full wind load in both along- and across-wind directions on the other half simultaneously. Recently, Tamura et al. (2008) and Keast et al. (2012) studied wind load combinations including torsion for medium-rise buildings. The first study shows the importance of considering the wind load combinations on the peak normal stress generated in the building columns. Based on testing of a limited number of building models, the latter study concludes that for rectangular buildings the peak overall torsion occurs simultaneously with 30-40% of the peak overall drag force. Additional experimental results for testing different building configurations are still required to confirm and generalize these results.

Figure 6.1 shows an example of the variation of the corresponding shear force ratio to the overall shear in X-direction when the 20-m high building was tested at different wind directions 0°, 30°, 45° and 90°. These selected wind directions were the

critical ones in which the maximum torsion was measured. Clearly, changing wind direction has significant effect on the reported shear force ratio to the overall maximum shear force in X-direction. It is also expected that wind load combinations will be affected much by changing the building height, roof slope. Therefore, this chapter examines the effect of building height, roof slope, and wind direction on wind load combinations; shear forces (in X- and Y- directions) occurring simultaneously with maximum torsion, as well as maximum shears and corresponding torsions.
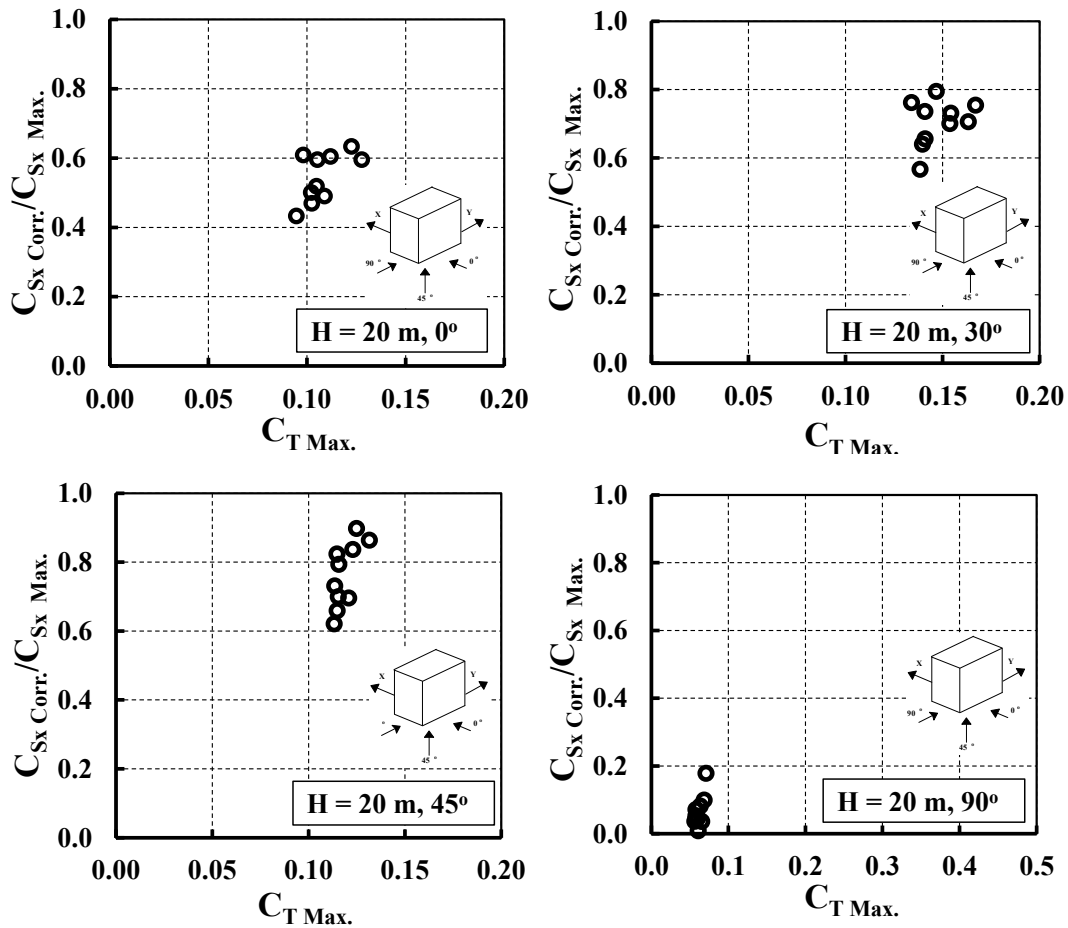
Figure 6.1: Corresponding shear force ratio in X- dir. ($C_{Sx\ corr.}/C_{Sx\ Max.}$), associated with maximum torsion ($C_{T\ Max.}$), for the 20 m building, flat-roof (wind directions; $0°$, $30°$, $45°$, $90°$)

6.2 SELECTION OF CRITICAL VALUES

All peak shear and torsional coefficients ($|C_{Sx}|_{Max.}$, $|C_{Sy}|_{Max.}$, $|C_T|_{Max.}$) were considered as the average of the maximum ten values picked up from a 1-hr full-scale equivalent time history of the respective signal. This approach has been considered as a good approximation to the mode value of detailed extreme value analysis and it has been used in previous wind tunnel studies. The corresponding shear forces ($C_{Sx\,corr.}$, $C_{Sy\,corr.}$) and torsion ($C_{T\,corr.}$) were evaluated as the average of ten values occurring at the time instances of the ten peaks used to define the respective source maximum value. These corresponding shear/torsion values were normalized by the overall shear/torsion - evaluated as the most critical values found from testing the buildings for all wind directions, i.e. $C_{Sx\,corr.}/C_{Sx\,overall}$, $C_{Sy\,corr.}/C_{Sy\,overall}$, $C_{T\,corr.}/C_{T\,overall}$.

6.3 MAXIMUM TORSION AND CORRESPONDING SHEAR FORCES IN X- AND Y-DIRECTIONS

As mentioned earlier, the two buildings with $0°$ and $45°$ gabled roof angles were tested in open terrain exposure at different eave heights (H = 6, 12, 20, 30, 40, 50 and 60 m) for different wind directions ($0°$ to $90°$ every $15°$). Figure 6.2a presents the variation of maximum torsion coefficient ($|C_T|_{Max.}$) with wind directions for both building configurations and all tested heights. Figures 6.2b and 6.2c show corresponding shear ratios from the overall maximum shear forces in X- and Y-directions respectively (i.e. $C_{Sx\,corr.}/C_{Sx\,overall}$, $C_{Sy\,corr.}/C_{Sy\,overall}$). As can be seen from the figures, the maximum

torsional coefficient increases significantly with increasing building height from 6 to 60 m. The lowest torsional coefficient values occur when the wind direction is around $60°$. Changing roof angle from $0°$ to $45°$ causes an increase of the torsional coefficient by about 50%. As expected, the corresponding shear ratio in X-axis decreases when the incident wind angle varies from $0°$ to $90°$. On the other hand, for the same wind range, the corresponding shear ratio in Y-axis increases. It is interesting to note that the maximum corresponding shear ratio is about 80% of the overall shear force for both X- and Y-directions, although for different wind directions. Moreover, the corresponding shear ratio has not been affected much by increasing building height or roof slope. The critical wind directions for torsion seem to be from $15°$ to $30°$ and $75°$ to $90°$. In the first range, torsion is associated with higher shear force in X- than in Y-direction, while in the other range the higher shear force is in the Y-direction.
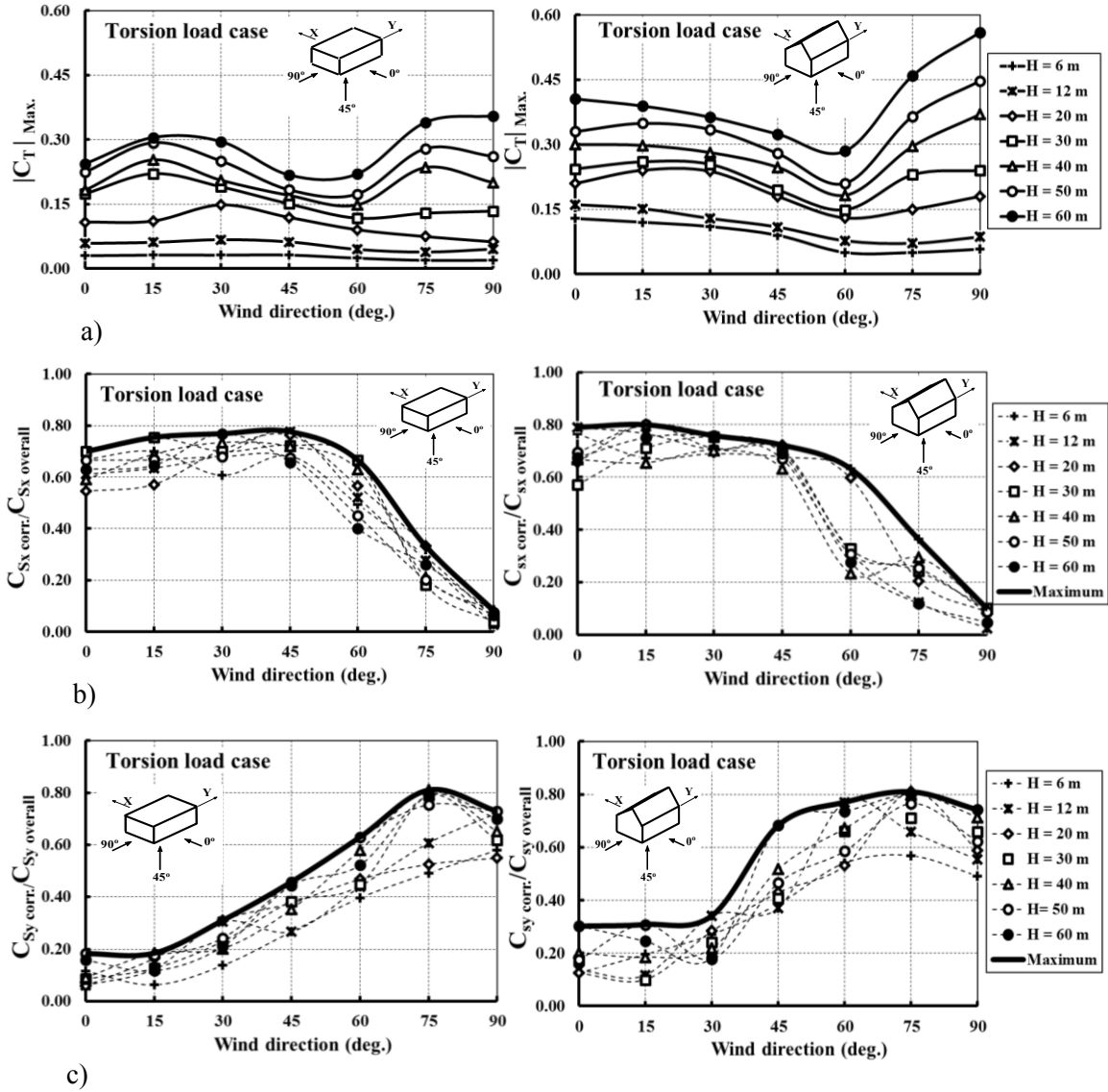
Figure 6.2: Torsional load case: a) maximum torsion, b) corresponding shear ratio in X-direction, c) corresponding shear ratio in Y-direction

6.4 Maximum shear force in X-direction, corresponding torsion and corresponding shear force Y-direction

In the same manner, Figure 6.3a presents the variation of the maximum shear force (X-component) evaluated for both building configurations and all tested heights for different wind directions. Figures 6.3b and 6.3c show the variation of corresponding torsion ratio ($C_{T\ corr.}/C_{T\ overall}$) and corresponding shear force ratio ($C_{Sy\ corr.}/C_{Sy\ overall}$) with wind direction, respectively. As can be observed in the figure, the maximum shear force coefficient ($|C_{Sx}|_{Max.}$) has increased significantly (almost triple and double for flat- and gabled-roof) by increasing the height of the building from 20 to 60 m. Changing roof angle from $0^{°}$ to $45^{°}$ results in increasing shear force coefficient ($C_{Sx\ Max.}$) by about 2.4 times for the 20 m building and 1.5 times for the 60 m building. This may be attributed to the reduction of the ratio of the inclined roof area facing the wind relative to the total surface building area resulting from increasing building height from 20 to 60 m. Thus, it is clear that the effect of increasing roof slope on the maximum shear force decreases with increasing building height. The maximum shear coefficient in X-direction has not been affected much by changing the wind direction from $0^{°}$ to $45^{°}$ while rapid decrease was noted from $45^{°}$ to $90^{°}$. The corresponding torsion ratio tends to reach its peak value for wind directions between $15^{°}$ and $30^{°}$ for the two tested buildings at different heights. On the other hand, the corresponding shear force ratio ($C_{Sy\ corr.}/C_{Sy\ overall}$) seems to be lower when wind directions are between $0^{°}$ and $45^{°}$ and higher between $45^{°}$ and $90^{°}$. Also, the peak corresponding shear force ratio ($C_{Sy\ corr.}/C_{Sy\ overall}$) was observed to occur at wind directions between $60^{°}$ and $75^{°}$ and to be about 80%. The shear load case in transverse

direction should account for the maximum shear force in X-direction, the corresponding torsion, and the corresponding shear in Y-direction for wind directions from $0°$ to $45°$. However, for wind directions ranging from $45°$ to $90°$, the shear in Y-direction will be maximized and this will be more critical for designing the building in the longitudinal direction, as it will be illustrated in the following sections.

a)

b)

c)
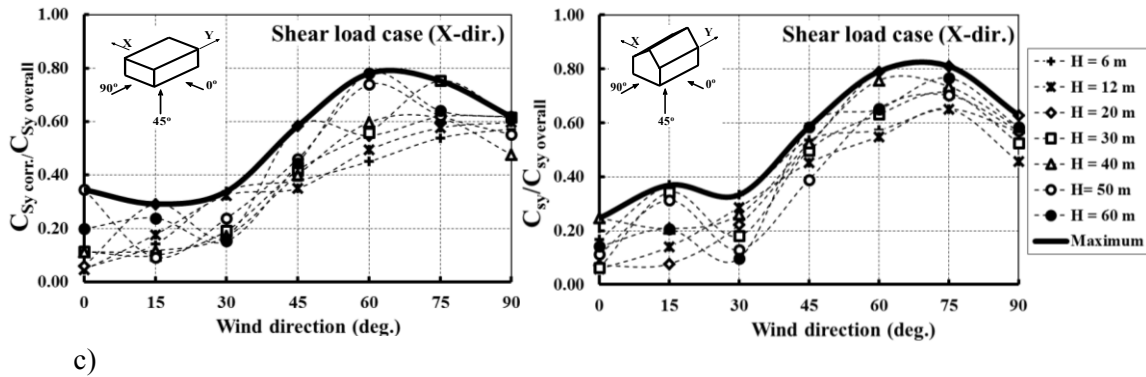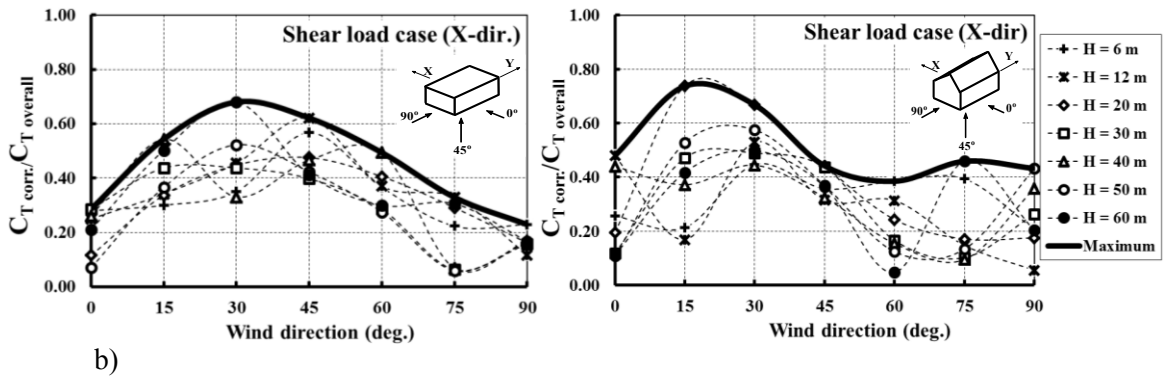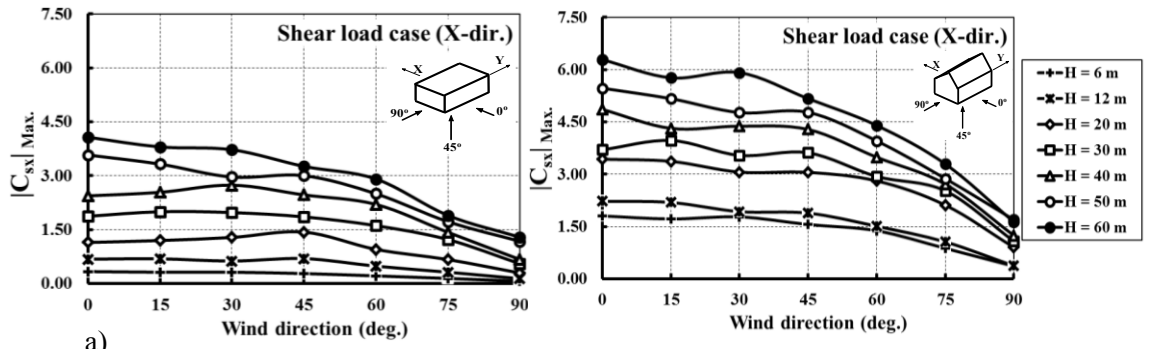
Figure 6.3: Shear load case (transverse direction): a) maximum Shear in X-direction, b) corresponding torsion ratio, c) corresponding shear ratio in Y-direction.

6.5 MAXIMUM SHEAR FORCE IN Y-DIRECTION AND CORRESPONDING TORSION AND SHEAR FORCE IN X-DIRECTION

Figure 6.4a presents the variation of the maximum shear force in Y-direction evaluated for different wind directions for the same building configurations. Also, Figures 6.4b and 6.5c show the variation of corresponding torsion ratio ($C_{T\ corr.}/C_{T\ overall}$) and corresponding shear force ratio ($C_{Sx\ corr.}/C_{Sx\ overall}$) with wind direction, respectively. Similar to the shear force in X-direction, the maximum shear force coefficient ($C_{Sy\ Max.}$) has increased significantly (about 2.8 times) by increasing the height of the flat-roofed building from 20 to 60 m and by about 1.8 times for the gabled-roof (45°) building. Changing roof angle from 0° to 45° results in almost doubling the shear force coefficient ($C_{Sy\ Max.}$) for the 20 m high building but in only 30% increase for the 60 m high building. The maximum shear coefficient in Y-direction has not been affected much by changing the wind direction from 45° to 90°. Accordingly, the corresponding torsion ratio reaches its peak value at wind direction of 75° for the two tested buildings at different heights. The corresponding shear force ratio ($C_{Sx\ corr.}/C_{Sx\ overall}$) seems to be lower for wind directions from 45° to 90°. The peak corresponding shear force ratio ($C_{Sx\ corr.}/C_{Sx\ overall}$) was found to be 0.8 for 0° wind direction. Although the effects of increasing roof slope from 0° to 45° lead to increasing the maximum torsion and shear forces for different wind directions - as mentioned earlier - the corresponding component ratios are similar for flat-roofed and gabled-roofed buildings. Likewise, the shear load case in longitudinal direction should account for the maximum shear force in Y-direction, the corresponding

torsion, and the corresponding shear ratio in X-direction for winds in the range of $45°$ to $90°$.
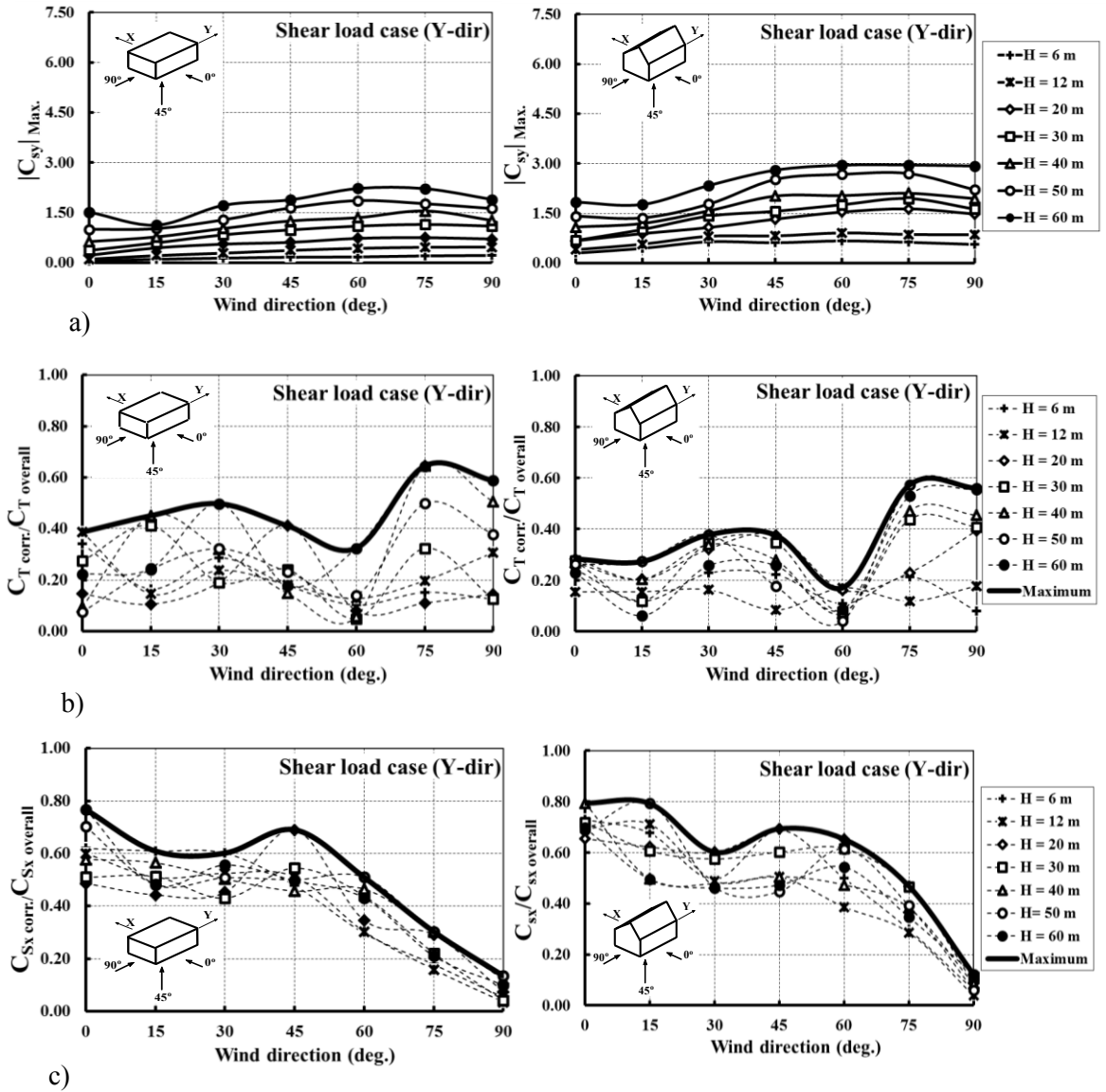
Figure 6.4: Shear load case (longitudinal direction): a) maximum Shear in Y-direction, b) corresponding torsion ratio, c) corresponding shear ratio in Y-direction.

6.6 COMPARISON WITH PAST STUDY BY KEAST ET AL. (2012)

A comparison of the results with those from a previous study by Keast et al. (2012) for a building with dimensions L = 40 x B = 20 x H = 60 m was made using the wind tunnel measurements in the current study for a modeled full-scale building with L = 61 x B = 39 m x H = 60 m. Keast et al. study (2012) have used shear and torsional coefficients defined as; C_v = Base shear/(q_H LH) and C_T = Base torsion/(q_H L^2H), respectively, where q_H = mean dynamic wind pressure at mean roof height, L = larger horizontal building dimension. Figure 8 presents the ten most critical torsion values recorded from all wind directions along with the corresponding shear force ratio measured by Keast et al. (2012) and the respective values from the current study. Results show relatively good agreement for the measured shear forces and torsion in the two studies. Small differences could be attributed to the difference in building dimensions, the scale used, and the number of pressure taps.
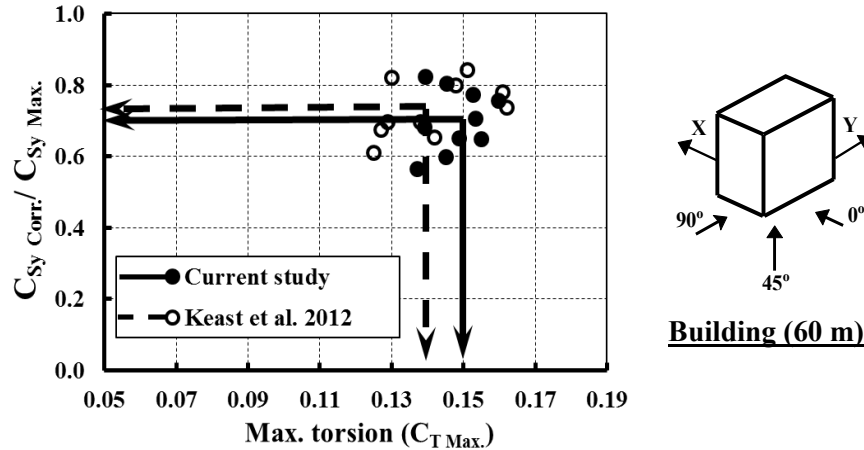
Figure 6.5: Overall shear ratio ($C_{Sy\ Corr.}$ / $C_{Sy\ Max.}$) at peak torsion for the flat-roof building with height 60 m evaluated by Keast et al. (2012) and the current study

6.7 PEAK TORSION AND SHEAR FORCES ASSOCIATED WITH CORRESPONDING VALUES

Table 6.1 summarizes the peak torsion ($C_{T\ overall}$) and shear force coefficients ($C_{Sx\ overall}$, $C_{Sy\ overall.}$) evaluated by the wind tunnel for the two buildings tested at all heights in open terrain exposure. Tables 6.2 and 6.3 present the corresponding wind force component ratios obtained from testing the two buildings with flat-roof ($0°$) and gabled-roof ($45°$) respectively, for all wind directions. The corresponding wind force component ratios reported in Tables 6.2 and 6.3 are the highest ratios obtained from testing all building heights, hence they are conservative. These values are associated to the peak torsion, peak shear force in X-direction, and peak shear force in Y-direction respectively.

Table 6.1: Peak torsion and shear force coefficients evaluated from all wind directions

Building height (m)	Flat-roof ($0°$)			Gabled-roof ($45°$)		
	$C_{T\ overall}$	$C_{Sx\ overall}$	$C_{Sy\ overall}$	$C_{T\ overall}$	$C_{Sx\ overall}$	$C_{Sy\ overall}$
6	0.03	0.33	0.22	0.13	1.80	0.67
12	0.07	0.69	0.46	0.16	2.22	0.91
20	0.15	1.45	0.80	0.24	3.43	1.63
30	0.22	2.00	1.20	0.26	3.97	1.94
40	0.25	2.75	1.60	0.37	4.86	2.10
50	0.30	3.60	1.90	0.45	5.47	2.70
60	0.36	4.10	2.25	0.56	6.29	2.96

Table 6.2: Peak corresponding force component ratio for building with flat-roof ($0°$) tested at all heights

	Wind direction (deg.)						
	0	15	30	45	60	75	90
Torsional load case:							
$C_{Sx\ corr./overall}$	0.70	0.75	0.77	0.76	0.67	0.33	0.08
$C_{Sy\ corr./overall}$	0.18	0.18	0.31	0.46	0.63	0.81	0.73
Shear load case (X-direction):							
$C_{T\ corr./overall}$	0.29	0.54	0.68	0.55	0.46	0.31	0.17
$C_{Sy\ corr./overall}$	0.34	0.29	0.24	0.58	0.78	0.75	0.62
Shear load case (Y-direction):							
$C_{T\ corr./overall}$	0.27	0.45	0.50	0.41	0.32	0.64	0.59
$C_{Sx\ corr./overall}$	0.77	0.56	0.56	0.69	0.51	0.30	0.13

Table 6.3: Peak corresponding force component ratio for building with gabled-roof (45°) tested at all heights

	Wind direction (deg.)						
	0	15	30	45	60	75	90
Torsional load case:							
$C_{Sx\ corr./overall}$	0.69	0.80	0.78	0.72	0.60	0.29	0.10
$C_{Sy\ corr./overall}$	0.30	0.31	0.28	0.60	0.74	0.81	0.74
Shear load case (X-direction):							
$C_{T\ corr./overall}$	0.44	0.74	0.67	0.44	0.24	0.46	0.43
$C_{Sy\ corr./overall}$	0.25	0.34	0.26	0.58	0.79	0.81	0.63
Shear load case (Y-direction):							
$C_{T\ corr./overall}$	0.28	0.27	0.38	0.36	0.14	0.57	0.56
$C_{Sx\ corr./overall}$	0.79	0.79	0.60	0.69	0.65	0.47	0.12

CHAPTER 7

PROPOSED WIND LOAD COMBINATIONS FOR DESIGN CODES

7.1 CODIFICATION APPROACH

Based on the wind tunnel results, Table 7.1 presents the suggested wind load combination factors for designing medium-rise buildings with rectangular plan. Shear and torsion load cases are provided for transverse and longitudinal directions, as illustrated in Figure 7.1. The shear load case in transverse direction was defined by applying the maximum shear force in X-direction (given in Table 6.1) with the corresponding torsion and shear in Y-direction. These corresponding values were introduced in a form of ratio from the maximum torsion or shear component and this ratio is the highest obtained from testing the two buildings in wind direction range 0° to 45°. For instance, the highest corresponding torsion ratio due to winds in transverse direction - wind direction range 0° to 45° - for the flat- and gabled-roof buildings are 0.68 and 0.74, respectively (see Tables 6.2 and 6.3). As indicated in Table 7.1, the corresponding torsion will be 0.75 (rounded number from 0.74) of the maximum torsion (given in Table 6.1). Likewise, the torsion load case in the transverse direction was defined by applying the maximum torsion and the corresponding shear forces in X- and Y-directions obtained for wind directions between 0° and 45°.

Table 7.1: Suggested design load combination factors for rectangular buildings

	Load case	C_T	C_{Sx}	C_{Sy}
Transverse direction	Shear	0.75	1	0.60
	Torsion	1	0.80	0.60
Longitudinal direction	Shear	0.65	0.70	1
	Torsion	1	0.35	0.80

b) Transverse directions   a) Longitudinal directions
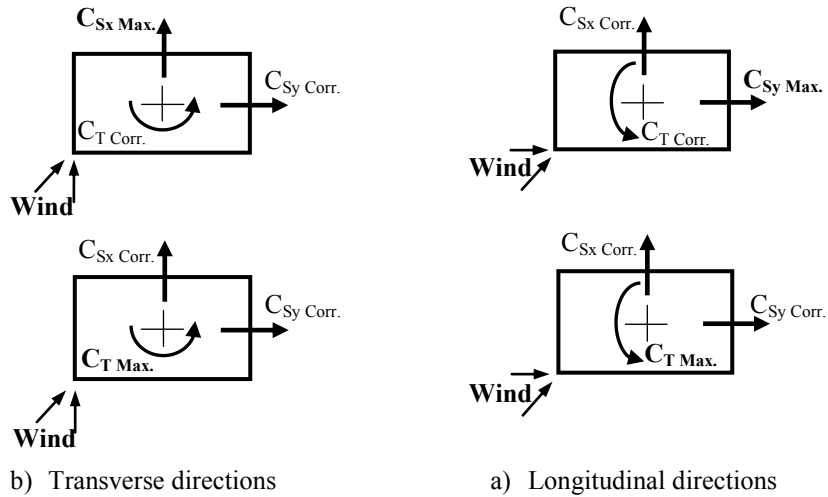
Figure 7.1: Illustration of the proposed shear and torsion wind load case in transverse and longitudinal directions for designing rectangular buildings

7.2 RECOMMENDATIONS FOR NBCC

Table 7.2 summarizes the shear force coefficients ($C_{Sx\ overall}$, $C_{Sy\ overall}$) evaluated by the wind tunnel for the two buildings (i.e. with flat- and gabled- roof) tested at all different heights in open terrain exposure. Based on the wind tunnel results, Table 7.3

presents the suggested wind load cases for the design of low- and medium-rise buildings with rectangular plan and different roof slopes. Shear and torsion load cases are provided for transverse and longitudinal directions. The shear load cases were defined by applying the maximum shear force in X-direction with an eccentricity e_y (%) from facing horizontal building dimension. For buildings with flat and gabled roofs, the corresponding torsion is presented for the suggested shear load cases by applying the maximum wind load at eccentricity of 5%, 15% from the facing horizontal building dimension in transverse and longitudinal direction, respectively. The torsion load case is defined by applying 80% of the maximum shear force but at higher eccentricities as it can be seen in Table 7.3. Although the current study tested only buildings with aspect ratio (L/B) of 1.6, it is believed that the proposed load cases could be applied for buildings with aspect ratios from 1.6 to 2. This is based on the comparisons with the few reported previous studies. For instance, Keast et al (2012) showed that for a 60 m high flat-roof building with aspect ratio (L/B) equal to 2, the maximum torsion was associated with 80% of the maximum shear force for wind directions $0^{°}$ and $90^{°}$. Also, the associated eccentricities were about 8%, 43% from the facing horizontal building dimension for $0^{°}$ and $90^{°}$ wind directions, respectively. It should be noted that the 43% eccentricity in the longitudinal direction is higher than the 35% proposed value obtained from considering only the torsion due to winds in longitudinal-direction. The difference may be attributed to the contribution to the total torsion of the corresponding shear force component in the transverse direction. Clearly, more experimental work for buildings with different aspect ratios would be significant to confirm and generalize the current findings.

It was also interesting to see the difference between the current analytical approaches stated in NBCC (2010) to evaluate torsion on buildings and the suggested load cases. Figures 7.2 and 7.3 show this comparison in transverse and longitudinal directions for buildings with flat and gabled roof. The suggested approach introduces significantly lower torsion in transverse direction, however, for the longitudinal direction higher torsion are introduced as it is underestimated by the NBCC (2010), as was shown in Figure 5.9.

Table 7.2: Most critical shear coefficients for flat and gabled roof buildings

Height (m)	Flat-roof Buildings		Gabled roof buildings	
	$C_{Sx\,overall}$	$C_{Sy\,overall}$	$C_{Sx\,overall}$	$C_{Sy\,overall}$
6	0.33	0.22	1.80	0.67
12	0.69	0.46	2.22	0.91
20	1.45	0.80	3.43	1.63
30	2.00	1.20	3.97	1.94
40	2.75	1.60	4.86	2.10
50	3.60	1.90	5.47	2.70
60	4.10	2.25	6.29	2.96

Table 7.3: Suggested load cases for the design of flat or gabled roof rectangular buildings

		Shear load case		Torsion load case	
		wind load	eccentricity	wind load	eccentricity
Flat-roof buildings	Transverse	P_X*	0.05 L	0.8 P_X	0.15 L
	Longitudinal	P_Y**	0.15 B	0.8 P_Y	0.35 B
Gabled-roof buildings	Transverse	P_X*	0.05 L	0.8 P_X	0.10 L
	Longitudinal	P_Y**	0.15 B	0.8 P_Y	0.30 B

P_X*= $C_{Sx\,overall}$*q_h*B^2 P_Y**= $C_{Sy\,overall}$ *q_h*B^2 Where values for $C_{Sx\,overall}$ and $C_{Sy\,overall}$ would be obtained from Table 7.2 for different building heights
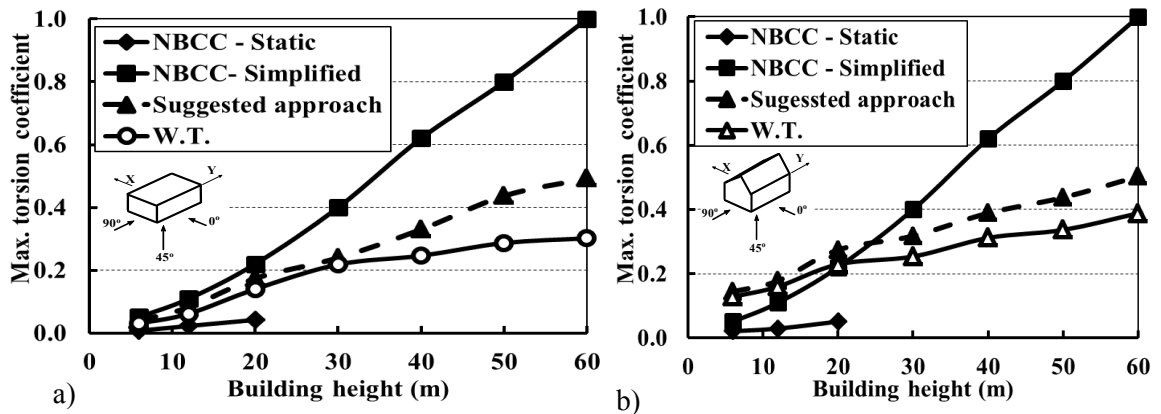
Figure 7.2: Maximum torsion evaluated using NBCC (2010), wind tunnel measurements, and suggested approach in transverse direction for buildings with: a) flat-roof, b) gabled roof (45°)
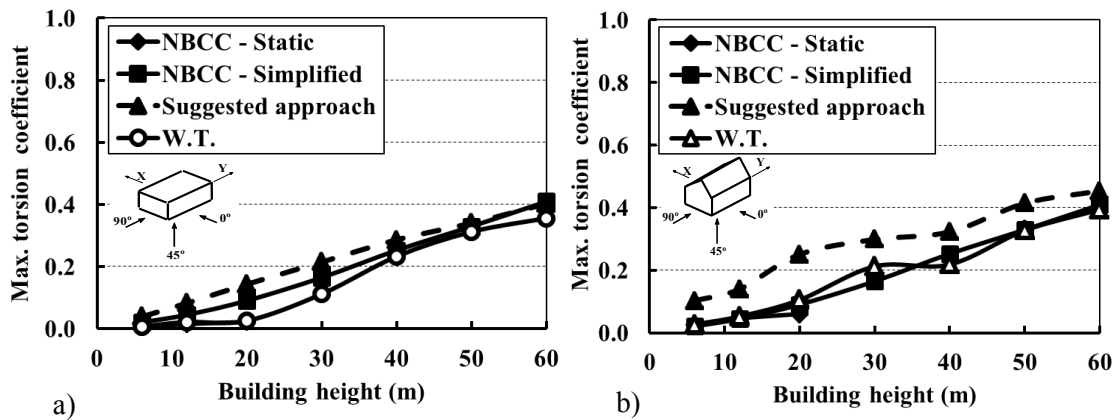
Figure 7.3: Maximum torsion evaluated using NBCC (2010) and wind tunnel measurements, and suggested approach in longitudinal direction for buildings with: a) flat-roof, b) gabled roof (45°)

108

7.2 Recommendations for ASCE 7 (2010)

The same load combinations proposed for potential use in the NBCC could be also used for future ASCE 7 provisions to better evaluate torsion on rectangular low- and medium-rise buildings. Figures 7.4 and 7.5 show this comparison in transverse and longitudinal directions for buildings with flat and gabled roof. The suggested approach introduces significantly lower torsion in transverse direction, however, for the longitudinal direction higher torsion is introduced as it is currently underestimated by the ASCE 7 (2010) –see Figure 7.5.

a)
b)
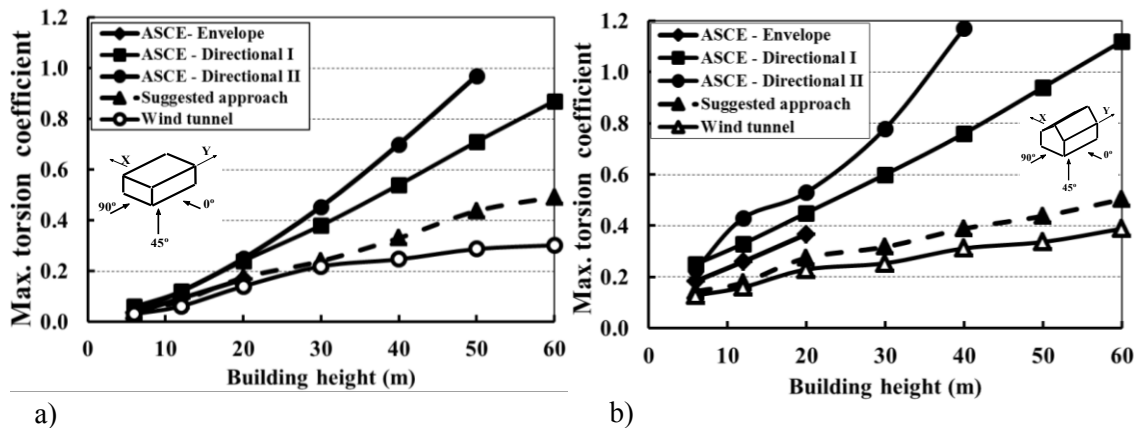
Figure 7.4: Maximum torsion evaluated using ASCE 7 (2010), wind tunnel measurements, and suggested approach in transverse direction for buildings with: a) flat-roof, b) gabled roof (45°)
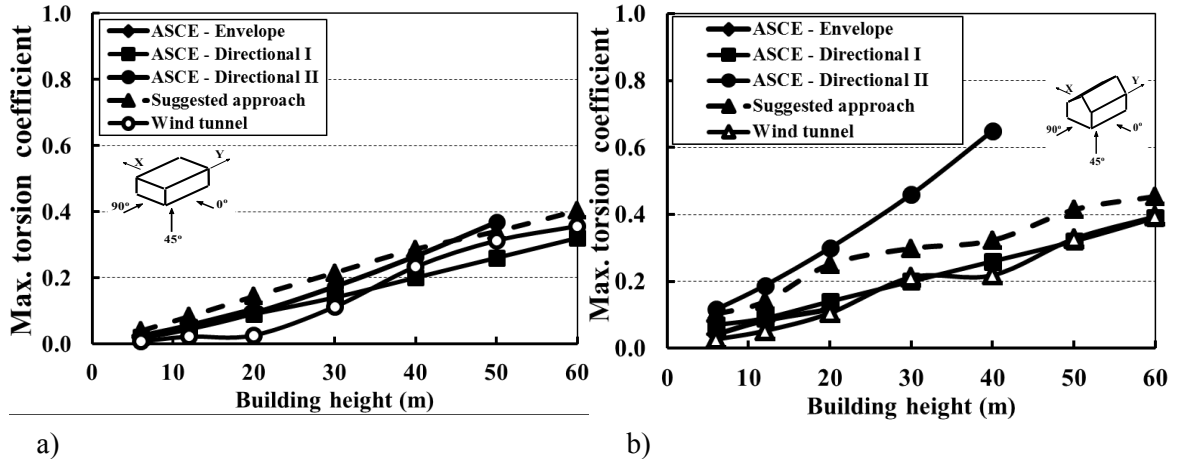
Figure 7.5: Maximum torsion evaluated using ASCE 7 (2010) and wind tunnel measurements, and suggested approach in longitudinal direction for buildings with: a) flat-roof, b) gabled roof (45°)

CHAPTER 8

CONCLUSIONS

8.1 RESEARCH SUMMARY AND CONTRIBUTIONS.

In spite of the continuous updates of wind codes and standards, the lack of knowledge about wind-induced torsion on buildings is clearly reflected in the current provisions. In this study, shear and torsional design wind load cases were investigated in a boundary layer wind tunnel. The first part of this thesis demonstrates that North American and European Codes and Standards have quite different provisions for wind-induced torsion acting on low- and medium-rise buildings with typical geometries – namely, horizontal aspect ratios (L/B) equal to 1, 2 and 3. For instance, the ASCE 7 (2010) applies torsion on low-rise buildings about three times the NBCC (2010) values, and about twice the European code values; for medium-rise buildings similar significant differences were found. Notwithstanding these differences among the mentioned wind load provisions, it is remarkable to mention that other codes/standards neglect torsion in the design of low- and medium-rise buildings. For instance, the Australian standard (AS/NZS 1170.2-2011) does not require wind-induced torsion to be considered for the design of buildings with heights lower than 70 m.

This established the need for the second part of this study, i.e. to investigate experimentally the wind-induced torsional loads on low- and medium-rise buildings. Wind-induced torsion and shears were measured in the wind tunnel for buildings with different roof slopes (0°, 18.4°, 45°) and heights ranging from 6 m to 60 m. The buildings were located in open and urban terrain exposures. Furthermore, the experimental results were compared with wind load provisions in NBCC (2010) and ASCE 7 (2010).

Several verifications were incorporated at various stages of this study, providing confidence in the experimental processes and equipment performance. The analysis of a considerable amount of experimentally and numerically acquired data generated findings of significant importance. In particular, the analysis of experimental results and comparisons with codes/standards demonstrate the following:

1- National Building Code of Canada

- The static method assigned for low-rise buildings underestimates torsion significantly.

- Significant differences were found between the simplified method and the wind tunnel results. In some cases, the simplified method requires torsion about double the measured, while in others underestimates torsion and shear force.

- The simplified method does not introduce any guidance for design of medium-rise buildings with gabled-roofs.

2- American Society of Civil Engineering (ASCE 7 (2010))

- The envelope method assigned for low-rise buildings shows generally good agreement with the wind tunnel measurements.

- Significant differences were found between the simplified method and the wind tunnel results. In some cases, the directional methods require torsion about three times the measured values.

Another key component with limited previous attention was the consideration of wind load combinations including torsion. Therefore, the present study examined the effect of building height, roof slope, and wind direction on wind load combinations; shear forces (in X- and Y- directions) occurring simultaneously with maximum torsion, as well as maximum shears and corresponding torsions. Emphasis was directed towards torsion and its correlation with peak shear forces in transverse and longitudinal directions. Two building models with the same horizontal dimensions but different gabled-roof angles ($0^{°}$ and $45^{°}$) were tested at different full-scale equivalent eave heights (6, 12, 20, 30, 40, 50, and 60 m) in open terrain exposure for all wind directions (every $15^{°}$). Wind-induced pressures were integrated over building surfaces and results were obtained for along-wind force, across-wind force, and torsional moment. Maximum wind force component was given along with the other simultaneously-observed wind force components normalized by the overall peak. The study found that for flat-roof buildings maximum torsion for winds in transverse direction is associated with 80% of the overall shear force perpendicular to the longer horizontal building dimension; and 45% of the maximum shear occurs perpendicular to the smaller horizontal building dimension. Comparison of the wind tunnel results with current torsion provisions in the American wind standard, the

Canadian and European wind codes demonstrate significant discrepancies. Suggested load combination factors were introduced aiming at an adequate evaluation of wind load effects on rectangular low- and medium-rise buildings. Significant differences were found between the suggested approach and current wind-induced loads provisions.

8.2 LIMITATIONS AND RECOMMENDATIONS FOR FUTURE WORK

The limitations of the current study, which may serve as recommendations for future work, can be summarized as follows:

- Wind-induced torsion known to be sensitive to building aspect ratio, plan building shape (i.e. L- and T-shapes), and building roof slope. It would be highly recommended to test more buildings with different configurations in different terrain exposures.

- Of great interest will be to study the effect of building surroundings and interference with neighbouring. These factors can significantly affect wind-induced torsional loads on buildings. This would be also very beneficial to provide general wind provisions that can be adequately help to reach the proper building design.

- Last but not least, as in any wind tunnel study; the findings are closely dependent to the geometry and properties of the specific test buildings. Additional experiments and research should be carried out to comprehend and support this effort.

References:

AAWE (2013). American Association of Wind Engineering web site on October 2, 2013, (http://www.aawe.org/gallery/?p=3&c=), February, 2, 2014.

ASCE 7 (2010). Minimum design loads for buildings and other structures. Structural Engineering Institute of ASCE, Reston, VA.

ASCE, 1999. Wind tunnel studies of buildings and structures. ASCE Manuals and Reports on Engineering Practice No. 67, ASCE, Reston, Virginia, 207 pp.

Boggs, D. W., Hosoya, N., and Leighton Cochran, L. Sources, (2000). Sources of torsional wind loading on tall buildings: Lessons from the wind tunnel, Proceedings of Structures Congress, Philadelphia, Pennsylvania, USA, Sponsored by ASCE/SEI, May 8-10.

CEN. (2005). Eurocode 1: Actions on Structures − Part 1-4: General actions − Wind actions. *Pr EN 1991-1-4*, Brussels.

Davenport, A.G., Surry, D. and Stathopoulos, T., (1977). Wind loading on low-rise buildings: final report on phases I and II, University of Western Ontario, Eng. Sci. Res. Rep., BLWT-SS8.

Davenport, A.G., Surry, D. and Stathopoulos, T., (1978). Wind loading on low-rise buildings: final report on phase III, University of Western Ontario, Eng. Sci. Res. Rep., BLWT-SS4.

Elsharawy, M., Stathopoulos, T. and Galal, K. (2012). Wind-Induced torsional loads on low buildings. Journal of Wind Engineering and Industrial Aerodynamics,104-106, 40-48.

Greig, G.L. (1980). Towards an estimate of Wind-Induced dynamic torque on tall buildings, Univ. of Western Ontario, M. Eng. Thesis, Sept. 1980.

Ho, T.C.E., Lythe, G.R. and Isyumov, N. (1999). Structural Loads from the Integration of Simultaneously Measured Pressures. Proc. ICWE- 10, Copenhagen, Denmark.

Holmes, J. D. (1983). Wind loads on low rise buildings − a review. CSIRO Div. of Building Research, Highett. Victoria, Australia.

Isyumov and Case, P. C. (2000). Wind-Induced torsional loads and responses of buildings, Proceedings of Structures Congress, Philadelphia, Pennsylvania, USA, Sponsored by ASCE/SEI, May 8-10.

Isyumov and Poole (1983). Wind induced torque on square and rectangular building shapes. Journal of Wind Engineering and Industrial Aerodynamics, 13(1-3), 183-196.

Keast, D.C., Barbagallo, A., and Wood, G.S. (2012). Correlation of wind load combinations including torsion on medium-rise buildings. Wind and Structures, An International Journal, 15(5), 423-439.

Krishna, P. (1995). Wind loads on low rise buildings – a review, Journal of Wind Engineering and Industrial Aerodynamics, 54-55, 383-396.

Lythe, G.R. and Surry, D. (1990). Wind-Induced torsional loads on tall buildings, Journal of Wind Engineering and Industrial Aerodynamics, 36, 225-234.

Melbourne, W.H. (1975). Probability distributions of response of BHP house to wind action and model comparisons. Journal of Wind Engineering and Industrial Aerodynamics, 1(2), 167-175.

NBCC (2010). User's Guide – NBC 2010, Structural Commentaries (part 4). Issued by the Canadian Commission on Buildings and Fire Codes, National Research Council of Canada.

Sanni, R. A., Surry, D. and Davenport, A. G. (1992). Wind loading on intermediate height buildings. Canadian Journal of Civil Engineering, 19, 148-163.

Standards Australia. Structural Design Actions Part2 Wind Actions. AS/NZS 1170.2-2011, Standards Australia; 2011.

Stathopoulos, T. (1979). Turbulent Wind Action on Low Rise Buildings. Ph.D., the University of Western Ontario (Canada).

Stathopoulos, T. (1984). Design and fabrication of a wind tunnel for building aerodynamics. Journal of Wind Engineering and Industrial Aerodynamics, 16, 361-376.

Stathopoulos, T. (1984). Wind Loads on Low-rise Buildings - A Review of the State of the Art. Engineering Structures, 6, 119–135.

Stathopoulos, T. and Dumitrescu-Brulotte, M. (1989). Design recommendations for wind loading on buildings of intermediate height. Canadian Journal of Civil Engineering, 16, 910-916.

Stathopoulos, T., Elsharawy, M., and Galal, K. (2013). Wind load combinations including torsion for rectangular medium-rise buildings. International Journal of High-Rise Buildings, 2(3), 1-11.

Surry, D., R.B. Kitchen, R.B., and A.G. Davenport, A.G., (1976). Design effectiveness of wind tunnel studies for buildings of intermediate height. In: Proceedings ASCE National Structural Engineering Conference, Aug., 22–25, 96–116.

Tallin, A., (1985). Analysis of torsional moments on tall buildings. Journal of Wind Engineering and Industrial Aerodynamics, 18, 191-195.

Tamura, Y., Kikuchi, H., Hibi, K. (2000). Wind load combinations and extreme pressure distributions on low-rise buildings. Wind and Structures, An International Journal, 3 (4).

Tamura, Y., Kikuchi, H., Hibi, K. (2003). Quasi-static wind load combinations for low- and middle-rise buildings. Journal of Wind Engineering and Industrial Aerodynamics, 91, 1613-1625.

Tamura, Y., Kikuchi, H., Hibi, K. (2008). Peak normal stresses and effects of wind direction on wind load combinations for medium-rise buildings. Journal of Wind Engineering and Industrial Aerodynamics, 96 (6-7), 1043-1057.

Van der Hoven, I. (1957). Power spectrum of wind velocities fluctuations in the frequency range from 0.0007 to 900 Cycles per hour. Journal of Meteorology, 14, 160-164.

Xie, J. and Irwin, (2000). Key factors for torsional wind response of Tall Buildings. Proceedings of Structures Congress 2000, Philadelphia, Pennsylvania, USA, Sponsored by ASCE/SEI, May 8-10.

Zhou, Y. and Kareem, A. (2000), Torsional load effects on buildings under wind. Proceedings of Structures Congress 2000, Philadelphia, Pennsylvania, USA, Sponsored by ASCE/SEI, May 8-10.

Zisis, I. (2007). Structural monitoring and wind tunnel studies of a low wooden building. M.A.Sc., Concordia University, Montreal, Canada, 2007, pages 150.

APPENDIX I

American Society of Civil Engineers (ASCE 7 (2010)) figures:

Main Wind Force Resisting System – Part 1		$h \le 60$ ft
Figure 28.4-1	**External Pressure Coefficients (GC$_{pf}$)**	**Low-rise Walls & Roofs**
Enclosed, Partially Enclosed Buildings		

Load Case A
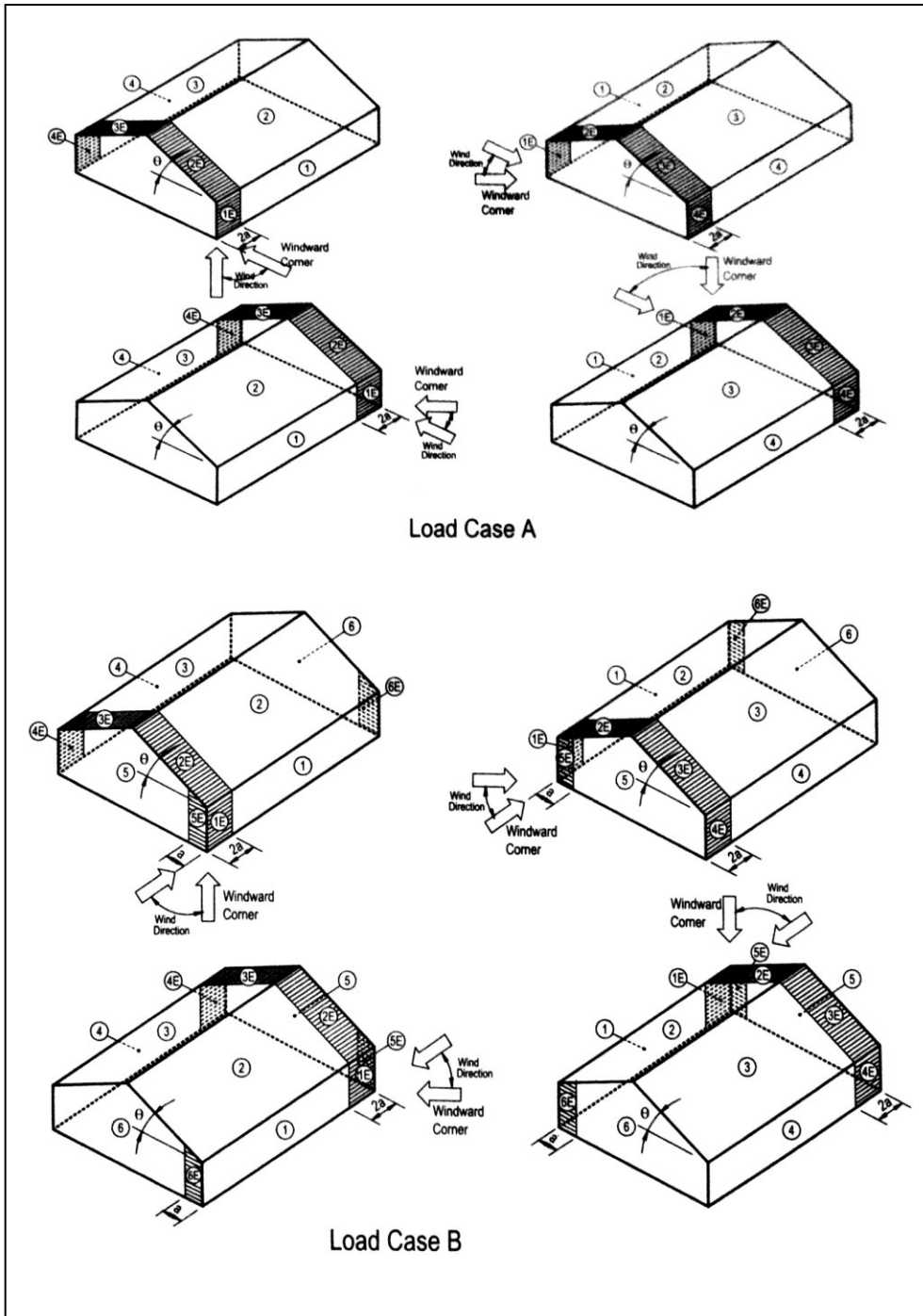
Load Case B

Main Wind Force Resisting System – Part 1		h ≤ 60 ft
Figure 28.4-1 (cont.)	**External Pressure Coefficients (GC$_{pf}$)**	**Low-rise Walls & Roofs**
Enclosed, Partially Enclosed Buildings		

Roof Angle θ (degrees)	LOAD CASE A							
	Building Surface							
	1	2	3	4	1E	2E	3E	4E
0-5	0.40	-0.69	-0.37	-0.29	0.61	-1.07	-0.53	-0.43
20	0.53	-0.69	-0.48	-0.43	0.80	-1.07	-0.69	-0.64
30-45	0.56	0.21	-0.43	-0.37	0.69	0.27	-0.53	-0.48
90	0.56	0.56	-0.37	-0.37	0.69	0.69	-0.48	-0.48

Roof Angle θ (degrees)	LOAD CASE B											
	Building Surface											
	1	2	3	4	5	6	1E	2E	3E	4E	5E	6E
0-90	-0.45	-0.69	-0.37	-0.45	0.40	-0.29	-0.48	-1.07	-0.53	-0.48	0.61	-0.43

Notes:

1. Plus and minus signs signify pressures acting toward and away from the surfaces, respectively.
2. For values of θ other than those shown, linear interpolation is permitted.
3. The building must be designed for all wind directions using the 8 loading patterns shown. The load patterns are applied to each building corner in turn as the Windward Corner.
4. Combinations of external and internal pressures (see Table 26.11-1) shall be evaluated as required to obtain the most severe loadings.
5. For the torsional load cases shown below, the pressures in zones designated with a "T" (1T, 2T, 3T, 4T, 5T, 6T) shall be 25% of the full design wind pressures (zones 1, 2, 3, 4, 5, 6).
   Exception: One story buildings with h less than or equal to 30 ft (9.1m), buildings two stories or less framed with light frame construction, and buildings two stories or less designed with flexible diaphragms need not be designed for the torsional load cases.
   Torsional loading shall apply to all eight basic load patterns using the figures below applied at each Windward Corner.
6. For purposes of designing a building's MWFRS, the total horizontal shear shall not be less than that determined by neglecting the wind forces on the roof.
   Exception: This provision does not apply to buildings using moment frames for the MWRFS.
7. For flat roofs, use θ = 0° and locate the zone 2/3 and zone 2E/3E boundary at the mid-width of the building.
8. The roof pressure coefficient (GC$_{pf}$), when negative in Zone 2 and 2E, shall be applied in Zone 2/2E for a distance from the edge of roof equal to 0.5 times the horizontal dimension of the building parallel to the direction of the MWFRS being designed or 2.5 times the eave height at the windward wall, whichever is less; the remainder of Zone 2/2E extending to the ridge line shall use the pressure coefficient (GC$_{pf}$) for Zone 3/3E.
9. Notation:
   a: 10 percent of least horizontal dimension or 0.4h, whichever is smaller, but not less than either 4% of least horizontal dimension or 3 ft (0.9 m).
   h: Mean roof height, in feet (meters), except that eave height shall be used for θ ≤ 10°.
   θ: Angle of plane of roof from horizontal, in degrees.

Case A Torsion

Transverse Direction

Case B Torsion

Longitudinal Direction

Torsional Load Cases

CASE 1

CASE 3

$M_T = 0.75\ (P_{WX}+P_{LX})B_X e_X$ $M_T = 0.75\ (P_{WY}+P_{LY})B_Y e_Y$ $M_T = 0.563\ (P_{WX}+P_{LX})B_X e_X + 0.563\ (P_{WY}+P_{LY})B_Y e_Y$

$e_X = \pm 0.15\ B_X$ $e_Y = \pm 0.15\ B_Y$ $e_X = \pm 0.15\ B_X$ $e_Y = \pm 0.15\ B_Y$

CASE 2

CASE 4

Case 1. Full design wind pressure acting on the projected area perpendicular to each principal axis of the structure, considered separately along each principal axis.

Case 2. Three quarters of the design wind pressure acting on the projected area perpendicular to each principal axis of the structure in conjunction with a torsional moment as shown, considered separately for each principal axis.

Case 3. Wind loading as defined in Case 1, but considered to act simultaneously at 75% of the specified value.

Case 4. Wind loading as defined in Case 2, but considered to act simultaneously at 75% of the specified value.

Notes:

1. Design wind pressures for windward and leeward faces shall be determined in accordance with the provisions of 27.4.1 and 27.4.2 as applicable for building of all heights.
2. Diagrams show plan views of building.
3. Notation:
   $P_{WX},\ P_{WY}$: Windward face design pressure acting in the x, y principal axis, respectively.
   $P_{LX},\ P_{LY}$: Leeward face design pressure acting in the x, y principal axis, respectively.
   $e\ (e_X,\ e_Y)$: Eccentricity for the x, y principal axis of the structure, respectively.
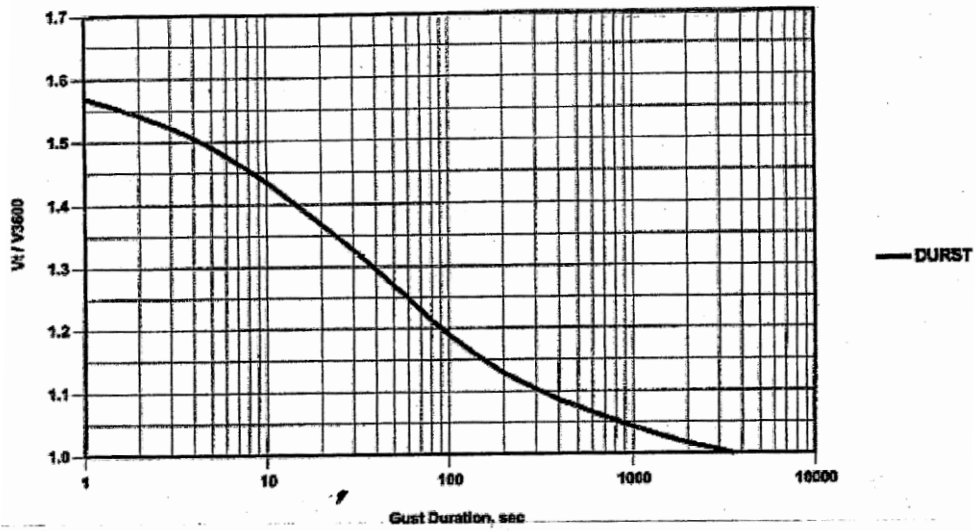 M_T: Torsional moment per unit height acting about a vertical axis of the building.

FIGURE C26.5-1 Maximum Speed Averaged over *t* s to Hourly Mean Speed.

GABLE, HIP ROOF

MONOSLOPE ROOF   (NOTE 4)

MANSARD ROOF   (NOTE 8)

Main Wind Force Resisting System – Part 1		All Heights
Figure 27.4-1 (cont.)	**External Pressure Coefficients, C_p**	**Walls & Roofs**
Enclosed, Partially Enclosed Buildings		

Wall Pressure Coefficients, C_p

Surface	L/B	C_p	Use With
Windward Wall	All values	0.8	q_z
Leeward Wall	0-1	-0.5	q_h
	2	-0.3	
	≥4	-0.2	
Side Wall	All values	-0.7	q_h

Roof Pressure Coefficients, C_p, for use with q_h

Wind Direction	h/L	Windward — Angle, θ (degrees)								Leeward Angle, θ (degrees)		
		10	15	20	25	30	35	45	≥60#	10	15	≥20
Normal to ridge for θ ≥ 10°	≤0.25	-0.7 / -0.18	-0.5 / 0.0*	-0.3 / 0.2	-0.2 / 0.3	-0.2 / 0.3	0.0* / 0.4	0.4	0.01 θ	-0.3	-0.5	-0.6
	0.5	-0.9 / -0.18	-0.7 / -0.18	-0.4 / 0.0*	-0.3 / 0.2	-0.2 / 0.2	-0.2 / 0.3	0.0* / 0.4	0.01 θ	-0.5	-0.5	-0.6
	≥1.0	-1.3** / -0.18	-1.0 / -0.18	-0.7 / -0.18	-0.5 / 0.0*	-0.3 / 0.2	-0.2 / 0.2	0.0* / 0.3	0.01 θ	-0.7	-0.6	-0.6

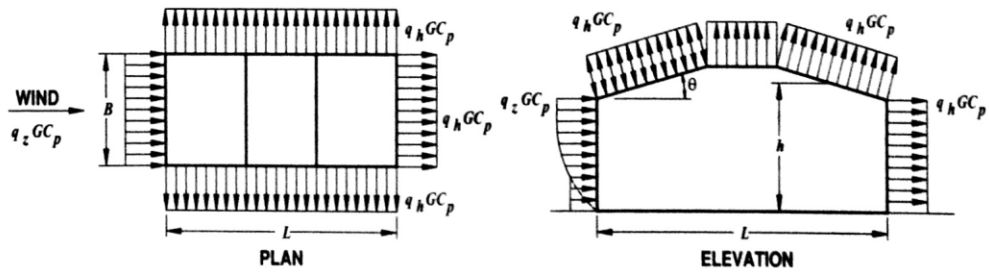| Wind Direction	h/L	Horiz distance from windward edge	C_p
Normal to ridge for θ < 10 and Parallel to ridge for all θ	≤ 0.5	0 to h/2	-0.9, -0.18
		h/2 to h	-0.9, -0.18
		h to 2 h	-0.5, -0.18
		> 2h	-0.3, -0.18
	≥ 1.0	0 to h/2	-1.3**, -0.18
		> h/2	-0.7, -0.18

*Value is provided for interpolation purposes.

**Value can be reduced linearly with area over which it is applicable as follows

Area (sq ft)	Reduction Factor
≤ 100 (9.3 sq m)	1.0
250 (23.2 sq m)	0.9
≥ 1000 (92.9 sq m)	0.8

Notes:
1. Plus and minus signs signify pressures acting toward and away from the surfaces, respectively.
2. Linear interpolation is permitted for values of L/B, h/L and θ other than shown. Interpolation shall only be carried out between values of the same sign. Where no value of the same sign is given, assume 0.0 for interpolation purposes.
3. Where two values of C_p are listed, this indicates that the windward roof slope is subjected to either positive or negative pressures and the roof structure shall be designed for both conditions. Interpolation for intermediate ratios of h/L in this case shall only be carried out between C_p values of like sign.
4. For monoslope roofs, entire roof surface is either a windward or leeward surface.
5. For flexible buildings use appropriate G_f as determined by Section 26.9.4.
6. Refer to Figure 27.4-2 for domes and Figure 27.4-3 for arched roofs.
7. Notation:
   B: Horizontal dimension of building, in feet (meter), measured normal to wind direction.
   L: Horizontal dimension of building, in feet (meter), measured parallel to wind direction.
   h: Mean roof height in feet (meters), except that eave height shall be used for θ ≤ 10 degrees.
   z: Height above ground, in feet (meters).
   G: Gust effect factor.
   q_z, q_h: Velocity pressure, in pounds per square foot (N/m^2), evaluated at respective height.
   θ: Angle of plane of roof from horizontal, in degrees.
8. For mansard roofs, the top horizontal surface and leeward inclined surface shall be treated as leeward surfaces from the table.
9. Except for MWFRS's at the roof consisting of moment resisting frames, the total horizontal shear shall not be less than that determined by neglecting wind forces on roof surfaces.

#For roof slopes greater than 80°, use C_p = 0.8

Main Wind Force Resisting System – Part 2		$h \leq 160$ ft.
Figure 27.5-1	**Building Class**	**Building Geometry Requirements**
Enclosed Simple Diaphragm Buildings		

$0.2L \leq B \leq 5L$

L

Plan

Mean roof ht.

$h \leq 60$ ft

Elevation

Class 1 Building

$0.5L \leq B \leq 2L$

L

Plan

Mean roof ht.

$h = 60 - 160$ ft

Class 2 Building

Elevation

Note: Roof form may be flat, gable, mansard or hip

128
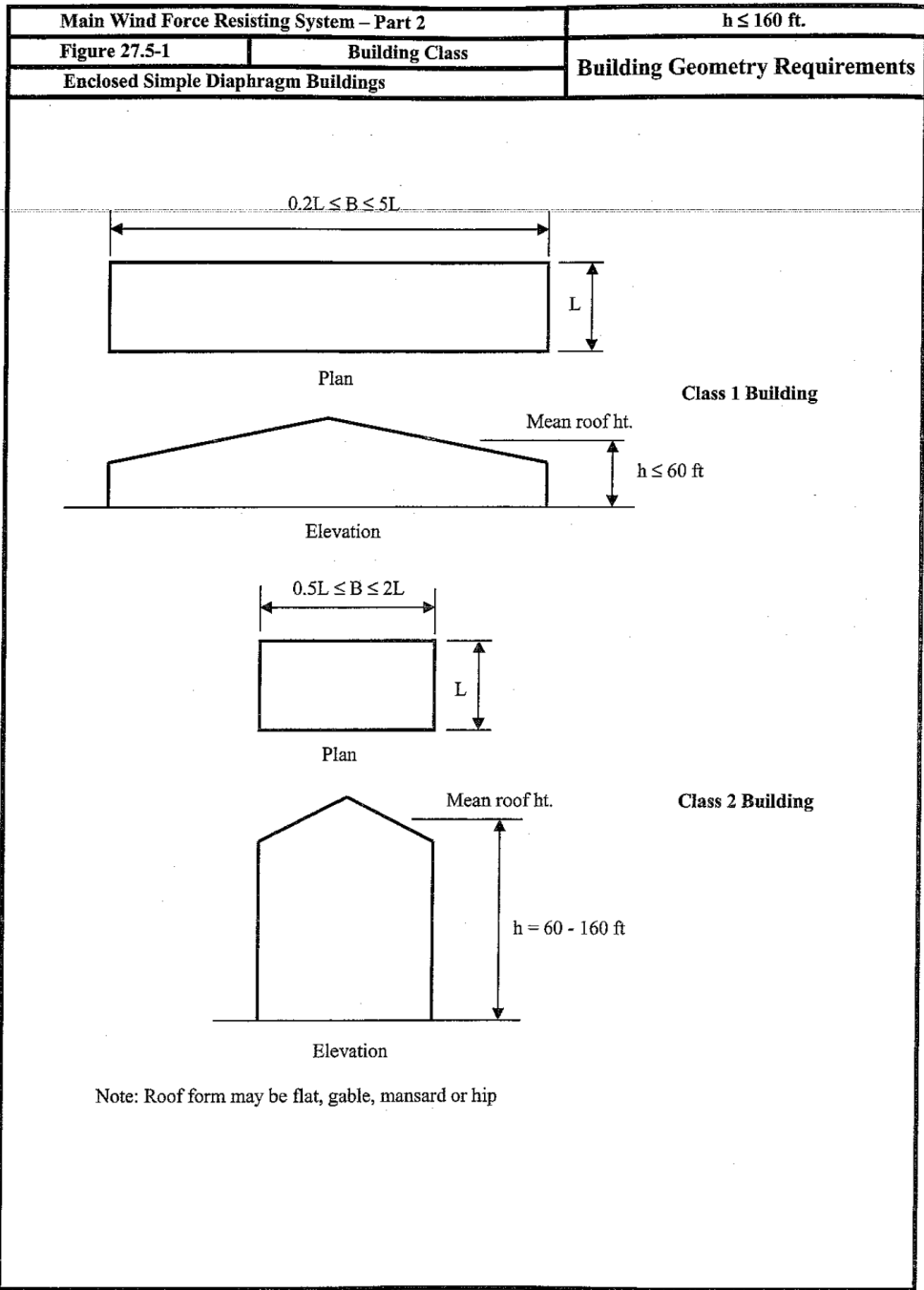
Main Wind Force Resisting System – Part 2		h ≤ 160 ft
Figure 27.6-1	Wind Pressures – Walls and Roof	Application of Wind Pressures See Tables 27.6-1 and 27.6-2
Enclosed Simple Diaphragm Buildings		

See Fig 27.6-2 for parapet wind pressures

Roof Pressures See Table 27.6-2

Mean roof ht.

θ

p_h

Wall Pressures See Table 27.6-1

h

p_o

Elevation

L

Wind

B

Plan
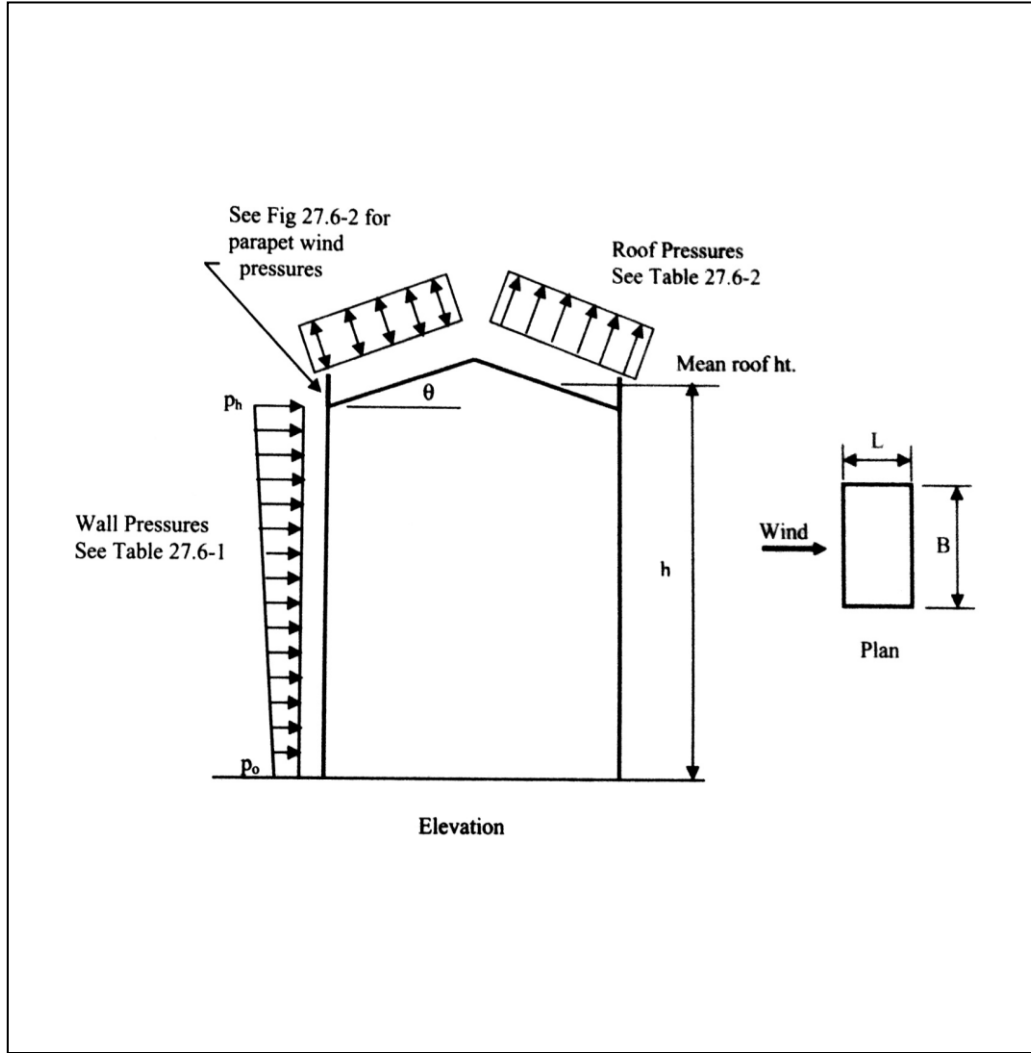
Main Force Resisting System – Part 2		$h \leq 160$ ft.
Table 27.6-1	**Wind Pressures - Walls**	**Application of Wall Pressures**
Enclosed Simple Diaphragm Buildings		

Plan   Wind Pressure   Elevation
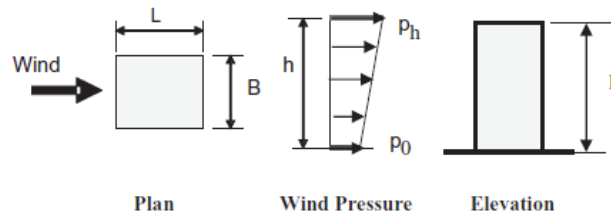
Notes to Wall Pressure Table 27.6-1:

1. From table for each Exposure (B, C or D), V, L/B and h, determine p_h (top number) and p_0 (bottom number) horizontal along-wind net wall pressures.
2. Side wall external pressures shall be uniform over the wall surface acting outward and shall be taken as 54% of the tabulated p_h pressure for $0.2 \leq L/B \leq 1.0$ and 64% of the tabulated p_h pressure for $2.0 \leq L/B \leq 5.0$. Linear interpolation shall apply for $1.0 < L/B < 2.0$. Side wall external pressures do not include effect of internal pressure.
3. Apply along-wind net wall pressures as shown above to the projected area of the building walls in the direction of the wind and apply external side wall pressures to the projected area of the building walls normal to the direction wind, simultaneously with the roof pressures from Table 27.6-2.
4. Distribution of tabulated net wall pressures between windward and leeward wall faces shall be based on the linear distribution of total net pressure with building height as shown above and the leeward external wall pressures assumed uniformly distributed over the leeward wall surface acting outward at 38% of p_h for $0.2 \leq L/B \leq 1.0$ and 27% of p_h for $2.0 \leq L/B \leq 5.0$. Linear interpolation shall be used for $1.0 < L/B < 2.0$. The remaining net pressure shall be applied to the windward walls as an external wall pressure acting towards the wall surface. Windward and leeward wall pressures so determined do not include effect of internal pressure.
5. Interpolation between values of V, h and L/B is permitted.

Notation:
  L = building plan dimension parallel to wind direction (ft.)
  B = building plan dimension perpendicular to wind direction (ft)
  h = mean roof height (ft.)
  p_h, p_0 = along-wind net wall pressure at top and base of building respectively (psf)

APPENDIX II

National Building Code of Canada (NBCC (2010)) figures:

Load case A: winds generally perpendicular to ridge

Roof slope	Building surfaces							
	1	1E	2	2E	3	3E	4	4E
0° to 5°	0.75	1.15	−1.3	−2.0	−0.7	−1.0	−0.55	−0.8
20°	1.0	1.5	−1.3	−2.0	−0.9	−1.3	−0.8	−1.2
30° to 45°	1.05	1.3	0.4	0.5	−0.8	−1.0	−0.7	−0.9
90°	1.05	1.3	1.05	1.3	−0.7	−0.9	−0.7	−0.9

Load case B: winds generally parallel to ridge

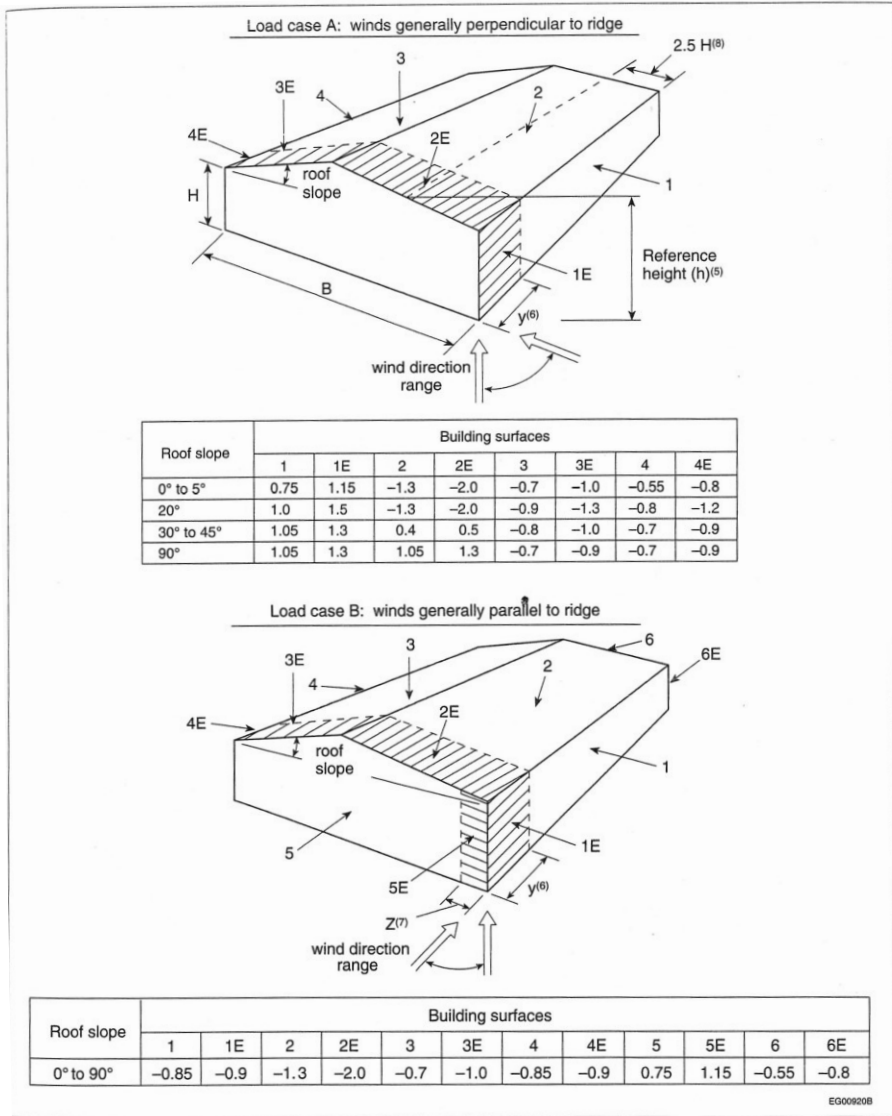| Roof slope	Building surfaces											
	1	1E	2	2E	3	3E	4	4E	5	5E	6	6E
0° to 90°	−0.85	−0.9	−1.3	−2.0	−0.7	−1.0	−0.85	−0.9	0.75	1.15	−0.55	−0.8

EG00920B

Figure I-7
External peak composite pressure-gust coefficients, $C_p C_g$, for primary structural actions arising from wind load acting simultaneously on all surfaces

Case A: Full wind pressure applied
in both directions separately

Case C: 75% of full wind pressure applied
in both directions simultaneously

Case B: Case A wind pressure applied
only on parts of wall faces

Case D: 50% of Case C wind load removed
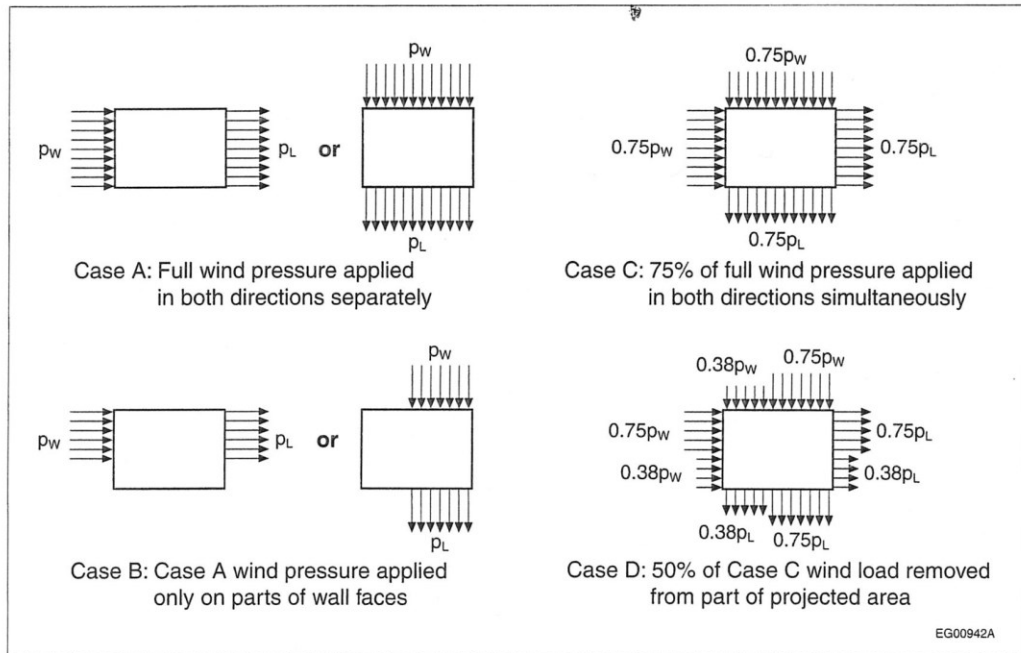from part of projected area

EG00942A

Figure I-16
Full and partial wind loads (see NBC Sentence 4.1.7.3.(1))

APPENDIX III

EN 1991-1-4 (2005): Actions on structures - General actions - Part 1-4: wind actions

a) For rectangular structures that are susceptible to torsional effects the pressure distribution given in Figure 7.1 should be applied for the representation of the torsional effects due to an inclined wind or due to lack of correlation between wind forces acting at different places on the structure.

b) For other cases an allowance for asymmetry of loading should be made by completely removing the design wind action from those parts of the structure where its action will produce a beneficial effect.
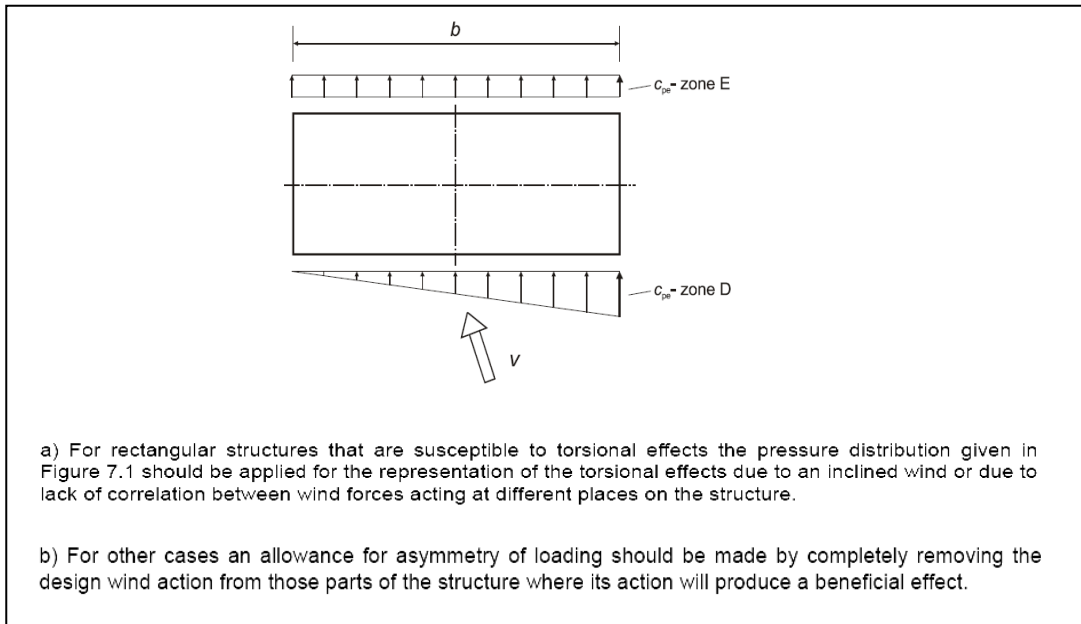
Figure 7.1: Pressure distribution used to take torsional effects into account (Eurocode (2005))